IL
NUOVO CIMENTO
ORGANO DELLA SOCIETÀ ITALIANA DI FISICA
SOTTO GLI AUSPICI DEL CONSIGLIO NAZIONALE DELLE RICERCHE

VOL. XI, N. 2 *Serie nona* 1° Febbraio 1954

Determination of the Mass of Slow Particles by the Constant Sagitta Method (×).

C. DILWORTH (*), S. J. GOLDSACK (+) and L. HIRSCHBERG

Centre de Physique Nucléaire de l'Université Libre - Bruxelles

(ricevuto il 13 Ottobre 1953)

Summary. — A method is described in which the measurement of scattering of tracks at the end of their range is carried out on sets of cells of varying length, chosen so that the second difference of the sagitta remains constant. This permits the measurements to be made always at the optimum cell length and eliminates the inconveniences and inaccuracies of the methods in which the track is broken into several sections for measurement. The mass values of a series of K and J-particles have been determined, together with those of a group of protons which serves as calibration.

Introduction.

The measurement of the mass of particles by the scattering range method, introduced by GOLDSCHMIDT *et al.* (2), has regained importance in the last year since the K-particles were observed in the photographic emulsion (3).

(×) This method, developed independently at the laboratories of Brussels and Bombay was presented as a joint communication at the Congress on Cosmic Rays at Bagnères de Bigorre, July 1953 (1).

(*) Aggregate member of the section of Milan of the Istituto Nazionale di Fisica Nucleare.

(+) Now at Physical Laboratories, University of Manchester.

(1) S. BISWAS, E. C. GEORGE and B. PETERS; C. DILWORTH, S. GOLDSACK and L. HIRSCHBERG: *Bagnères Conference*, in press.

(2) Y. GOLDSCHMIDT-CLERMONT, G. KING, H. MUIRHEAD and D. M. RITSON: *Proc. Phys. Soc.*, **61**, 183 (1948).

(3) C. O'CEALLAIGH: *Phil. Mag.*, **42**, 1032 (1951).

In this paper is described a convenient and accurate technique for making these measurements, by which the second difference of the sagitta of scattering is kept constant over the whole residual range.

A calibration has been made on a group of protons and the masses of 8 K-particles, 3 τ-particles and 3 J-particles are given.

Of these 4 K-particles were found in the Laboratory of Brussels, 4 K-particles, 1 τ and 3 J-particles were kindly lent by the laboratories of Genoa and of Milan and 2 τ's by the laboratory of Padova for measurement by this method.

The resolving power of the method is discussed.

Principle of the method.

The energy of a particle of mass M, chage Ze and residual range R can, when R is not too small, be written approximately

$$E = 0.251\, Z^{1.16} M^{0.42} R^{0.58}, \tag{1}$$

where E is in MeV, R in microns and M in units of proton mass.

The angle of scattering in a cell of t microns is given by

$$\alpha = K_s Z t^{\frac{1}{2}} / p\beta \cdot 10^{-1} \quad \text{(degrees)}, \tag{2}$$

where p is the momentum, β the velocity of the particle and K_s is the scattering « constant ».

In the non-relativistic approximation $p\beta = 2E$, and therefore

$$\alpha = 0.199\, K_s t^{\frac{1}{2}} R^{-0.58} Z^{-0.16} M^{-0.42}. \tag{3}$$

Thus α varies rapidly with R towards the end of the range.

The existing techniques ([2, 4]), consist in treating α as constant over a given portion of the track, and measuring it at constant cell length. This has the disadvantage:

a) of requiring either a fitting of $\bar{\alpha} - R$ curves or a weighting of several values of $\bar{\alpha}$ from several portions of track;

b) of rendering it impossible to maintain the measurement at strictly optimum cell-length over the sections of track in which α is supposed constant;

c) of requiring separate correction for noise level and separate cut-off of large angles in each section.

It seemed reasonable to try to vary the cell of measurement continuously along the track in such a way as to remain always at the optimum cell length. If at the same time the parameter of scattering remains constant, then the

([4]) M. G. K. MENON and O. ROCHAT: *Phil. Mag.*, **42**, 1232 (1951).

calculation is considerably simplified. These two conditions can be fulfilled simultaneously only in the sagitta method.

From (3) the second difference D of the sagitta is given by

$$D = \alpha t = 0.00348\, K_s R^{-0.58} Z^{-0.16} M^{-0.42} t^{\frac{3}{2}} . \tag{4}$$

Since the noise level, ε, in the measurement of sagitta is practically independent of the cell-length for the short cells employed for slow particles, the signal to noise ratio D/ε is independent of t, if D is maintained constant. The cell-length t is chosen so that

$$t^{\frac{3}{2}} \propto K_s^{-1} R^{0.58} Z^{0.16} M^{0.42} . \tag{5}$$

Fig. 1 shows the variation of cell length in function of range for various particles, if K_s is supposed constant, for $D/\varepsilon \cong 4$. Then, since D/ε is constant,

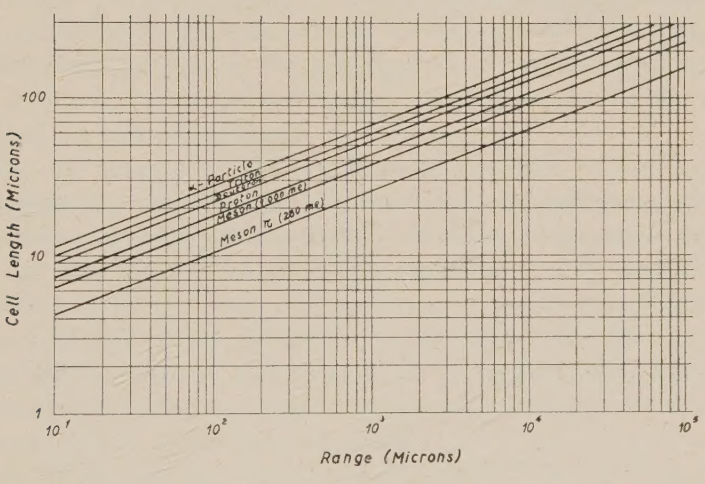

Fig. 1. – Relationship between Range and Cell Length to obtain constant Sagittal Scattering: $\overline{\delta} \propto t^{\frac{3}{2}} R^{-0.58} M^{-0.42} Z^{-1.16}$. Using the cell given here $D = 0.49$ microns (Arithmetic mean)

measurement can be made at optimum cell length over the whole track. Since D is constant, a straight mean can be taken and the mass M deduced either from the constants in equation (2) or by comparison with the mean sagitta $\overline{D}_N$ obtained on tracks of known particles:

$$M/M_N = (\overline{D}_N/\overline{D})^{2.38} . \tag{4}$$

The correction for noise and the cut-off of large angles can be applied over the whole track, since both corrections are made with respect to $\overline{D}$.

The standard error on the determination of mass is calculated taking the statistical error on $\overline{D}$ to be $0.75/\sqrt{N}$, with cut off at 4 times the mean angle of scattering and noise elimination between two cell lengths, N being the num-

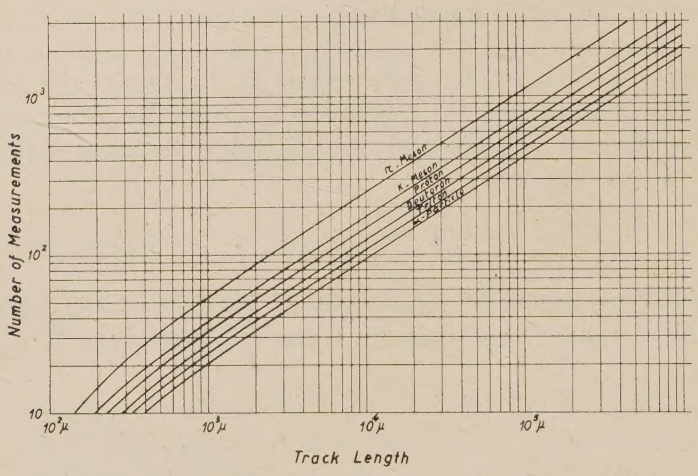

Fig. 2.

ber of independent measurements (see Fig. 2). In Fig. 3 is shown the percentage error on the mass in function of the length of track. The error being

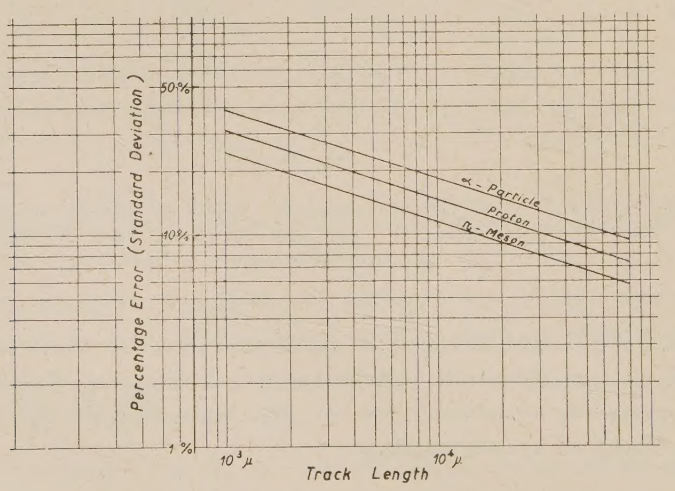

Fig. 3.

relatively small for lengths of more than 1 mm is taken symmetric here.

Variation of K_s of the range-energy exponent, and extension to relativistic velocities.

Equation (4) is not strictly correct, at low energies since the range-energy relation is not the simple power law of (1), and at high velocities for which $p\beta \neq 2E$. Thus the set of cells defined by (5) are not those for which D is truly constant. In addition, the scattering « constant » K_s is in reality a slowly varying function of R and t and not a constant as has been supposed in drawing the curves of Fig. 1.

There are two possible ways of taking into account these three effects. We can either construct a set of cells for which t is truly proportional to $(K_s/p\beta)^{-\frac{2}{3}}$ or, since the errors involved are small, use the simple sets of Fig. 1 and apply an overall correction to the resulting $\overline{D}$. We have employed the latter technique for two reasons. In the first place, improvements in the available knowledge of the range energy relation and the scattering constant, and possible slight changes in the constitution of the emulsion, do not make necessary a change in the cell-series used for measurements, but only in the constant used in the calculation.

Secondly, the lengths of cell for different particles at a given range are simply proportional to each other. It is therefore possible to make measurements, without prior assumptions about the mass, with a series of cells, say half those suitable for a π-meson (see Appendix II). The mean scattering is then calculated from the same measurements at increasing cell lengths, until the observed scattering is sufficiently greater than the noise level. Noise elimination can be carried out exactly as for mono-energetic tracks. For example a π-meson can be calculated at twice the fundamental cell, a K particle at three times and a proton at four times.

Using these cell sets we reduce the measured $\overline{D} = 1/N \sum_0^N D$, where N is the number of cells of measurement, to a standard D_s by applying a correction factor λ^{-1} which is a function of the range and of the mass determined. Values of λ^{-1} are given in Appendix I. With the values we have chosen, we find for protons

$$D_{sp} = 0.565 .$$

Thus to calculate the mass of an unknown particle we write

$$M/M_p = (D_{sp}/D_s)^{2.38} = (0.565/\lambda^{-1}\overline{D})^{2.48}$$

Experimental technique.

As in the normal sagitta method, the track is aligned parallel to the

movement of the stage and readings taken of the position of the central grains in successive cells. It is more convenient in this case to displace the track at given values of the residual range R, rather than with the appropriate value of the cell length. Tables of residual ranges at which the measurements are to be made can be constructed for each type of particle (with a normally good micrometer screw and stage displacements can be made with a precision of 1 μ) or, if the simple uncorrected cell sets are to be used and noise eliminated between two cell lengths, a basic table such as that given in Appendix II for half π cell lengths can be used for the measurement of any track.

If the more rigorous sets of curves are used, preliminary measurements must be made to determine approximately the mass of the particle, and the set of ranges chosen accordingly (*).

It is important to keep the track closely parallel to the stage movement, as otherwise the second difference does not quite represent the scattering angle. The error can be shown to be negligible if the first difference δ_1 satisfies

$$\delta_1 \leqslant t/5$$

where t is the cell length.

This condition is rather stringent for π-mesons near the end of the range, and frequent reorientation is often necessary.

Steeply dipping tracks are not really suitable for these measurements. A correction must be applied if the dip is significant (cf. MENON and O'CEALLAIGH [5]). If φ is the angle of dip, in the unshrunk emulsion the range is greater than the projected range by a factor $(\cos\varphi)^{-1}$ reducing the scattering by a factor $(\cos\varphi)^{0.58}$. The projected scattering is greater than the true scattering by the factor $(\cos\varphi)^{-\frac{3}{2}}$. In a uniformly dipping track the overall correction to the scattering is approximately a factor $(\cos\varphi)^{0.92}$ corresponding to a correction in the mass of $(\cos\varphi)^{-2.19}$.

These corrections are not serious in tracks long enough for useful measurement in a single emulsion, except, perhaps, at the end of the range, but in a stack of stripped emulsions a track may be steep and still be long enough for measurement.

Experimental results.

Measurements were made with the proton cell series on a group of tracks stopping in the emulsion of plates exposed in the Sardinia balloon flights of

(*) Such sets of ranges are being calculated at Göttingen for the proceedings of the Varenna Summer School (Società Italiana di Fisica, 1953).

(5) M. G. K. MENON and C. O'CEALLAIGH: *Phil. Mag.*, **44**, 1291 (1953).

1952. The mass spectrum is shown in Fig. 4. The proton group is well enough separated for a mean value of its mass to be determined. This gives

$$M_p = 1\,790 \pm 40\ m_e\,,$$

TABLE I.

Particle (*)	Range, μ	Mass, m_e	Error, m_e	$\frac{P_K}{P_J}$
K – M_1	2 000	1 270	290	$8.4 \cdot 10^{1}$
M_2	5 260	1 030	165	$3.0 \cdot 10^{7}$
M_4	1 470	1 360	340	$4.7 \cdot 10^{0}$
M_6	3 400	970	185	$2.7 \cdot 10^{6}$
B_1	3 000	800	160	$1.2 \cdot 10^{8}$
B_2	2 000	750	170	$4.9 \cdot 10^{7}$
B_3	1 400	985	255	$1.3 \cdot 10^{3}$
B_4	20 000	1 100	110	$1.0 \cdot 10^{16}$
J – M_1	16 000	2 210	260	$1.2 \cdot 10^{-7}$
M_2	1 250	2 340	680	$6.7 \cdot 10^{-2}$
M_3	900	2 330	770	$1.2 \cdot 10^{-1}$
τ – M_1	4 000	933	170	—
P_1	7 000	840	190	—
P_2	5 000	925	200	—

(*) The particles marked M are from Milan and Genoa, B from Brussels and P from Padova.

which is within a statistical deviation of the true value and gives us confidence in the method.

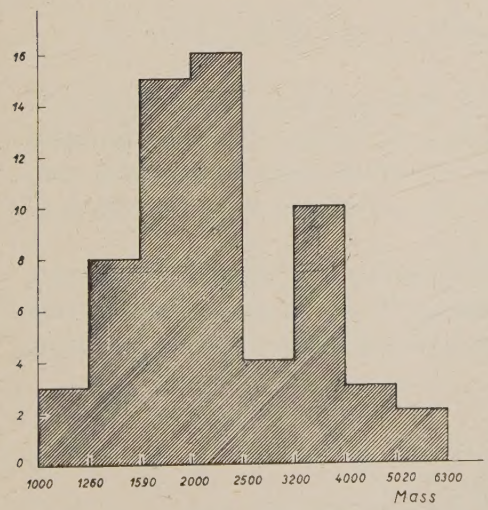

Fig. 4. – Distribution of mass of particles stopping in the emulsion.

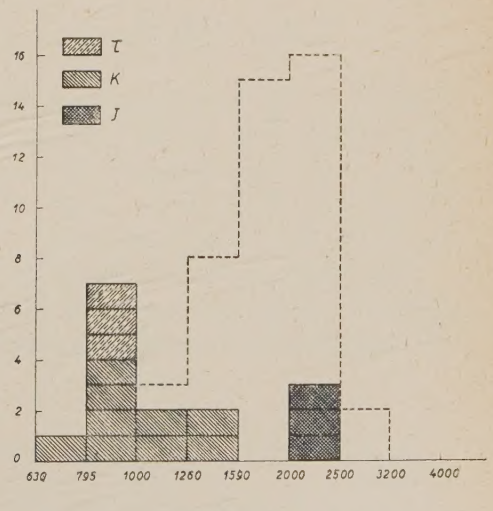

Fig. 5. – Distribution of mass of K-, τ-, and J-particles.

The mass values of a group of 8 K-particles, 3 τ's and 3 J's were also determined. The results are given in Table I and Fig. 5. The mean values obtained were:

$$M_K = 990 \pm 60 \ m_e ,$$

$$M_\tau = 910 \pm 110 \ m_e ,$$

$$M_J = 2\,260 \pm 210 \ m_e .$$

The constancy of D was checked over the longest tracks by taking the means of 10 cells. The results are shown in Fig. 6.

Discussion.

The validity of the constant sagitta method seems to have been established. It should in principle be more precise than the preceding methods.

It is of interest to consider the resolving power of the method. We may take as examples two problems of current interest, the resolution of those K and J-particles which decay into fast secondaries, and the resolution of Kϱ's from protons (see below).

The former problem has been posed by BONETTI *et al.* ([6]). These two groups of particles differ considerably in mass, but on short tracks some overlap is possible. If we consider a track on which measurement of scattering-range on N cells gives a value $\overline{D}$ of the mean second difference, the ratio of the probability P_K of its being a K-particle to that P_J of its being a J-particle is

$$P_K/P_J = P_0 \overline{D}_J/\overline{D}_K \exp\left[-\{(1-\overline{D}/\overline{D}_K)^2 - (1-\overline{D}/\overline{D}_J)^2\}\right]/2\varepsilon^2,$$

where P_0 is the ratio of the number of K to J-particles, and $\varepsilon = 0.75/\sqrt{N}$. It is evident that for $M = 1\,570 \ m_e$, $P_K/P_J = P_0 D_J/D_K$, whatever the value of N. From the indication of the relative intensities given by BONETTI *et al.* (loc. cit.) at $M = 1\,570 \ m_e$, $P_K/P_J = 1.4$. In table I are given the values of P_K/P_J for the K and J-particles.

The second problem is that of the possible existence of negative K-particles captured without giving a nuclear disintegration. These, by analogy with the old phenomenological nomenclature of OCCHIALINI and POWELL ([7]) we can call Kϱ's.

([6]) A. BONETTI, R. LEVI-SETTI, M. PANETTI and G. TOMASINI: Private communication.

([7]) G. P. S. OCCHIALINI and C. F. POWELL: *Nature*, **162**, 168 (1948).

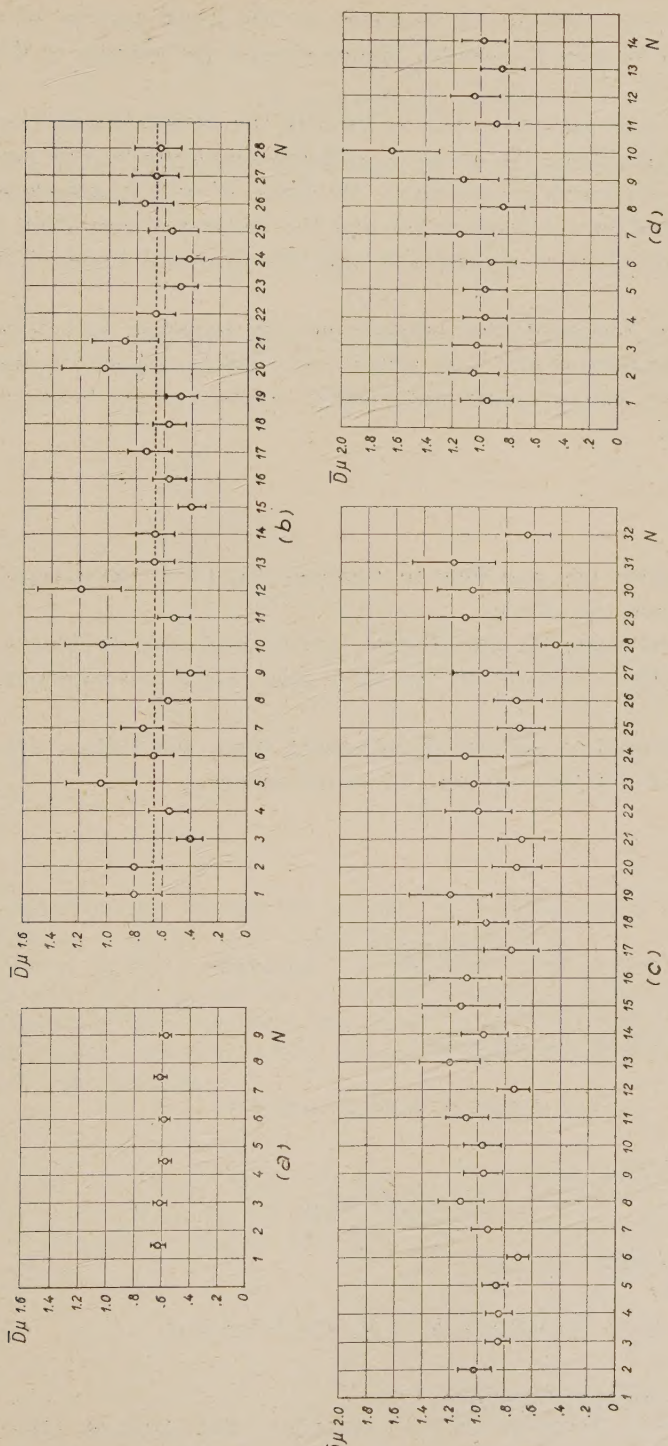

Fig. 6. – Constancy of D: (*a*) Proton group; (*b*) One long proton; (*c*) Group of K-mesons; (*d*) Group of τ-mesons.

The possibility of their existence is suggested by the small number of disintegrations produced by slow K-particles compared with the number of K-particles which decay ([8]).

The scattering range method is not necessarily the most efficient to apply to such a statistical problem. To obtain a sufficient resolution by this method, tracks of at least 2 cm length are required. On tracks of such length the ionization at the beginning of the track is low and the method of ionization range is quicker, a consideration of a certain weight when several hundred tracks must be measured.

When this paper was ready for publication, our attention was drawn to the article of HOLTEBEKK *et al.* ([9]), in which the variable cell length method had been developed independently and applied to discriminate between ^{3}He and ^{4}He fragments.

Acknowledgements.

We wish to express our gratitude to Professor G. P. S. OCCHIALINI who proposed and directed this work.

We thank our colleague D. HIRSCHBERG for his invaluable assistance, and Mrs. CORNIL and Miss VANDENCAMP for their help in the measurement and calculation.

We are very grateful to our friends of Genoa Milan and Padua, who lent us an important part of the material for measurement.

APPENDIX I.

We take as standard the constant

$$D_s = 0.199 \cdot 24 \cdot R^{-0.58} M^{-0.42} Z^{-0.16} l^{\frac{2}{3}} .$$

The measured value

$$D = K_s Z t^{\frac{2}{3}} / p\beta .$$

At each cell therefore we have

$$D_s/D = 0.199 \cdot 24 \cdot R^{-0.58} M^{-0.42} Z^{-0.16} p\beta / K_s Z$$

([8]) *Discussion of Bagnères Conference*, 1953.

([9]) T. HOLTEBEKK, N. ISACHSEN and S. O. SÖRENSEN: *Phil. Mag.*, **44**, 1037 (1953).

i.e.

$$\frac{D_s}{\overline{D}} = \frac{24}{\overline{K_s}} \frac{E/M}{0.251(R/MZ)^{0.58}} \frac{p\beta}{2E} = \delta_K \delta_{ER} \delta_{p\beta} .$$

The mean value of D is obtained by summing over the number N of cells of measurements

$$\overline{D} = D_s \sum_0^N (\delta_K \delta_{ER} \delta_{p\beta})^{-1}/N = \overline{\lambda}^{-1} D_s .$$

The correction factor $\delta_K = 24/K_s$ is determined from the values of K_s given by GOTTSTEIN *et al.* ([10]). $\delta_{ER} = E/M/0.251(R/MZ)^{0.58}$ is calculated from

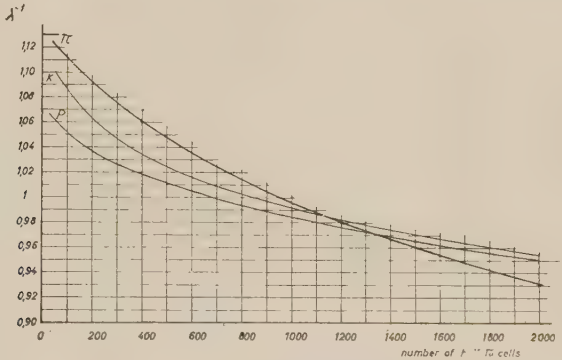

Fig. 7.

the range-energy curves for protons of ROTBLAT ([11]). The relativistic correction $\delta_{p\beta} = p\beta/2E = (1 + E/2Mc^2)(1 + E/Mc^2)^{-1}$.

Curves of $\delta^{-1} = (\delta_K \delta_{ER} \delta_{p\beta})^{-1}$ in function of the number of π cells in the track have been drawn for π-mesons, K-particles and protons and integrated numerically. The resultant values of λ^{-1} in function of N are given in fig. 7. These values are calculated for cell sets of t_π for π-mesons. $3t_\pi/2$ for K-particles and $2t_\pi$ for protons.

([10]) K. GOTTSTEIN, M. G. K. MENON, J. H. MULVEY, C. O'CEALLAIGH and O. ROCHAT: *Phil. Mag.*, **42**, 708 (1951), Curve with cut-off.

([11]) J. ROTBLAT: *Nature*, **167**. 550 (1951).

Appendix II.

Table of ranges for half π cells.

No.	R	No.	R	No.	R	No.	R
1	48	51	372	101	907	151	1 616
2	52	52	381	102	920	152	1 632
3	56	53	390	103	932	153	1 648
4	60	54	399	104	945	154	1 664
5	64	55	408	105	958	155	1 680
6	69	56	417	106	971	156	1 696
7	73	57	426	107	984	157	1 712
8	78	58	436	108	997	158	1 728
9	82	59	445	109	1 010	159	1 744
10	87	60	455	110	1 023	160	1 760
11	92	61	464	111	1 036	161	1 776
12	97	62	474	112	1 050	162	1 793
13	102	63	483	113	1 063	163	1 809
14	108	64	494	114	1 077	164	1 826
15	113	65	504	115	1 090	165	1 842
16	119	66	514	116	1 104	166	1 859
17	124	67	524	117	1 117	167	1 875
18	130	68	534	118	1 131	168	1 892
19	136	69	544	119	1 144	169	1 909
20	142	70	554	120	1 158	170	1 926
21	148	71	564	121	1 172	171	1 943
22	154	72	575	122	1 186	172	1 960
23	160	73	585	123	1 200	173	1 977
24	167	74	596	124	1 214	174	1 995
25	173	75	606	125	1 228	175	2 012
26	180	76	617	126	1 242	176	2 030
27	186	77	627	127	1 256	177	2 047
28	193	78	638	128	1 271	178	2 065
29	200	79	649	129	1 285	179	2 082
30	207	80	660	130	1 300	180	2 100
31	214	81	671	131	1 314	181	2 117
32	221	82	682	132	1 329	182	2 135
33	228	83	692	133	1 343	183	2 153
34	236	84	704	134	1 358	184	2 171
35	243	85	715	135	1 372	185	2 189
36	251	86	727	136	1 387	186	2 207
37	258	87	738	137	1 402	187	2 225
38	266	88	750	138	1 417	188	2 243
39	273	89	761	139	1 432	189	2 261
40	281	90	773	140	1 447	190	2 279
41	289	91	785	141	1 462	191	2 297
42	297	92	797	142	1 477	192	2 315
43	305	93	809	143	1 492	193	2 333
44	313	94	821	144	1 507	194	2 352
45	321	95	833	145	1 522	195	2 370
46	330	96	845	146	1 538	196	2 389
47	338	97	857	147	1 553	197	2 407
48	347	98	870	148	1 569	198	2 426
49	355	99	882	149	1 584	199	2 444
50	364	100	895	150	1 600	200	2 463

Table of ranges for half π cells.

No.	R	No.	R	No.	R	No.	R
201	2 481	251	3 485	301	4 612	351	5 852
202	2 500	252	3 507	302	4 636	352	5 878
203	2 518	253	3 528	303	4 659	353	5 904
204	2 537	254	3 550	304	4 683	354	5 930
205	2 555	255	3 571	305	4 707	355	5 956
206	2 574	256	3 593	306	4 631	356	5 982
207	2 593	257	3 614	307	4 755	357	6 008
208	2 612	258	3 636	308	4 779	358	6 035
209	2 631	259	3 658	309	4 803	359	6 061
210	2 650	260	3 680	310	4 827	360	6 088
211	2 669	261	3 702	311	4 851	361	6 114
212	2 689	262	3 724	312	4 876	362	6 141
213	2 708	263	3 746	313	4 900	363	6 167
214	2 728	264	3 768	314	4 925	364	6 194
215	2 747	265	3 790	315	4 949	365	6 220
216	2 767	266	3 812	316	4 974	366	6 247
217	2 786	267	3 834	317	4 998	367	6 274
218	2 806	268	3 856	318	5 023	368	6 301
219	2 825	269	3 878	319	5 047	369	6 328
220	2 845	270	3 901	320	5 072	370	6 355
221	2 865	271	3 923	321	5 096	371	6 382
222	2 885	272	3 946	322	5 121	372	6 409
223	2 905	273	3 968	323	5 145	373	6 436
224	2 925	274	3 991	324	5 170	374	6 463
225	2 945	275	4 013	325	5 194	375	6 490
226	2 965	276	4 036	326	5 219	376	6 518
227	2 985	277	4 058	327	5 244	377	6 545
228	3 005	278	4 081	328	5 269	378	6 573
229	3 025	279	4 103	329	5 294	379	6 600
230	3 046	280	4 126	330	5 319	380	6 628
231	3 066	281	4 148	331	5 344	381	6 655
232	3 087	282	4 171	332	5 369	382	6 683
233	3 107	283	4 194	333	5 394	383	6 710
234	3 128	284	4 217	334	5 419	384	6 738
235	3 148	285	4 240	335	5 444	385	6 765
236	3 169	286	4 263	336	5 969	386	6 793
237	3 190	287	4 286	337	5 494	387	6 820
238	3 211	288	4 309	338	5 520	388	6 848
239	3 232	289	4 332	339	5 545	389	6 875
240	3 253	290	4 355	340	5 571	390	6 903
241	3 274	291	4 378	341	5 596	391	6 930
242	3 295	292	4 401	342	5 622	392	6 958
243	3 316	293	4 424	343	5 647	393	6 985
244	3 337	294	4 448	344	5 673	394	7 013
245	3 358	295	4 471	345	5 698	395	7 040
246	3 379	296	4 495	346	5 724	396	7 068
247	3 400	297	4 518	347	5 749	397	7 095
248	3 421	298	4 542	348	5 775	398	7 123
249	3 442	299	4 565	349	5 800	399	7 150
250	3 464	300	4 589	350	5 826	400	7 178

RIASSUNTO (*)

Si descrive un metodo col quale la misura dello scattering delle tracce a fine range si esegue su gruppi di celle di lunghezza variabile, scelte in modo che la seconda differenza della saetta rimanga costante. Ciò permette di eseguire la misura sempre alla lunghezza più favorevole della cella ed elimina le inesattezze e gli inconvenienti dei metodi in cui la traccia è divisa, per l'esecuzione della misura, in diverse sezioni. I valori delle masse di una serie di particelle K e J sono stati determinati, per confronto, assieme a quelli di un gruppo di protoni.

(*) *Traduzione a cura della Redazione.*

Sulla dissipazione delle onde elastiche nel piombo ad alta temperatura.

P. G. Bordoni e M. Nuovo

Istituto Nazionale di Ultracustica « O. M. Corbino » - Roma

(ricevuto il 9 Novembre 1953)

Riassunto. — A completamento di precedenti ricerche si è misurata la dissipazione delle onde elastiche estensionali nel piombo puro, per frequenze comprese tra 10 e 40 kHz e temperature variabili tra 300 e 600 °K Si è trovato che la dissipazione aumenta gradualmente al crescere della temperatura e al diminuire della frequenza. Di tale risultato è stata data una giustificazione teorica mostrando come esso sia legato alle deformazioni progressivamente crescenti nel tempo (*creep*) che si producono nei solidi ad alta temperatura sotto l'azione di una sollecitazione costante.

1. – Scopo del lavoro.

Nel corso di precedenti ricerche è stata determinata la velocità delle onde elastiche di tipo estensionale nel piombo puro in tutto l'intervallo di temperatura compreso tra 4,5 °K e 557 °K [1], [2], e dei risultati ottenuti è stata data una soddisfacente giustificazione valendosi della teoria statistica dei solidi [3], [4]. Limitatamente all'intervallo 4,5 °K - 300 °K è stata inoltre misurata la dissipazione relativa allo stesso tipo di onde elastiche [1], ed anche di questi risultati è stata indicata una interpretazione teorica di carattere statistico [5]. Nel presente lavoro ci si è proposti di completare le attuali conoscenze relative alla propagazione delle onde estensionali nel piombo, determinandone la dissipazione anche per le temperature comprese tra 300 °K ed il punto di fusione.

Le misure effettuate mostrano che al disopra di 300 °K la dissipazione cresce gradualmente insieme con la temperatura, fino a raggiungere valori dello stesso ordine di quelli che si hanno in corrispondenza al massimo nei fenomeni di rilassamento; a differenza però di quanto si verifica per questi

ultimi, l'aumento della dissipazione ha luogo in un intervallo di temperatura di parecchie centinaia di gradi. Tale risultato è in ottimo accordo con le misure effettuate da I. BARDUCCI sul piombo puro e su alcune sue leghe mediante vibrazioni flessionali [6] ed estensionali [19]. Un andamento analogo della curva dissipazione-temperatura è stato inoltre osservato dagli autori nel corso di una precedente ricerca sullo stagno [7] e da T. S. KÊ nel caso dell'alluminio [8], del rame, del magnesio, del ferro e dell'ottone [20].

I risultati delle misure di dissipazione relative al piombo sono ripetibili finchè non si supera la temperatura di 520-540 °K; se invece si effettua un riscaldamento prolungato in aria a temperature superiori a quelle indicate si osserva una progressiva diminuzione della dissipazione al crescere del tempo. Tale diminuzione, che è particolarmente sensibile se il materiale è portato a qualche grado dalla sua temperatura di fusione, persiste anche a temperatura ordinaria dando luogo ad una curva dissipazione-temperatura che si trova tutta al disotto di quella rilevata durante il riscaldamento.

L'applicazione del calcolo operatorio alla teoria della dissipazione elastica [10] ha permesso di dare una giustificazione teorica dei risultati sperimentali precedentemente illustrati, mettendo in luce lo stretto legame esistente tra l'aumento della dissipazione con la temperatura e la *deformazione crescente progressivamente nel tempo* che notoriamente ha luogo ad alta temperatura sotto l'azione di uno sforzo costante. La teoria svolta mostra che la dissipazione è prevalentemente dovuta al moto di un numero di dislocazioni crescente insieme con la temperatura nell'intervallo considerato.

Le curve sperimentali dissipazione-temperatura presentano anche dei massimi assai poco accentuati in corrispondenza a temperature di circa 360 °K e 505 °K. Al crescere della frequenza i massimi si spostano verso le alte temperature ed il calcolo dei relativi calori di attivazione, effettuato in base a tale spostamento, fornisce proprio valori dello stesso ordine di grandezza di quelli che si hanno nella diffusione dei metalli. Sembra pertanto che i massimi osservati vadano attribuiti a fenomeni di rilassamento del tipo abituale.

2. – Metodo di misura.

Come misura della dissipazione si è preso l'inverso del coefficiente di risonanza Q di una sbarretta di piombo priva di ogni sensibile vincolo esterno e vibrante su uno dei suoi modi estensionali, analogamente a quanto è stato fatto dagli autori in precedenti ricerche [1], [7] e da altri sperimentatori [6], [8], [9], [10]. La conoscenza di Q consente di determinare immediatamente il decremento logaritmico d delle vibrazioni di una sbarretta di lunghezza finita ed il coefficiente di attenuazione μ riferito alla lunghezza d'onda, e relativo ad un'onda estensionale che si propaghi lungo una sbarra sottile di lunghezza

infinita. Infatti finchè Q^{-1} è abbastanza piccola rispetto all'unità tra Q, d e μ sussistono, con ottima approssimazione, le relazioni [9], [10], [11]

$$d = \pi Q^{-1}; \qquad \mu = 2\pi Q^{-1}, \tag{1}$$

in modo che, indicando con $\mathcal{J}(x)$ l'intensità dell'onda in corrispondenza all'ascissa x e con λ la relativa lunghezza d'onda, si ha:

$$\mathcal{J}(x) = \mathcal{J}(0) \exp\left[-\mu \frac{x}{\lambda}\right] = \mathcal{J}(0) \exp\left[-2\pi Q^{-1} \frac{x}{\lambda}\right]. \tag{2}$$

I valori di Q sono stati ottenuti eccitando le vibrazioni della sbarretta mediante una forza variabile nel tempo con legge sinusoidale. Mantenendo costante l'ampiezza massima della forza e variandone la frequenza si è misurata l'ampiezza di vibrazione in funzione della frequenza, in prossimità di uno dei primi modi di vibrazione estensionali; la differenza $\nu' - \nu''$ tra le frequenze corrispondenti ad un'ampiezza di vibrazione eguale ad $1/\sqrt{2}$ dell'ampiezza massima, divisa per la frequenza ν_m corrispondente a quest'ultima fornisce allora il valore di Q^{-1}

$$Q^{-1} = \frac{|\nu' - \nu''|}{\nu_m}. \tag{3}$$

L'apparecchiatura elettroacustica per l'eccitazione e la misura delle vibrazioni è sostanzialmente quella stessa dettagliatamente descritta in una nota precedente [12], che è già stata adoperata in diverse ricerche di tipo analogo [1], [2], [6], [7]. Essa consente la determinazione di Q con valori dei coefficienti di deformazione dell'ordine di 10^{-8}, e richiede l'uso di un solo elettrodo per l'eccitazione e la misura delle vibrazioni; normalmente l'elettrodo è posto alla distanza di circa 5/100 mm da una delle basi della sbarretta, ed il dielettrico è costituito dallo straterello d'aria interposto. Le dilatazioni della sbarretta e le deformazioni di origine termica del sostegno richiedono però frequenti ritocchi nella posizione dell'elettrodo, i quali non sempre riescono agevoli ad alta temperatura. Si è eliminata tale difficoltà valendosi di un recente perfezionamento apportato al metodo sperimentale [13], consistente nell'appoggiare direttamente l'elettrodo sulla sbarretta, con l'interposizione di un foglio di mica dello spessore circa 5/100 mm come dielettrico (fig. 1*a*). In tal modo la distanza tra l'elettrodo e la sbarretta e quindi anche la sensibilità dell'apparato, risultano indipendenti dalla temperatura. Nello stesso tempo le piccole irregolarità delle superficie metalliche e della mica fanno sì che il contatto meccanico fra di esse abbia luogo soltanto in qualche punto, in modo che, nonostante la presenza dell'elettrodo, l'estremità superiore della sbarretta vibra ancora come se fosse libera.

Per ridurre al minimo i vincoli esterni l'insieme elettrodo-sbarretta è disposto verticalmente ed è sostenuto mediante tre punte di acciaio del dia-

metro di 1 mm disposte a 120° tra di loro, e contenute in un piano nodale, come è stato fatto per le misure di velocità ad alta temperatura [2]. Il contatto elettrico con la sbarretta è assicurato dalle punte stesse che la sostengono, mentre l'elettrodo è collegato agli apparecchi di misura mediante un filo d'argento del diametro di 0,1 mm. Confrontando i valori di Q misurati nel modo indicato con quelli che si hanno quando l'elettrodo è separato dalla sbarretta da uno straterello di aria si è verificato che, nel campo di temperatura considerato, la dissipazione aggiuntiva dovuta all'appoggio è sempre abbastanza piccola rispetto alla dissipazione interna del piombo.

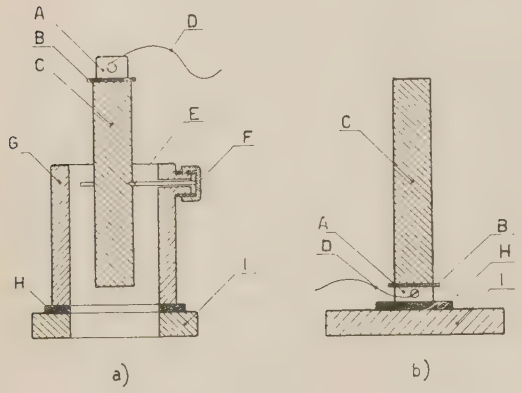

Fig. 1. – Disposizione sperimentale per la misura della dissipazione relativa a vibrazioni estensionali. *A* elettrodo; *B* foglio di mica (spessore circa 5/100 mm); *C* sbarretta di piombo; *D* filo di contatto dell'elettrodo; *E* punte di acciaio; *F* viti di pressione delle punte; *G* sostegno; *H* materiale isolante; *I* base.

La disposizione sperimentale può essere ulteriormente semplificata appoggiando direttamente la sbarretta sull'elettrodo, con l'interposizione di un sottile foglio di mica (fig. 1*b*), in modo da eliminare il sostegno a punte. In questa maniera la dissipazione aggiuntiva risulta però alquanto maggiore di quella che si riscontra nel caso precedente, pur restando sempre tollerabile in confronto ai valori della dissipazione interna.

Durante le misure la sbarretta, il suo sostegno e l'elettrodo sono collocati nella muffola cilindrica di un forno elettrico, la cui temperatura è regolata automaticamente con l'approssimazione di un grado mediante un termometro a mercurio provvisto di contatto mobile. Come nelle precedenti misure di velocità [2] la temperatura è misurata con una termocoppia ferro-costantana, tarata in corrispondenza al punto di fusione del piombo, e posta vicinissima alla sbarretta. Il raggiungimento dell'equilibrio termico tra quest'ultima e l'aria che la circonda è indicato dalla costanza nel tempo della frequenza di risonanza.

3. – Risultati sperimentali.

Le misure sono state effettuate su tre sbarrette cilindriche di piombo Merck T. P. aventi diversa lunghezza, le cui caratteristiche principali sono indicate nella Tab. I. La fusione è stata effettuata in lingottiera di alluminio

(diametro 20 mm; lunghezza 250 mm) preriscaldata a circa 250 °C, e le singole sbarrette sono state ricavate per tornitura dalla parte centrale di *lingotti diversi*.

TABELLA I. – *Caratteristiche delle sbarrette.*

Sbarretta n.°	Materiale	Lavorazione prima delle misure	Lunghezza mm	Diametro mm	Frequenza di risonanza fondamentale a 20 °C (Hz)
1	Piombo Merck T.P.	Fusione e tornitura	24,15	9,89	28 149
2			48,6	9,95	13 723
3			48,0	10,08	13 149

Per ottenere risultati ripetibili si è trovato conveniente iniziare le misure dalla temperatura più elevata, dopo aver lasciato trascorrere un tempo sufficientemente lungo (dell'ordine di qualche ora) in modo che la frequenza di risonanza e la dissipazione non subissero più variazioni nel tempo. Se non si supera una temperatura di 520 ÷ 540 °K, le misure effettuate in *discesa*, cioè facendo diminuire la temperatura, non differiscono da quelle eseguite in *salita*, cioè con temperature successivamente crescenti. Infatti nella fig. 2 i punti sperimentali contrassegnati in maniera diversa, che appartengono a diverse serie di misure relative alla sbarretta n. 1 si dispongono su di una stessa curva (a tratto continuo). A scopo di confronto si sono riportati anche i valori di Q^{-1} relativi all'intervallo 200-300 °K ottenuti in una precedente ricerca alle basse temperature [1] (curva tratteggiata). A parte la presenza di un massimo assai poco accentuato, corrispondente alla temperatura di circa 380 °K, la dissipazione cresce gradualmente da 200 °K fino alla massima temperatura raggiunta. Tale accrescimento risulta particolarmente

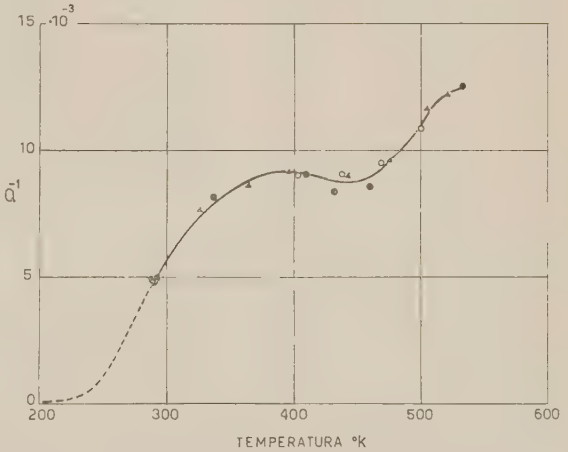

Fig. 2. – Dissipazione in funzione della temperatura nella sbarretta n. 1. O prima serie di misure, in discesa; ● seconda serie di misure, in salita; ▲ terza serie di misure, in salita.

marcato nell'intervallo 200-300 °K, mentre al disopra di questa ultima temperatura la pendenza media della curva è considerevolmente minore.

Sulla sbarretta n. 2, la cui frequenza fondamentale è circa la metà di quella precedente, sono stati ottenuti risultati del tutto analoghi finchè la temperatura non ha superato i 540 °K (fig. 3, curva a tratto continuo). Al disopra di tale valore si è osservata una graduale diminuzione dell'assorbimento *a temperatura costante* accompagnata da un aumento della frequenza di risonanza. Abbassando successivamente la temperatura si sono trovati valori della dissipazione tutti inferiori a quelli ottenuti precedentemente, mentre i valori della frequenza di risonanza sono risultati tutti maggiori di quelli misurati prima del riscaldamento. I nuovi valori di Q^{-1} risultano perfettamente ripetibili, come si rileva dalla fig. 3, nella quale i punti contrassegnati in maniera differente ed appartenenti a diverse serie di misure, si dispongono tutti su di un'unica curva (tratteggiata); naturalmente in queste ultime misure si è avuto cura di non superare la temperatura massima raggiunta nel riscaldamento iniziale. La diminuzione della dissipazione rende assai più evidente la presenza di un massimo a 350 °K; si osserva inoltre che al disopra di 540 °K i valori di Q^{-1} anche dopo il riscaldamento rimangono sempre molto elevati.

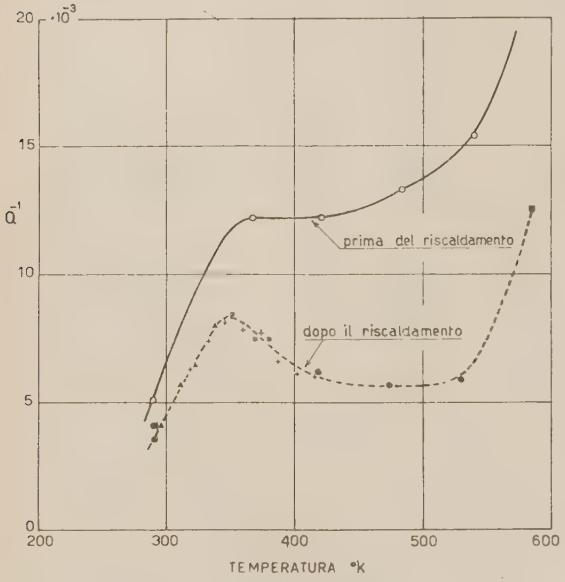

Fig. 3. – Dissipazione in funzione della temperatura nella sbarretta n. 2. ○ prima serie di misure, in salita ($T \leqslant 592$ °K); ● seconda serie di misure, in salita ($T \leqslant 585$ °K); ▲ terza serie di misure, in salita ($T \leqslant 339$ °K); + quarta serie di misure, in salita ($T \leqslant 416$ °K); ■ quinta serie di misure in salita ($T \leqslant 398$ °K).

La differenza che si riscontra tra i valori della velocità misurati dopo il riscaldamento oltre i 540 °K e quelli anteriori al riscaldamento stesso (fig. 4) cresce leggermente insieme con la temperatura; ad esempio a 300 °K essa è di 35 ms^{-1} mentre a 540 °K raggiunge i 44 ms^{-1}. Oltre ad uno spostamento verso l'alto della curva velocità-temperatura si nota quindi una lieve diminuzione della sua pendenza, diminuzione che è particolarmente sensibile alle temperature più elevate.

Occorre tener presente che le variazioni indicate, per quanto piccole, risul-

tano apprezzabili con sicurezza, poichè il metodo di misura adoperato consente la determinazione della velocità con un errore relativo dell'ordine di $1 \div 2 \cdot 10^{-3}$ [2]. Nel caso del piombo tale errore non supera quindi 2,5 ms^{-1}.

Limitatamente alle temperature comprese tra 290 e 430 °K le misure di dissipazione sono state ripetute sulla sbarretta n. 2 determinando *contemporaneamente* i valori di Q^{-1} relativi ai primi due modi di vibrazione estensionali. Il confronto tra le due curve ottenute (fig. 5) mostra che il massimo dell'assorbimento si sposta verso le alte temperature al crescere della frequenza.

La diminuzione permanente della dissipazione risulta ancora più accentuata se la sbarretta viene tenuta abbastanza a lungo ad una temperatura molto prossima a quella di fusione. La curva a tratto continuo della fig. 6 indica i valori di Q^{-1} misurati sulla sbarretta n. 3 dopo un primo riscaldamento a 584 °K; la curva tratteggiata caratterizza invece la dissipazione nella stessa sbarretta dopo un trattamento di 3^h a 598 °K e risulta tutta notevolmente inferiore alla precedente. A differenza di quanto si è osservato nella sbarretta n. 2, in questo caso la dissipazione si mantiene abbastanza limitata anche alle alte temperature. Inoltre nella curva rilevata dopo il riscaldamento non si osserva più traccia del piccolo massimo a 360 °K, il quale d'altronde nella curva originale era assai meno accentuato che in quelle relative alle sbarrette n. 1 e 2. Invece dopo il riscaldamento risulta assai più netto il massimo a 510 °K, la cui presenza è appena accennata nella fig. 2, mentre non appare nella fig. 3 in cui i punti sperimentali sono più lontani tra di loro.

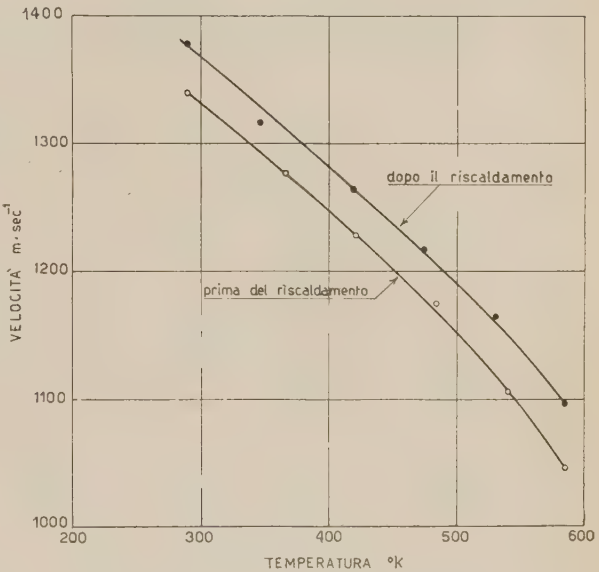

Fig. 4. – Velocità in funzione della temperatura nella sbarretta n. 2. ○ prima serie di misure, in salita, con riscaldamento fino a circa 590 °K; ● seconda serie di misure, in salita ($T \leqslant 585$ °K).

4. – Discussione dei risultati.

Il risultato più importante tra quelli precedentemente illustrati è senza dubbio costituito dal graduale aumento della dissipazione interna che ha luogo quando si passa dalla temperatura ambiente a valori prossimi alla temperatura di fusione.

Tale aumento, pur non essendo stato studiato in maniera sistematica, è stato osservato incidentalmente anche in metalli diversi dal piombo e con tipi di vibrazioni differenti da quelle estensionali. Ad esempio in una breve nota [7] precedentemente pubblicata, gli autori hanno segnalato, nel caso dello stagno, un andamento della curva dissipazione-temperatura del tutto simile a quello ora riscontrato nel piombo. Risultati analoghi per entrambi i metalli indicati sono stati ottenuti da I. Barducci mediante vibrazioni flessionali [6] e, più recentemente, con vibrazioni estensionali di frequenza considerevolmente più bassa di quelle impiegate nel presente lavoro [19]; si può osservare che anche sotto l'aspetto quantitativo i valori di Q^{-1} relativi a vibrazioni flessionali si trovano in ottimo accordo con quelli ottenuti mediante vibrazioni estensionali, quando si tenga conto della notevole differenza tra le frequenze alle quali sono state effettuate le misure. Infine nelle curve dissipazione-temperatura relative all'alluminio, al magnesio, al rame, al ferro ed all'ottone, rilevate da S. T. Kê con vibrazioni torsionali di bassissima frequenza [8], [9], [10], oltre alla presenza di massimi abbastanza acuti dovuti a fenomeni di rilassamento, si nota anche un aumento graduale della dissipazione con la temperatura proprio dello stesso tipo di quello indicato dalle fig. 2, 3, 6.

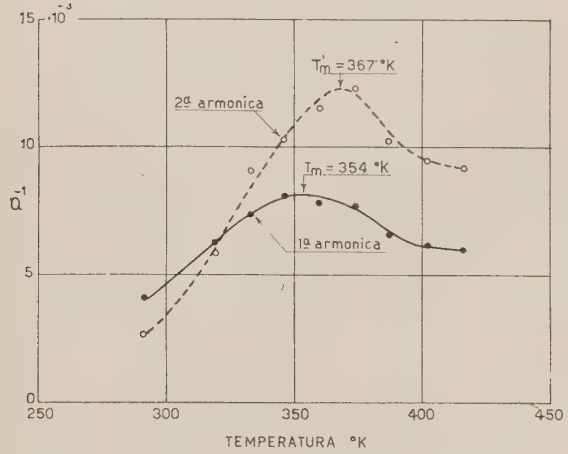

Fig. 5. – Spostamento verso le alte temperature della dissipazione massima al crescere della frequenza nella sbarretta n. 2. Prima armonica: frequenza a 354 °K = 13 592 Hz; seconda armonica: frequenza a 367 °K = 2 555 Hz.

Per ottenere una giustificazione teorica dell'accrescimento graduale di Q^{-1} con la temperatura che abbia un carattere abbastanza generale, come è richiesto dalle considerazioni precedenti, conviene innanzi tutto osservare che un aumento analogo è stato osservato anche in alcuni liquidi allo stato pseudo-solido in

corrispondenza alle temperature di transizione [14]. Come si è fatto in quel caso si può quindi ammettere che l'operatore differenziale che lega una sollecitazione di trazione o pressione semplice variabile nel tempo $\sigma(t)$ al coefficiente di deformazione $\varepsilon(t)$ relativo alla stessa direzione [10], si riduca, in assenza di forze di inerzia, al quoziente di due funzioni lineari di Δ, e che inoltre il numeratore sia privo di termine noto, cioè [14],

$$(4) \qquad \sigma(t) = E_U \frac{\tau\Delta}{1 + \tau\Delta} \varepsilon(t) ,$$

dove E_U è una costante avente le dimensioni di un modulo di elasticità; Δ rappresenta l'operazione di derivazione rispetto al tempo t; τ è una costante avente le dimensioni di un tempo.

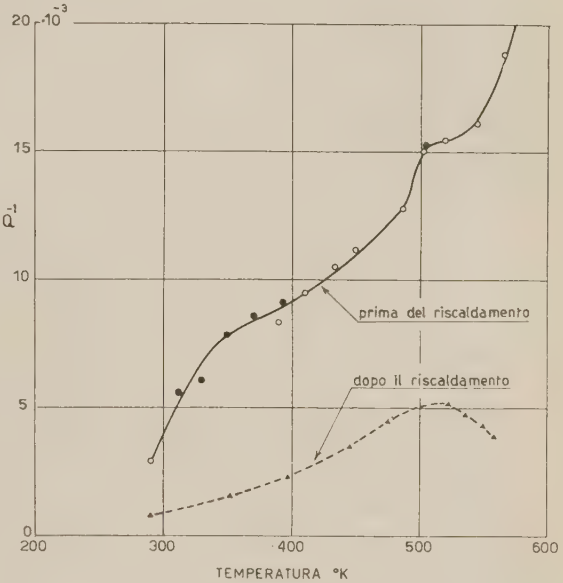

Fig. 6. – Dissipazione in funzione della temperatura nella sbarretta n. 3. ○ Prima serie di misure in discesa ($T \leqslant 584$ °K); ● seconda serie di misure in salita ($T \leqslant 504$ °K); ▲ terza serie di misure, in salita, dopo un trattamento di 3^h a 598 °K.

Se a partire dall'istante $t = 0$ si impone bruscamente al corpo una deformazione di ampiezza $\bar{\varepsilon}$ la quale resti costante in tutti gli istanti successivi, il teorema di espansione [10], [14] dà:

$$(5) \qquad \sigma(t) = E_U \bar{\varepsilon} \exp[-t/\tau] \ldots, \qquad t \geqslant 0 .$$

La costante E_U coincide quindi con il valore del modulo di trazione misurato immediatamente dopo l'applicazione della deformazione. Al crescere di t il secondo membro della (5) tende esponenzialmente a zero: nel semplice schema adottato si ha quindi rilassamento completo dello sforzo di tensione.

Se invece il coefficiente di deformazione varia sinusoidalmente rispetto al tempo, sostituendo nella (4) $\bar{\varepsilon} \exp[j\omega t]$ al posto di $\varepsilon(t)$ si ha:

$$(6) \qquad \sigma(t) = E_U \frac{j\omega\tau}{1 + j\omega\tau} \bar{\varepsilon} \exp[j\omega t] .$$

Il modulo di elasticità risulta quindi una grandezza complessa, dipendente dal prodotto $\omega\tau$, e la sollecitazione ha una componente « *in quadratura* »

rispetto alla deformazione, ed « *in fase* » con la velocità, dando così luogo ad ad una dissipazione di energia.

La (6) può essere direttamente applicata al calcolo del coefficiente di risonanza di un sistema ad un grado di libertà costituito da una sbarretta elastica, in cui la relazione tra lo stress sia del tipo (4), e le cui forze di inerzia siano trascurabili rispetto a quelle di una massa $\mathcal{M}$ ad essa collegata ed oscillante rigidamente. Si verifica facilmente che, in questo caso, l'inverso del coefficiente di risonanza è dato, a meno del fattore $1/\pi$ dal rapporto tra il coefficiente della parte immaginaria e la parte reale del modulo, cioè in base alla (6):

$$Q^{-1} = \frac{1}{\pi} \cdot \frac{1}{\omega\tau} . \tag{7}$$

La (7) risulta anche valida con ottima approssimazione nel caso di una sbarra sottile vibrante su uno dei suoi modi estensionali. Si può infatti osservare che anche quando la dissipazione è diversa da zero la distribuzione della velocità di vibrazione lungo la sbarra segue *sensibilmente* una legge sinusoidale, almeno finchè Q^{-1} è abbastanza piccolo rispetto all'unità. Adottando una simile distribuzione ci si riduce al caso di un sistema oscillante ad un grado di libertà già considerato, e di conseguenza Q^{-1} è ancora dato dalla (7). In base a quest'ultima relazione, in corrispondenza ad un valore assegnato della temperatura la dissipazione deve risultare funzione decrescente della frequenza. Le misure dei valori di Q^{-1} effettuati in corrispondenza alle prime tre armoniche della sbarretta n. 3, a temperatura ambiente (tabella II), mostrano che effettivamente Q^{-1} diminuisce al crescere della frequenza, ma in misura alquanto minore di quella che sarebbe richiesta dalla proporzionalità ad $1/\omega\tau$.

Tabella II.

Dissipazione in funzione della frequenza nella sbarretta n. 3 a temperatura ambiente.

Armonica	Frequenza Hz	Q^{-1}
1	12 564	$0{,}80 \cdot 10^{-3}$
2	24 262	0,68
3	35 170	0,53

Per esaurire le conseguenze della (4) conviene risolverla rispetto ad $\varepsilon(t)$ e supporre che, in corrispondenza all'istante $t = 0$, una sollecitazione di trazione o pressione semplice avente ampiezza costante σ sia bruscamente applicata

al corpo; la relativa deformazione è allora data da:

$$\varepsilon(t) = \frac{\bar{\sigma}}{E_U}\left(1 + \frac{t}{\tau}\right) \ldots , \qquad t \geqslant 0 . \tag{8}$$

e si compone quindi di una parte *elastica* σ/E_U che si produce immediatamente dopo l'applicazione dello stress, e di una *deformazione progressiva*, crescente linearmente nel tempo. Quest'ultimo tipo di deformazione è stato effettivamente riscontrato in diversi metalli ad alta temperatura [9], [15], [16], [17], [20], anche in corrispondenza a sforzi considerevolmente minori del limite di elasticità, ed è generalmente attribuito al moto delle dislocazioni preesistenti nel solido ed alla formazione di nuove dislocazioni. L'esperienza mostra inoltre che la curva che caratterizza al variare del tempo la deformazione prodotta da uno sforzo costante ha una pendenza $d\varepsilon/dt$ che cresce con la temperatura secondo una legge esponenziale del tipo [15],

$$\frac{d\varepsilon}{dt} = A \exp[-H/RT] , \tag{9}$$

dove A è una costante avente le dimensioni dell'inverso di un tempo; H è il calore di attivazione del fenomeno considerato (cal·mole^{-1}), ed R è la costante dei gas = 1,987 cal·grado^{-1}·mole^{-1}. Se si deriva la (8) rispetto al tempo e la si confronta con la (9), si ricava la legge di dipendenza del tempo caratteristico τ dalla temperatura.

$$\tau = \frac{\sigma}{AE_U} \exp[H/RT] . \tag{10}$$

Indicando per brevità con τ_0 la costante $\bar{\sigma}/AE_U$, che ha proprio le dimensioni di un tempo, e sostituendo nelle (7), (8), si hanno le relazioni

$$Q^{-1} = \frac{1}{\pi} \frac{\exp[-H/RT]}{\omega\tau_0} , \tag{11}$$

$$\varepsilon(t) = \frac{\sigma}{E_U}\left(1 + \frac{t}{\tau_0} \exp[-H/RT]\right) . \tag{12}$$

La (11) giustifica pienamente sotto l'aspetto qualitativo i risultati sperimentali indicati nelle figg. 2, 3, 6, in quanto mostra che per un valore sensibilmente costante della frequenza, la dissipazione deve risultare funzione *sempre crescente* della temperatura.

Si può inoltre osservare che la (11) e la (12) si presentano come conseguenze diverse, ma entrambe dirette, dell'ipotesi fondamentale (4) e della legge sperimentale (9). Viene così messo in evidenza — ed è questo il pregio essen-

ziale della semplice teoria proposta — l'intimo legame esistente tra l'aumento graduale della dissipazione che si verifica al crescere della temperatura, e la deformazione progressiva che si produce al passare del tempo sotto l'azione di una sollecitazione costante ed a temperatura costante. Sembra pertanto ragionevole attribuire, come ha fatto T. S. Kê, entrambi i fenomeni ad una stessa causa strutturale, e precisamente al moto delle dislocazioni.

In un precedente lavoro [1] si è mostrato come una parte delle dislocazioni prodotte in alcuni metalli (Pb, Cu, Al, Ag) da deformazioni di tipo permanente, possa muoversi a temperatura ambiente in un tempo assai breve sotto l'azione delle fluttuazioni statistiche dell'energia termica e di una sollecitazione meccanica. Infatti se si determina il modulo di trazione di questi metalli mediante sollecitazioni alternative aventi la frequenza di alcune decine di kHz, si trova che a temperatura ordinaria esso diminuisce per effetto di una deformazione permanente mentre aumenta in seguito ad un rinvenimento. Si è pure trovato che il moto delle dislocazioni diviene meno rapido quando la temperatura diminuisce, tanto che a 4,5 °K non si osserva più nessuna differenza tra il modulo di un metallo incrudito e quello dello stesso metallo dopo un rinvenimento. A conferma di questi risultati si è constatata l'esistenza di una temperatura intermedia alla quale il tempo associato al moto delle dislocazioni diviene paragonabile al periodo delle vibrazioni e di conseguenza la dissipazione raggiunge un massimo.

Evidentemente le dislocazioni che si muovono liberamente a temperatura ordinaria sono quelle associate ai valori più bassi delle barriere di potenziale, e costituiscono soltanto una piccola parte di tutte le dislocazioni preesistenti nel solido. Al crescere della temperatura aumenta anche il valore quadratico medio delle fluttuazioni locali dell'energia termica; di conseguenza, per un valore assegnato della sollecitazione massima e della frequenza di vibrazione, si possono muovere dislocazioni associate a barriere di potenziale sempre più elevate: aumenta quindi il *numero totale* delle dislocazioni in movimento ed insieme ad esso deve aumentare la dissipazione di energia elastica. Si può inoltre osservare che a temperatura elevata, anche con sollecitazioni molto piccole, la formazione di nuove dislocazioni può divenire abbastanza probabile, e ciò costituisce evidentemente un'ulteriore causa suscettibile di produrre un graduale aumento della dissipazione con la temperatura.

Le considerazioni precedenti mostrano che un aumento nel numero delle dislocazioni, prodotto da un preventivo incrudimento del materiale, deve provocare un corrispondente aumento sia nella dissipazione, sia nella rapidità con cui ha luogo la deformazione progressiva: entrambi questi effetti sono stati ripetutamente osservati [9], [16], [18], [20]. Inversamente la diminuzione permanente nella dissipazione che ha luogo in seguito ad un riscaldamento prolungato (figg. 3, 6) può essere fondatamente attribuita ad una diminuzione nel numero delle dislocazioni, o ad una riduzione della loro mobilità.

Le curve sperimentali delle fig. 5, 6 oltre a mostrare il graduale aumento della dissipazione che è stato sinora discusso, presentano anche dei massimi poco accentuati.

Se si ammette che i relativi tempi caratteristici variino con la temperatura secondo una legge del tipo della (10), come generalmente avviene per quasi tutti i fenomeni di rilassamento, il confronto tra i valori T_1 e T_2 della temperatura in corrispondenza ai quali l'assorbimento diviene massimo alle frequenze ν_1 e ν_2 consente di calcolare il calore di attivazione H mediante la formula

$$H = 2{,}30 \frac{R \log \frac{\nu_2}{\nu_1}}{\frac{1}{T_1} - \frac{1}{T_2}} . \tag{13}$$

Sostituendo nella (13) i valori che si ricavano dalla fig. 5, si trova $H \approx 14\,000$ cal·mole^{-1}; tale valore è abbastanza prossimo al calore di attivazione della diffusione di alcuni metalli nel piombo [9]. Si ha infatti per l'oro $H = 13\,000$ cal·mole^{-1}; per il bismuto $H = 18\,000$ cal·mole^{-1}. Sembra quindi probabile che il massimo osservato sia dovuto alla presenza di impurità.

Quanto all'altro massimo che si produce a temperatura più elevata (fig. 6) è probabile che si tratti di quello stesso osservato da I. Barducci a 463 °K con una frequenza di circa 750 Hz. Sostituendo questi valori nella (13), insieme con quelli forniti dalla fig. 6, si trova $H = 30\,000$ cal·mole. Tale valore è abbastanza prossimo a quello associato con i fenomeni di diffusione piombo-piombo e ciò sembra confermare l'ipotesi fatta dall'autore citato che attribuisce il massimo al rilassamento degli sforzi di taglio sulla superficie dei grani cristallini.

5. – Conclusioni.

La dissipazione che accompagna la propagazione di onde elastiche estensionali nel piombo puro aumenta al crescere della temperatura nell'intervallo 300-600 °K ed al diminuire della frequenza nel campo compreso tra 10 e 10 kHz.

Considerazioni di carattere teorico mostrano che tale comportamento è intimamente legato al noto fenomeno della deformazione progressiva (*creep*) che si produce ad alta temperatura sotto l'azione di una sollecitazione costante. Per i valori indicati della temperatura e della frequenza la dissipazione sembra quindi prevalentemente dovuta alla stessa causa che produce la deformazione progressiva, e cioè al moto di un numero crescente di dislocazioni al crescere della temperatura.

BIBLIOGRAFIA

[1] P. G. Bordoni: *Ric. Scient.*, **23**, 1193 (1953).

[2] P. G. Bordoni e M. Nuovo: *Nuovo Cimento*, **10**, 386 (1953); *Ric. Scient.*, **23**, 593 (1953).

[3] P. G. Bordoni: *Rend. Acc. Naz. Lincei*, **6**, 597 (1949).

[4] P. G. Bordoni: *Nuovo Cimento*, **10**, 268 (1953).

[5] P. G. Bordoni: *Ric. Scient.*, **19**, 851 (1949).

[6] I. Barducci: *Ric. Scient.*, **22**, 1733 (1952).

[7] P. G. Bordoni e M. Nuovo: *Nuovo Cimento, Suppl.* n. 2, **7**, 161 (1950).

[8] T. S. Kê: *Phys. Rev.*, **72**, 41 (1947).

[9] C. Zener: *Elasticity and anelasticity of metals* (Chicago, 1948), cap. VI.

[10] P. G. Bordoni: *Nuovo Cimento, Suppl.* n. 2, **7**, 144 (1950).

[11] E. Heidemann: *Grundlagen und Ergebnisse der Ultraschallforschung* (Berlin, 1939) cap. III, n. 3.

[12] P. G. Bordoni: *Nuovo Cimento*, **4**, 177 (1947).

[13] P. G. Bordoni e M. Nuovo: *Généralisation d'une méthode électrostatique pour la mesure ultrasonore des constantes élastiques et anélastiques des solides* (in corso di pubblicazione sugli *Atti dell'International Electro-Acoustic Congress*, Delft, (1953).

[14] P. G. Bordoni e M. Nuovo: *Ultrasonic absorption in the pseudo solid state of liquids.* « Colloque International sur les ultrasons dans les gaz et les liquides » Bruxelles, Juin 1951), publié par la Koninklijke Vlaamse Akademie voor Wetenschappen, Letteren en Schone Kunsten van Belgie, p. 164.

[15] F. Seitz: *The physics of metals* (New York, 1943) 1ª ediz., cap. IX, X.

[16] G. E. Doan e E. M. Mahla: *The principles of physical metallurgy* (New York, 1941), 2ª ediz., cap. III.

[17] W. Boas: *Physics of metals and alloys.* (New York, 1947), 1ª ediz., cap. III, nn. 16, 22.

[18] W. G. Burgers: *Handbuch der Metallphysik* (Leipzig, 1941), p. 504.

[19] I. Barducci: *Frottement interne du Plomb à haute température* (in corso di pubblicazione sui *Compt. Rend.*).

[20] T. S. Kê: *Journ. Appl. Phys.*, **21**, 414 (1950).

SUMMARY

The elastic and anelastic behaviour of lead was investigated in previous papers by the authors [1], [2] and the experimental data have been explained from a theorethical standpoint, according to the statistical theory of solids [3], [4], [5], [10]. The damping of extensional vibrations has now been measured in the range from 10 to 40 kHz and for temperatures between 300 °K and 600 °K with the same electrostatic method formerly described [12] and recently improved [13] which was employed in previous experimental research [1], [2], [14]. Damping has been evaluated by means of the inverse value of the resonance coefficient Q. It was found that Q^{-1} increases continuously with increasing temperatures, from values of $3 \div 5 \cdot 10^{-3}$ up to $15 \div 20 \cdot 10^{-3}$

(fig. 3, 6); for a given temperature Q^{-1} decreases with increasing frequency. The experimental runs can be repeated if the maximum temperature does not exceed $520 \div 540$ °K. When the lead sample is kept at higher temperatures for several hours, a permanent decrease in Q^{-1} is found in the whole temperature range. The damping vs. temperature curve, besides the steady rise, shows also two small bumps at about 360 °K and 505 °K; the first one is displaced towards higher temperatures by a rise in frequency (fig. 5). To explain the gradual increase in Q^{-1} with temperature it has been observed that a similar behaviour is exhibited by liquids in the pseudo-solid state [14] for which the stress-strain relation is of the type (4), when both are considered as functions of time [10], [14]. This relation has been applied to a steady sinusoidal stress and to a constant one, suddenly applied at time zero. In the first case Young's modulus is a complex number, according to (6); moreover equation (7) shows that damping increases when frequency decreases, in agreement with the experimental results shown in Table II. In the second case it has been found that a fixed stress gives raise to creep, which adds to the true elastic strain, as it is shown by (8). This result agrees with the previous one and with the experimental data: the creep rate has been observed to change with temperature according to equation (9), substituting it in (6) damping is found to increase with temperature, as it is pointed out by (11) and as can be seen from figures 2, 3, 6. The above theory shows that the rise in Q^{-1} with temperature and creep are only two sides of the same phenomenon, that is the motion of number of dislocations which increases together with temperature. An attempt is also made to evaluate the activation energy associated with the two flat maxima shown by the experimental curve, and the values of 14 000 and 30 000 cal mole^{-1} are found; the latter, being very near to the diffusion energy of lead atoms in lead, seems to point out that the relaxation observed is due to the viscous behaviour of grain boundaries.

IL NUOVO CIMENTO Vol. XI, N. 2 1° Febbraio 1954

Non Perturbation Treatment of Scattering in Quantum Field Theory.

M. Cini and S. Fubini

Istituto di Fisica dell'Università - Torino
Istituto Nazionale di Fisica Nucleare - Sezione di Torino

(ricevuto il 24 Novembre 1953)

Summary. — A sequence of approximations to the S and K operators is obtained by means of a variational method. The form of the approximations is such that discussions on general questions like convergence and renormalization become possible without any weak coupling assumption. The method is particularly suited for the study of two body collision problems: in this case the difficulties in the treatment of the higher order approximations are reduced to the problem of evaluating the perturbation S-matrix elements.

1. – Introduction.

It is well known that, owing to the large value of the coupling constant, the perturbation expansion of the S matrix does not give results in agreement with experiment in problems involving meson fields, such as nucleon-nucleon and pion-nucleon scattering. Different approaches have been proposed to take somehow into account the reaction effects of the interacting particles, independently from any weak coupling assumption. The first one, originally proposed by Tamm and Dancoff [1] for the proton neutron system, consists in assuming that all representatives of the wave function with more than a given number Q of particles are equal to zero. The fundamental hypothesis is that, if Q is sufficiently large, the results of the calculations will be insen-

[1] I. Tamm: *Journ. Phys. (USSR)*, **9**, 449 (1945); S. M. Dancoff: *Phys. Rev.*, **78**, 382 (1950) in the following denoted as T.D.method.

sitive to the value of Q and will tend to a limit as Q tends to infinity ([2]). The T.D. method has been used, in the lowest approximation, to study the $T = 3/2$ pion-nucleon scattering with a substantial improvement in comparison with the weak coupling results ([3-5]).

Against this procedure one can raise the criticism that it is practically impossible to apply the method consistently in higher order approximations, because one gets coupled integral equations which must not be solved by iteration.

Furthermore in this method it seems impossible to treat the radiative processes without making an expansion in powers of g. For this reason an alternative four-dimensional formulation has been originally introduced by SALPETER and BETHE ([6]) for the two nucleons problem in which integral equations are deduced for Feynman kernels. This method is appropriate for the study of the $T = 1/2$ pion-nucleon scattering in which divergent contributions must be eliminated by means of renormalization. Owing to the circumstance that in lowest order no four dimensional integration appears, the calculations can be performed, and also in this case reasonable results are found ([7-9]). Nevertheless when one has to deal with the integral equations, the presence of singular functions in the kernel discourages any attempt of solution. Furthermore, when after renormalisation the « bare » propagators S_F and D_F are replaced in the integrals with the modified propagators S_F' and D_F', the new unphysical poles of these functions give rise to new infinities which cause serious troubles for the consistency of the theory ([10]).

A non-perturbation approach to scattering problems which overcomes some of the difficulties outlined above is the one proposed in this paper. With the

([2]) For a full discussion of this question and of the relationship between the « proper T.D. method » and the Lévy-Klein method ([2a]), see F. J. DYSON: *Phys. Rev.*, **91**, 1543 (1953).

([2a]) M. M. LEVY: *Phys. Rev.*, **88**, 72, 725 (1952); A. KLEIN: *Phys. Rev.*, **90**, 1101 (1953); **91**, 740 (1953).

([3]) G. CHEW: *Phys. Rev.*, **89**, 591 (1953).

([4]) F. J. DYSON, S. S. SCHWEBER and W. M. VISSHER: *Phys. Rev.*, **90**, 372 (A) (1953) and *Proceedings Third Annual Rochester Meeting*, Dec. 1952, pag. 78.

([5]) S. FUBINI: *Nuovo Cimento*, **10**, 564 (1953).

([6]) E. SALPETER and H. A. BETHE: *Phys. Rev.*, **84**, 1232 (1951).

([7]) A. K. BRUCKNER, M. GELL-MANN and M. GOLDBERGER: *Phys. Rev.*, **90**, 476 (1953).

([8]) R. KARPLUS, M. KIVELSON and P. C. MARTIN: *Phys. Rev.*, **90**, 1072 (1953).

([9]) S. FUBINI: *Nuovo Cimento*, **10**, 851 (1953).

([10]) G. FELDMAN: *Modified Propagators in Field Theory* – preprint. We are indebted to Dr. FELDMAN who sent to us a prepublication copy of his work.

use of a variational principle proposed by LIPPMANN and SCHWINGER ([11]) and the same «ansatz» introduced in a previous paper ([12]) we obtain a sequence of approximations to the K reaction operator in which at each stage only a limited number of mesons and pairs is taken into account.

The variational principle is chosen in such a way that each approximation for K remains Hermitian, thus insuring the unitarity of the S matrix. Any given approximation $K^{(n)}$ to K is determined by a set of linear operator equations involving only the terms K_i of the perturbation expansion of K. A corresponding approximation $S^{(n)}$ for the S matrix can be derived from the preceding $K^{(n)}$ and involves only the terms S_i of the perturbation expansion of S. The divergent contributions are handled by means of a prescription which makes use of the analysis of DYSON and MATTHEWS and reduces to the usual procedure of renormalization for small values of the coupling constant. This renormalization procedure is not subject to the criticism raised against the B.S. method, because no four dimensional integration involving the modified propagators S'_F and D'_F appears.

The operator equations defining $K^{(n)}$ or $S^{(n)}$ can be easily solved for the two body collisions by introducing a suitable representation in which the constants of the collision are made simultaneously diagonal. Thus, in most of the physical interesting cases, the difficulties met in the methods previously discussed in the treatment of higher order approximations are here reduced to the numerical problem of evaluating, e.g. by means of Feynman-Dyson techniques, the perturbation S matrix elements.

2. – The sequence of approximations to the K and S operators.

We will introduce the well known field operators $V(t)$ and K given by:

$$V(t) = 1 - i\int_{-\infty}^{+\infty} H(t')V(t')\varepsilon(t-t')\,dt', \tag{1}$$

where

$$\varepsilon(t-t') = \begin{cases} \frac{1}{2} & t > t' \\ -\frac{1}{2} & t < t' \end{cases},$$

([11]) B. A. LIPPMANN and J. SCHWINGER: *Phys. Rev.*, **79**, 569 (1950), denoted in the following as LS. See also: M. CINI and L. A. RADICATI: *Nuovo Cimento*, **7**, 905 (1950) and M. CINI: *Nuovo Cimento*, **7**, 910 (1950).

([12]) M. CINI and S. FUBINI: *Nuovo Cimento*, **10**, 1695 (1953), hereafter denoted as I.

and

$$K = \int_{-\infty}^{+\infty} H(t')V(t')\,\mathrm{d}t' . \tag{2}$$

The iteration of equation (1) yields the two power series in g

$$V(t) = 1 + V_1(t) + V_2(t) + \ldots + V_i(t) + \ldots \tag{1'}$$

$$K = K_1 + K_2 + \ldots + K_i - \ldots \tag{2'}$$

where the suffix i denotes the power of g in each term.

The S matrix is expressed in terms of K by means of:

$$S = \frac{1 - (i/2)K}{1 + (i/2)K} . \tag{3}$$

LIPPMANN and SCHWINGER have shown that, if we define K' by means of [13]

$$K' = \int_{-\infty}^{+\infty} \Big\{ H(t)V(t) + V^*(t)H(t) - V^*(t)H(t)V(t) - \\ - i\int_{-\infty}^{-\infty} \mathrm{d}t'\, V^*(t)H(t)H(t')V(t')\varepsilon(t-t') \Big\}\,\mathrm{d}t, \tag{4}$$

then K' is stationary and equal to K when $V(t)$ satisfies eq. (1).

We introduce in eq. (4) a variational « ansatz » analogous to the one used in I, given by:

$$V(t) = A_1 + V_1(t)A_2 + \ldots + V_{n-1}(t)A_n , \tag{5}$$

with A_l time independent operators. Then eq. (4) becomes

$$K' = \sum_{i=1}^{n} \big\{ K_i A_i + A_i^* K_i - \sum_{k=1}^{n} A_i^* (K_{i+k-1} - K_{i+k}) A_k \big\} . \tag{6}$$

Our n-th approximation $K^{(n)}$ is obtained by introducing in eq. (6) those values $A_l^{(n)}$ of A_l which make the variation K' vanish. Thus we get:

$$K_i = \sum_{k=1}^{n} (K_{i+k-1} - K_{i+k}) A_k^{(n)} \qquad 1 \leqslant i \leqslant n, \tag{7}$$

$$K^{(n)} = \sum_{i=1}^{n} K_i A_i^{(n)} \tag{8}$$

[13] We notice that our $\varepsilon(t-t')$ differs by a factor 1/2 from the same quantity defined in LS.

or, in a more symmetrical form [14]

$$K^{(n)} = \sum_{k=1}^{i} K_k + \sum_{k=1}^{n} K_{k+i} A_k^{(n)} \qquad 0 \leqslant i \leqslant n. \tag{7'}$$

The operator $K^{(n)}$ defined by these equations is obviously Hermitian.

It is apparent that, in the general case the solution of the system (7') is by no means simple since the K_i are operators in second quantization connecting states with different number of particles. The important point is, nevertheless, that all the matrices K_i connect states with equal energy. This property limits considerably, in the general case, the available states, and allows one to obtain a simple solution in all the two body problems.

In order to be able to make use of the well known techniques developed by FEYNMAN, DYSON and WICK it is convenient to introduce the terms of the perturbation expansion of the S matrix. The expansion analogous to (2') is

$$S = 1 + S_1 + S_2 + \ldots + S_i + \ldots . \tag{9}$$

The introduction of the series (2') and (9) in eq. (3) yields:

$$2iS_r = \sum_{k=1}^{r-1} K_k S_{r-k} + 2K_r \qquad 1 \leqslant r \leqslant 2n. \tag{10}$$

Definining the n-th order approximation of the S matrix by means of:

$$S^{(n)} = \frac{1 - (i/2)K^{(n)}}{1 + (i/2)K^{(n)}}, \tag{11}$$

we obtain, with the help of (10) as shown in Appendix, the following system for $S^{(n)}$ [15]:

$$S^{(n)} = \sum_{k=0}^{i} S_k + \sum_{k=1}^{n} S_{k+i} \Gamma_k^{(n)} \qquad 0 \leqslant i \leqslant n. \tag{12}$$

It is noteworthy that $S^{(n)}$ (which, as a consequence of eq. (11), is unitary) is obtained in our method by the same system which gives $K^{(n)}$ simply by replacing the perturbation terms K_i of K with the perturbation terms S_i of S. One might think that this result would follow simply by introducing a convenient « ansatz » in the variational principle (L.S. 1.21): this is not the case because the unitarity of S is not preserved by that variational principle.

[14] Eqs. (7') form a system of $n+1$ equations in the $n+1$ variables $K^{(n)}$, $A_k^{(n)}$.
[15] Obviously $S_0 = 1$, while $K_0 = 0$.

3. – The treatment of divergent contributions.

The terms S_k appearing in the system (12) contain the well known divergent contributions. With the purpose of making use of standard mass and coupling constant renormalization procedure ([16]) we perform the following transformation on the $\Gamma_k^{(n)}$. Let us introduce $n+1$ operators $\Delta_l^{(n)}$ defined by

$$\Gamma_k^{(n)} = \sum_{l=k}^{n} \Delta_l^{(n)}, \qquad 1 = \sum_{l=0}^{n} \Delta_l^{(n)} \tag{13}$$

then eqs. (12) become

$$S^{(n)} = \sum_{l=0}^{n} \sigma_{i-l} \Delta_l^{(n)} \qquad 0 \leqslant i \leqslant n \tag{14}$$

where

$$\sigma_i = \sum_{l=0}^{i} S_l \,. \tag{15}$$

Our prescription for the elimination of the divergences arising from radiative processes is simply to use the standard procedure of renormalization in all the σ_i ([17]). Denoting with σ_i' and S_l' the convergent remainder (after renormalizations have been performed) of σ_i and S_l it is easy to go back to a form analogous to (12):

$$S^{(n)'} = \sum_{k=0}^{i} S_k' + \sum_{k=1}^{n} S_{k+i}' \Gamma_k^{(n)} \qquad 0 \leqslant i \leqslant n. \tag{16}$$

By making use of the relations

$$\sum_{r=0}^{k} S_r' S_{k-r}'^{*} = 0 \qquad r \geqslant 0 \tag{17}$$

([16]) F. J. Dyson: *Phys. Rev.*, **75**, 1736 (1949); P. T. Matthews: *Phil. Mag.*, **41**, 185 (1950).

([17]) We have not been able to define the renormalized constants otherwise than by means of the usual power series in g. This is unsatisfactory from a conceptual point of view because in the same approximation $S^{(n)}$, different perturbation approximations of these constants appear contained in the different σ_i.

which follow from the unitarity of the renormalized power series ([18])

$$1 + S_1' + \ldots + S_i' + \ldots \tag{18}$$

it turns out that all the approximations $S^{(n)'}$ are unitary.

We will see that there are good reasons for believing that, for for values of g such that the series (18) diverges, the sequence of $S^{(n)'}$ defined by (16) still converges. It is clear that our prescription (which we assume to be valid whenever the sequence converges) is unambiguous and that the limit of the sequence coincides with the limit of the renormalized power series (18) for values of the coupling constant for which (18) converges. A support to the consistency of the renormalization procedure may also be found in a recent investigation by FERRETTI ([19]) who has shown that the expansion in power series of g is not a necessary condition for the validity of the renormalization procedure.

4. – Application to two-body collisions.

We want to show in this section, that for the two-body collisions the system (16) can be reduced to a very simple form and easily solved by introducing a suitable representation. As we have pointed above our equations, in contrast with those of the T.D. method, contain only matrix elements between states with equal energy. Therefore the study of a collision between two particles, whose kinetic energy in the c.m. system is below the threshold for the production of a new particle, involves only the variables of these two particles ([20]). In these collisions the total energy E, the total angular momentum J with its component J_z, the parity P and the total isotopic spin T with its component T_z, commute with all the S_i'. The choice of a representation in which all these operators are simultaneously diagonal simplifies considerably the system (16).

In the particular case of nucleon-nucleon scattering also the total spin S is a good quantum number. Then for the singlet collision ($S = 0$) E, J and T determine completely the states and equations (16) reduce to a numerical system of equations. In the triplet collisions ($S = 1$) we may have

([18]) The relations (17) derived with the assumption that the series (18) converges for sufficiently small values of g, are independent from the magnitude of the coupling constant.

([19]) B. FERRETTI: *Nuovo Cimento*, **10**, 1079 (1953).

([20]) For example the treatment of nucleon nucleon scattering with our method at energies below the threshold for pion production is essentially different from that at higher energies.

$L = J+1;\ J;\ J-1$. Because of parity conservation the state $L = J$ combines only with itself and not with $L = J \pm 1$: thus eqs. (16) split into a numerical system and a system between two-by-two matrices.

In the case of pion nucleon scattering we have $L = J \pm 1/2$: for the same parity reasons these two states do not combine and eqs. (16) reduce to a numerical system.

Following this procedure the lowest approximation for the S matrix elements is found to be

$$\langle \alpha\ S|\alpha\rangle = 1 + \langle \alpha|\, S_2'|\,\alpha\rangle \frac{\langle \alpha|\, S_2'|\,\alpha\rangle}{\langle \alpha|\,(S_2' - S_4')|\,\alpha\rangle}\,, \tag{19}$$

where $|\alpha\rangle$ denotes shortly the eingestate of E, J, L, T.

It is worthwhile to notice that the two cases of isotopic spin $T = 1/2$ and $T = 3/2$ are treated on the same footing. This is important in connection with the study of photoproduction of pions, since the isotopic spin is not a good quantum number: thus far no consistent treatment of this problem was available.

5. – Discussion.

The form of the sequence of approximations given by our method for the K and S matrices is such that discussions on some general features of the theory, like convergence and renormalization, become possible without any weak coupling assumption. The first requirement for the validity of our method is that, for sufficiently small values of g the perturbation expansion of S is convergent or at least semiconvergent. This seems plausible in analogy with the case of electrodynamics.

We have a conducted preliminary investigation in the case in which the divergence of the power series in g for the value $g = G$ corresponding to the physical meson field is assumed to be due to a finite number of poles in the complex plane of g for $|g| < G$. The result is that in this case our sequence of approximations is convergent. (Clearly if the power series for small values of g is semiconvergent only the first terms of our sequence will decrease). The assumption previously stated is closely related to the physical assumption that the failure of perturbation theory in mesodynamics compared with electrodynamics depends only on the existence of isobaric states which may lead to resonances in the scattering cross-sections.

In what concerns renormalization, from the form of eq. (16) it is clear that the separation of the finite parts from the divergent graphs is unambiguous and that the divergent parts can be absorbed in suitable lowest order diagrams.

The question of defining new renormalized constants gives rise to some difficulties of principle. Namely we have to use the definition of these constants as power series given by Dyson which does not fit satisfactorily in the framework of the method.

The present method allows also to derive an approximate expression for the operator $V(t)$, although less reliable than the approximation for K. This happens because K is made stationary by our variational principle while $V(t)$ is only the « best value » of the « trial function ». We notice that the reasons referred above for the convergence of the sequence $K^{(n)}$ do not hold for the sequence $V^{(n)}$. The fact that here the operators on the energy shell K and S are placed in a privileged position does not seem to us a disadvantage of the present method, considering the difficulties connected with the concept of relativistic wave functions in field theory ([21]).

For the application to practical calculations the present method is particularly suited to the two body scattering problems. The lowest approximation requires the evaluation of the elements S_2 and S_4 of the perturbation expansion of S. The following approximation involves S_6 and S_8 and so on. Anyone acquainted with calculations of radiative corrections using the methods available at present realizes the computational difficulties that will be met. Nevertheless these difficulties are not even comparable with the formidable task of solving the set of coupled integral equations appearing in other non-perturbation methods. One may also hope that the order of magnitude of the higher order terms could be estimated by means of some qualitative arguments analogous to those used by KLEIN and LÉVY ([2a]).

The contributions to a given S_n arising from the different graphs can be classified, at least for convergent parts, according to the following considerations:

a) The contribution is larger when the maximum number of γ_5 creates or annihilates nucleon pairs.

b) The contribution is larger when the maximum number of intermediate states contain as many particles as the initial state.

Obviously this procedure is reliable only when the selected contributions do not cancel in the denominators, namely in conditions far from resonance.

As an example we see that for $T = 3/2$ pion-nucleon scattering our lowest approximation (19) can be reduced to a very simple form since in S_4 only one

([21]) F. J. DYSON: *Phys. Rev.*, **91**, 1543 (1953).

graph fulfills at the same time both conditions *a*) and *b*) ([22]). This very crude solution possesses already many of the satisfactory features of the results obtained by means of T.D. method ([3]) ([23]).

The situation is rather different in the case of nucleon-nucleon scattering, because in S_4 we find that some contributions fulfil condition *a*) and some condition *b*), but none satisfies both simultaneously. For this reason we can expect that the results of our lowest approximation for this problem will differ substantially from the solution of the lowest order T.D. integral equation.

Appendix

We rewrite the system (7′) introducing a new set of $2n$ operators L_k, defined as follows:

$$\text{(1.A)} \qquad \begin{cases} L_k = 1 & 1 \leqslant k \leqslant n \\ L_k = A^{(n)}_{k-n} & n+1 \leqslant k \leqslant 2n\,, \end{cases}$$

then (7′) becomes

$$\text{(2.A)} \qquad \begin{cases} K^{(n)} = \sum_{k=1}^{n+i} K_k L_{k+n-i} & 0 \leqslant i \leqslant n \\ 1 = L_{n-i} & 0 \leqslant i \leqslant n-1. \end{cases}$$

Now we define the new variables J_k by means of

$$\text{(3.A)} \qquad L_{n-j} = \sum_{l=1}^{n+j} S_l J_{l+n-j} + 2J_{n-j} \qquad -n \leqslant j \leqslant +n\,.$$

Eqs. (2.A) become, in terms of these variables, and with the use of eq. (10):

$$\text{(4.A)} \qquad \begin{aligned} K^{(n)} &= 2i \sum_{k=1}^{n+i} S_k J_{k+n-i} && 0 \leqslant i \leqslant n \\ 1 &= 2J_{n-i} + \sum_{k=1}^{n+i} S_k J_{k+n-1} && 0 \leqslant i \leqslant n-1\,. \end{aligned}$$

([22]) The selection according to condition *a*) is valid for matrix elements of S between eigenstates of momentum, and one must be careful when the representation of eigenstates of angular momentum is chosen: when all the γ_5 annihilate pairs, for example, the graph contributes only to S waves.

([23]) *Note added in proof.* – Dr. H. R. Dalitz has kindly referred to us an interesting remark of Dr. M. Goldberger. It can be shown that in the Thomson limit, and when μ/M (ratio of the meson to the nucleon mass) is made to approach zero, the correct phases for the $T = 1/2$ and $T = 3/2$ pion-nucleon scattering must become equal. This condition is not satisfied by the solutions of the T.D. and B.S. equations, but is instead fulfilled at any order by the terms of our sequence.

From these one obtains immediately

$$1 + \frac{i}{2} K^{(n)} = 2J_{n-i} \,. \qquad 0 \leqslant i \leqslant n-1 \,. \tag{5.A}$$

Finally defining

$$G_{n-i} = 2J_{n-i}\left(1 + \frac{i}{2} K^{(n)}\right)^{-1}, \tag{6.A}$$

the following system follows immediately

$$\begin{cases} S^{(n)} = 1 + \sum_{k=1}^{n+i} S_k G_{k+n-i} & 0 \leqslant i \leqslant n \\ 1 = G_{n-i} & 0 \leqslant i \leqslant n-1 \end{cases} \tag{7.A}$$

which determines completely $S^{(n)}$.

This is the equivalent of the system (2A) for $K^{(n)}$ and can be written in the form (12) by setting

$$G_k = \Gamma^{(n)}_{k-n} \qquad n+1 \leqslant k \leqslant 2n \,. \tag{8.A}$$

RIASSUNTO

Si ottiene per mezzo di un principio variazionale una successione di approssimazioni non perturbative per gli operatori K ed S. La forma delle approssimazioni successive è tale che sono possibili discussioni generali sulla convergenza e sulla rinormalizzazione del metodo senza far ricorso ad alcuna ipotesi sulla grandezza della costante di accoppiamento. Il metodo è particolarmente adatto allo studio dei problemi di collisione fra due corpi: in questo caso le difficoltà per la valutazione delle approssimazioni di ordine più elevato si riducono al calcolo di elementi di matrice S perturbativi.

A Stable High Speed Multichannel Pulse Analyzer.

E. Gatti
Laboratori CISE - Milano

(ricevuto il 30 Novembre 1953)

Summary. — A twenty channel pulse analyzer with a resolving power of 3 μs is described. Its chief feature is that pulse selection is accomplished by a single discriminator for each channel whose threshold is set at a height corresponding to the upper boundary of the channel and the channel width is determinated by suitably shaping the incoming pulses.

The problem of pulse amplitude analysis has acquired increased importance and has been widely investigated in the last few years.

In the literature have been described several new instruments: ([1,2]) and bibl. of ([6]); and have appeared many reviews of the features of the problem and of the solutions and instruments already developed ([3-6]).

The reader is referred to those papers for a general statement of the problem; in the present paper we are only concerned with the description of a new instrument.

Principle of operation.

The principle of operation of the present pulse analyser is, we believe, entirely new, and is a further elaboration of a method proposed by the author in collaboration with F. Piva, in a preliminary note ([7]).

([1]) E. Breitenberger: *Phil. Mag.*, **44**, 987 (1953).
([2]) H. Guillon: *Journ. de Phys. et le Rad.*, **14**, 128 (1953).
([3]) J. H. Parsons: *P.I.R.E.*, **37**, 564 (1949).
([4]) A. B. Van Runnes: *Nucleonics*, July 1952, p. 20; Aug. 1952, p. 22; Sept. 1952, p. 32; Oct. 1952, p. 50.
([5]) G. W. Hutchinson: *Nucleonics*, February 1953, p. 24.
([6]) E. Balndinger and W. Haeberly: *Ergebn. d. exacten Naturwiss.*, **27**, 248 (1953).
([7]) E. Gatti and F. Piva: *Nuovo Cimento*, **10**, 984 (1953).

The classification of the pulses in the different channels is accomplished by a single discriminator for each channel, instead of two having thresholds corresponding to the boundaries of the channel, as done in conventional types of fast pulse analysers.

The use of a single discriminator for each channel is made possible through a shaping of the incoming pulses so that they are made to carry an element containing the information relative to the channel width, while preserving the original information relative to the height of the pulse itself. Then the thresholds of the discriminators need only to define the position of the channels, no more their width.

In this way two interesting features are obtained: fluctuations on threshold values do not influence any more the width of channels but only their position, and the width is constant for all channels because it is defined through a single physical system, that is the pulse-shaper circuit.

Actually (fig. 1) the incoming pulse having height V (fig. 1 no. 1) is first squared preserving its height (fig. 1 no. 3), then, and with a suitable delay, a standard square pulse of height d (henceforth called calibrated pulse) is added on the top (fig. 1 no. 7). This composite pulse is fed to the discriminators. The output of each of them, suitably differentiated, is brought to a coincidence circuit, one for each channel, together with a square pulse sincronous with the calibrated pulse. Then a pulse appears at the output of a coincidence only when the corresponding discriminator has been triggered by the step of height d on the top of the shaped pulse. Therefore, in a channel whose discriminator has the threshold level set at V_0 volts, are recorded only those pulses that have a height lying between $V_0 - d$ and V_0 volts.

Functional Arrangement.

The block diagram and associated waveforms for the complete instrument are given in fig. 1.

Waveforms are drawn for two typical input events, that is for a single pulse in row I and for a pair of pulses spaced 4 μs apart in row II. The single blocks are defined in fig. 1 *a*) through their operational function. As shown, some blocks are « gated », that is they perform two different operations depending on whether or not a « gate pulse » is applied.

The operation of the complete instrument can be seen easily by direct inspection of the block diagram and its associated waveforms and captions, therefore we think unnecessary to make here a detailed description of the whole performance and we limit ourselves to describe the less obvious features.

Pulse lengthener *PL* shapes the incoming pulse of height V and gives it

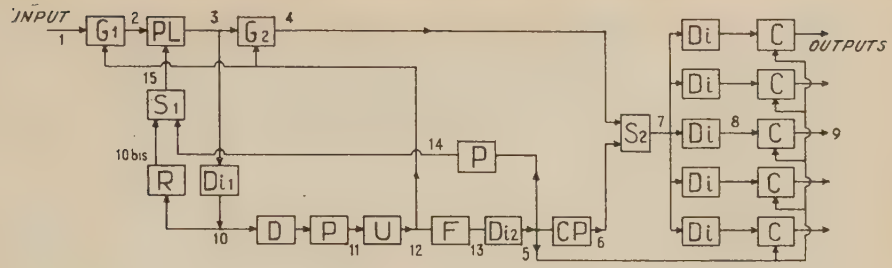

Fig. 1. – a) *Definition of blocks.*

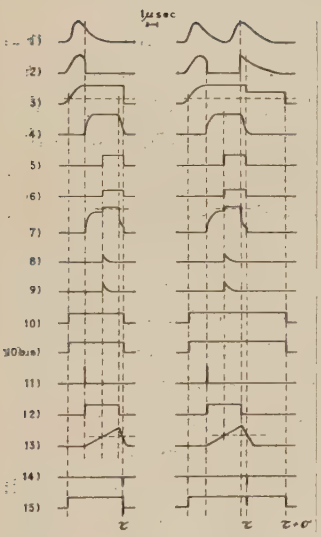

Abbreviation	*Name*	*Gate pulse*	*Functional behaviour*
G_1	Gate	V_{12} { absent / present	$V_2 = V_1$ / $V_2 = 0$
PL	Pulse lengthener	V_{15} { absent / present	$V_3 = V_2$ / $V_3(t) =$ to the largest value of V_2 in the interval beginning with the presence of V_{15} and ending with t.
G_2	Gate	V_{12} { absent / pre-ent	$V_4 = 0$ / $V_4 = V_3$
U	Univibrator	V_{11}	Generates a square standard pulse of 3μs having leading edge coincident with V_{11}.
R	Reset		$V_{10\,bis} = V_{10}$ but if V_{10} stays > 0 for more than 8 μs, $V_{10\,bis}$ recovers to 0.
F	Forming circuit		It converts the square pulse 12 into a triangular one: 13.
CP	Calibrated pulse generator	V_5	It generates an amplitude calibrated pulse sincronous with V_5.
p	Differentiators		
Di_1, Di_2, Di	Threshold discriminators		
S_1, S_2	Summing circuits		
C	Coincidence circuits		

b) *Waveforms (rows I and II).*

1) Input pulse. 2) Input pulse after the action of gate G_1 which is driven from « gate pulse » 12. 3) Output of pulse lengthener *PL*. (Step in row II is due to istantaneous disappearance of the « gate pulse » 15 at time τ, henceforth and up to time $\tau+\sigma$ the pulse lengthener is again in action; only at the instant τ relation $V_3(\tau) = V_2(\tau)$ holds. 4) Output of gate G_2 which, driven by « gate pulse » 12 takes away from V_3 its original leading edge and substitutes it with a standard one. 5) Output of Di_2, it is « gate pulse » for the calibrated pulse generator *CP* and coincidence pulse for coincidence circuit *C*. 6) Calibrated pulse which sets the channel witdh. It is generated by *CP*. 7) Pulse obtained by addition of calibrated pulse to pulse 4. 8) Output of that of the discriminators *Di* which has the threshold shown by the dotted line in waveform 7. 9) Output of coincidence *C* connected with discriminator *Di* of the preceding item. This pulse is fed to scalers. 10) Output of discriminator Di_1 which has threshold shown by the dotted line in waveform 3. 10 *bis*) It is the same of 10) in the case shown on row I. In the case shown on row II $V_{10\,bis}$ will recover to zero at the time $\tau+\sigma$ also if V_{10} will not. The recovering to zero of V_{10} follows, in this case, from the return to zero of V_{10bis}, because 10 *bis* brings to an end the lengthening operation and this resets Di_1. 11) Pulse obtained from the leading edge of pulse 10 suitably delayed. 12) Output of univribator driven by pulse 11: it is « gate pulse » for G_1 and G_2. 13) Output of forming circuit *F*. The forming circuit *F* and following discriminator Di_2 generate a pulse delayed with respect to the input pulse 12. The delay is set by the threshold of Di_2 that is shown by the dotted line in waveform 13. 14) Resetting pulse, obtained from the trailing edge of pulse 5. 15) Pulse obtained by addition of 14 and 10 *bis*: it is « gate pulse » for pulse lengthener *PL*.

a flat top so that the following addition of the delayed calibrated pulse of height d produces a step starting from height V and ending at height $V+d$.

Gate G_2 gives to each pulse a standard leading edge independent of the shape of the input pulses. Gate G_2 is driven by a suitably delayed pulse generated from the discriminator Di_1.

The threshold level of Di_1 is adjusted to a value inferior to the smallest pulses to be recorded. The delay time between the triggering of Di_1 and of G_2 is adjusted to a value larger than the maximum rise time of the input pulses.

The leading edge of pulses has been standardized because otherwise thresholds of channel discriminators could be influenced by a possibly too steep leading edge.

Gate G_1 safeguards against the possibility of wrong recordings due to couples of pulses very close to each other. In fact, in absence of gate G_1 the second pulse would superpose itself on the flat top of the preceding one and interfere with its associated calibrated pulse thus changing the channel width.

The resetting of the instrument after a pulse, is accomplished by pulse 14 that stops the operation of lenghtening. However it could happen that (row II of fig. 1) at the time τ of arrival of pulse 14 (that causes V_3 to become equal to $V_2(\tau)$), $V_2(\tau)$ be larger than the threshold value V_0 of Di_1. In such a case Di_1 would not recover and the whole instrument would remain indefinitely blocked.

R is provided to help that. It works letting V_{15} become zero at the time $\tau+\sigma$ so that afterwards $V_3(t) = V_2(t)$. Then Di_1 recovers to the initial state later on, when it gets below this value. In this way no spurious recordings are made. The whole instrument behaves itself as if it were provided with the known « inspector » circuit [8].

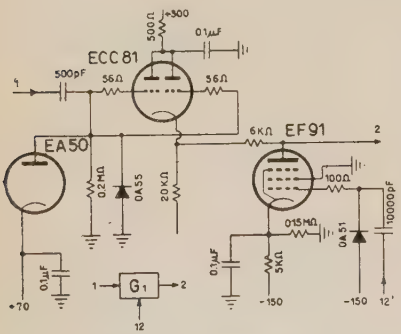

Fig. 2. – Gate G_1.

Circuits diagrams.

General. – The diagrams of the individual circuits will be found in the figures from 2 to 9. In every one of them is shown the corresponding section of the block diagram.

The reader will observe that sometimes connections synthetysed on the block diagram by a single bar correspond in the real circuits to two or more inputs or outputs in which the same pulse may have different available power or sign. Where confusion might arise for such reason, apexes have been added

[8] A. B. Van Rennes: *Nucleonics*, October (1952), p. 52.

to the numbers of the connections in order to distinguish the corresponding bars of the interconnected circuits.

All circuits which work on the input pulse, that is G_1 PL, G_2 S_2 and Di's, are designed for a maximum input pulse amplitude of 70 volts.

The time resolution of the instrument can be directly deduced from the time scale of the waveforms of fig. 1.

Gate G_1. – Gate G_1 consists of a cathode follower and a pentode EF91, connected as shown in fig. 2.

The pentode is normally below cut-off, and when it receives the « gate pulse » 12 becomes conducting, and the anode current develops across the 6 kΩ resi-

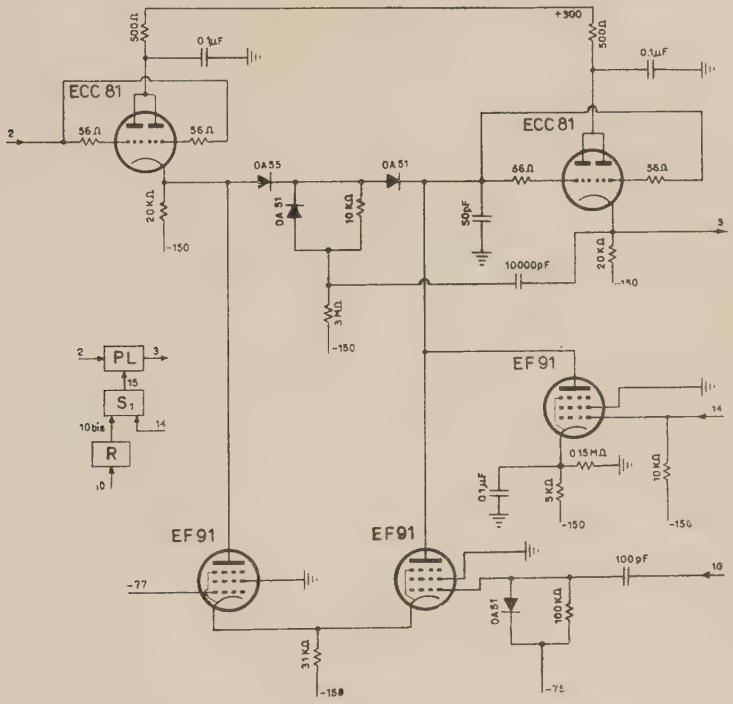

Fig. 3. – Pulse lengthener PL.

stence a potential drop sufficient to cut off the input cathode follower of block PL whatever the height of the pulse applied to the input of the gate. A diode limiter cuts down all pulses higher than 75 volts.

The input cathode follower is designed for accepting pulses up to 75 volts and 0,1 µs rise time without driving grid current.

Pulse Lenghtener PL (fig. 3). – The pulse lenghtener is of the type introduced by KELLEY (9) with three diodes.

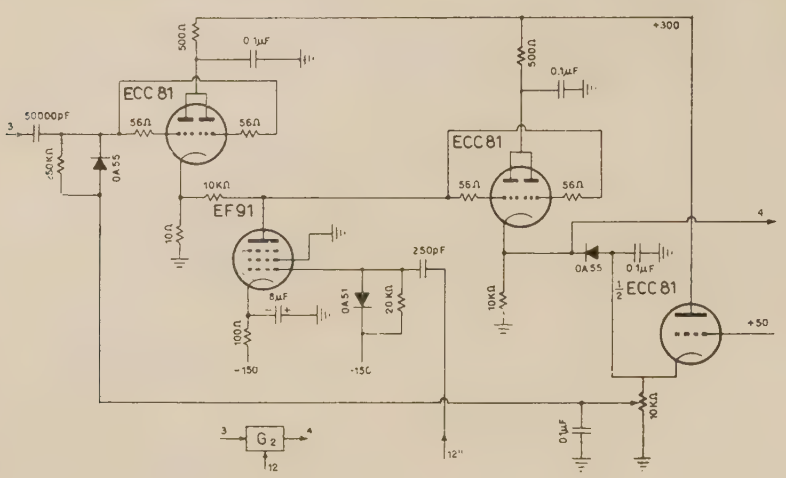

Fig. 4. – Gate G_2.

In our case one of the features of this type of pulse lenghtener results particularly useful, that is its property to maintain, in first approximation, a

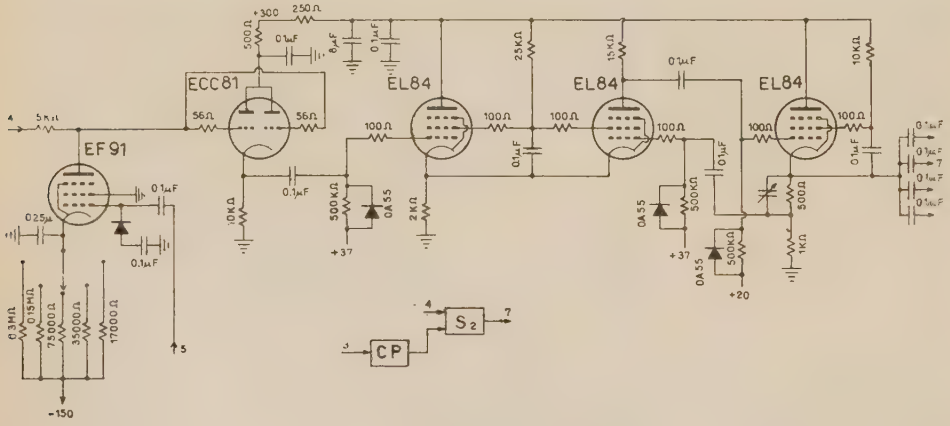

Fig. 5. – Calibrated pulse generator *CP* and adding circuit S_2.

constant inverse voltage across the lenghtener diode OA51 and consequently a constant leak current of the storage condenser.

In fact let us consider the effect of the leak current of the storage con-

(9) A. B. VAN RENNES: *Nucleonics*, October (1952), p. 51.

denser in the two different cases of constant leak current and of leak current proportional to the voltage (fig. 10, 1 e 2).

In both cases the step of the calibrated pulse appears to the discriminators *Di* partially hidden, and that gives rise to a reduction in the channel width, but in the latter case this reduction is proportional to the height of the pulse, that is, it is different for pulses of different height; in the former case instead it is constant for all pulses.

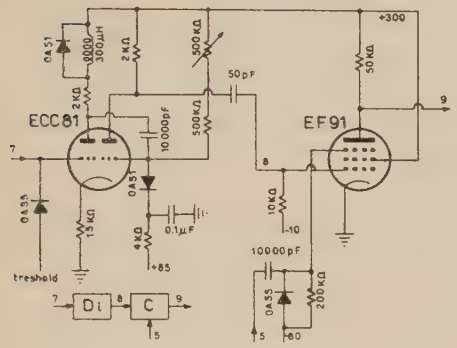

Fig. 6. – Discriminator *Di* and associated coincidence *C*.

That is, the deviation from ideal behaviour of the pulse lenghtener results, for constant leak current, in a reduction of the channel width constant for all channels.

The rate of discharge of the storage condenser has been measured and has resulted to be of 0.025 V/μs, which amounts to a reduction in channels width of 0.025 V/μs time 1.5 μs, that is 0.037 V.

Some care has been taken in the construction for keeping this discharge current constant and for that reason the OA51 has been kept away from heat sources.

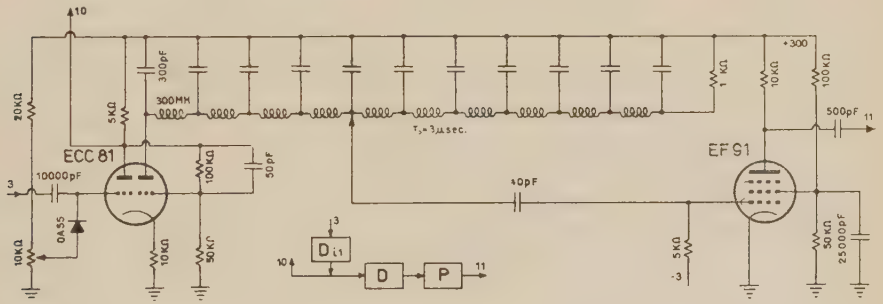

Fig. 7. – Auxiliary circuits.

It will be noticed that all the time constants of couplings in the circuits which follow the pulse lenghtener are unusually large. This has been done in order to have a negligible added sag of the flat parts of the pulses.

Gate G_2 (fig. 4). – It is very similar to gate G_1 and needs no further comment.

Calibrated pulse generator CP and summing circuit S_2 (fig. 5). – Also very similar to G_2. The anode current of the EF91 is accurately set by cathode

feedback to a stabilyzed value such as to produce across the 5 kΩ resistor (plus the output impedance of the preceding cathode follower) a potential drop equal to the desired amplitude d of the calibrated step.

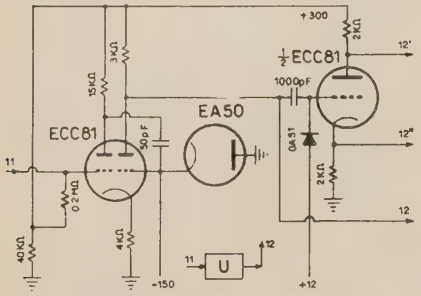

Fig. 8 Auxiliary circuits.

The constancy of the anode current is secured by the high internal resistance and by the constancy of the repartition of cathode current between anode and screen of the pentode EF91 for a sufficiently wide range of anode voltages.

Channel width is selected by changing the value of the cathode resistor of the EF91.

As output stage feeding the discriminators it has been found necessary to use a feedback amplifier in order to get a very low impedance (11 ohms).

Actually it happens that the discriminators triggered by the leading edge of a pulse feed back to the input circuit a small pulse through the grid-anode capacitance of their input tube.

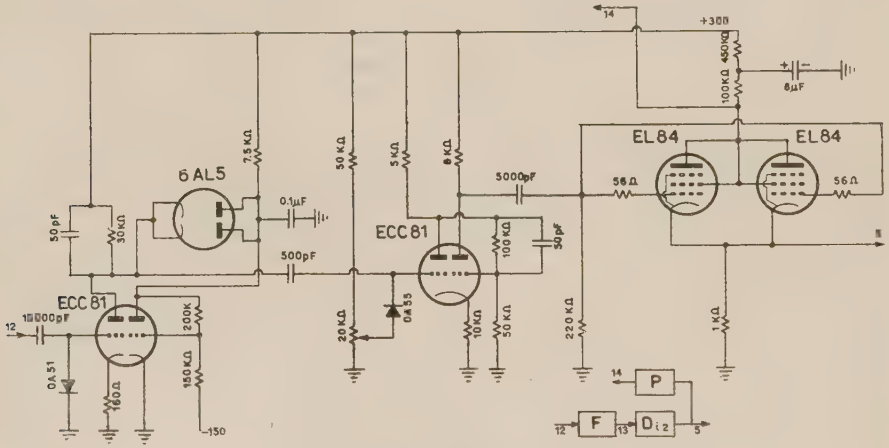

Fig. 9. – Auxiliary circuits.

The amplitude of these pulses across the line feeding the channel discriminators is, of course, proportional to the impedance shunting the same line, that is to the output impedance of the driver stage. It has been found necessary to reduce this impedance to about 10 Ω in order to minimize the influence of this effect on the channel width. The output stage is designed for a gain of 1.25 in order to compensate for the loss in the preceeding cascaded cathode followers.

Channel Circuits. – The bias to the discriminators is taken from a voltage divider built with wire resistors and fed from a voltage stabilized source.

Each coincidence circuit is followed from a scale of two, and a 100 scaler built with two decades Philips E1T.

Other circuits (fig. 6-7-8-9) do not present special features.

Bench Tests.

Linearity has been tested feeding calibrated pulses to the analyser and giving a corresponding bias to one of the channel discriminators so that pulses

Fig. 10. – Demonstrative figure (not to scale) of the effect on the shape of the pulse and actual channel width of the leakage of the storage capacitor of *PL*. *s* is the sag produced by leakage. $d - s$ is the resultant actual channel width. *s* is constant for all pulses in case I.

did fall in that channel. Results are shown in fig. 11. Channel width identity has been tested by means of pulses with random time distribution and having amplitude distribution equal to the probability value of position of a classical harmonic point oscillator. Channels of 1 volt width have proved to be equal within 1% without any adjustment of discriminator circuits.

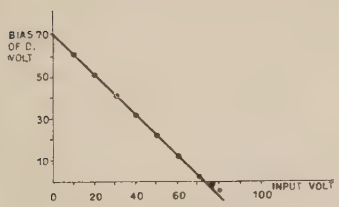

Fig. 11. – Linearity test.

Aknowledgements.

The author wishes to thank Prof. G. Bolla for his kind interest, Mr. C. Cottini for help in development work, construction and tests of the instrument and Dr. Giannelli for aid in preparing and editing the manuscript.

RIASSUNTO

Viene descritto un discriminatore di ampiezza a 20 canali avente alta stabilità e piccolo tempo di insensibilità (3 μs). La classificazione in ampiezza degli impulsi è effettuata a mezzo di un solo discriminatore a soglia per ogni canale: le posizioni di soglia definiscono le posizioni dei canali, mentre l'ampiezza di questi risulta determinata mediante una opportuna « messa in forma » degli impulsi da classificare.

Una camera a diffusione con campo magnetico per fisica nucleare.

A. Lovati e C. Succi

Istituto di Scienze Fisiche dell'Università - Milano
Istituto Nazionale di Fisica Nucleare - Sezione di Milano

(ricevuto il 5 Dicembre 1953)

Riassunto. — Vengono descritte una camera a diffusione dotata di campo magnetico e le apparecchiature ausiliarie per la ripresa delle fotografie. In questa camera il fondo vien mantenuto alla temperatura di — 45 °C mediante un evaporatore al Freon 22, azionato da un compressore industriale. Due bobine, raffreddate con circolazione d'acqua, permettono di mantenere nella zona sensibile della camera un campo magnetico massimo di circa 1000 gauss. In base ai risultati ottenuti utilizzando alcool metilico, etilico e propilico puri e miscele di questi alcooli diffondentisi in diversi gas, vengono fatte alcune considerazioni circa le migliori condizioni di funzionamento della camera.

In questi ultimi anni sono state realizzate numerose camere a diffusione [1], del tipo di quella di Langsdorf, continuamente sensibili alla radiazione ionizzante: risultati notevoli sono stati ottenuti sinora solo con strumenti ad alta pressione. Si può però ritenere che anche a pressione normale la camera a diffusione sia un efficace strumento di ricerca e che possa, per alcuni problemi, sostituire vantaggiosamente la camera di Wilson: pregio principale della camera a diffusione è infatti l'assenza o quasi di «tempo morto». I suoi immediati campi d'impiego sono quelli della radioattività e della fisica nucleare, rimanendo però praticamente escluso, data la geometria della zona sensibile, il campo della radiazione cosmica.

[1] A. Langsdorf jr.: *R.S.I.*, **10**. 91 (1939); A. Voisin: *Journ. Phys. et Radium*, **14**. 459 (1953) e bibliografia ivi contenuta; W. Rielzler e R. Werz: *Naturw.*, **4**. 138 (1953).

In base all'esperienza fatta con una prima camera a diffusione [2], simile a quella di COWAN [3], siamo passati alla realizzazione di uno strumento più completo, atto a ricerche di fisica nucleare.

1. – La camera.

La camera ha sezione circolare ed è a doppia parete di vetro: il cilindro interno ha diametro di 35 cm ed altezza di 18 cm.

Il fondo della camera è costituito da un disco di bronzo, incorporato in un anello di bachelite: alla faccia inferiore del disco è saldato il serpentino frigorifero di un compressore monofase a due cilindri al Freon 22, della potenza di 2 kW, capace di assorbire 3000 kcal nominali all'ora e di abbassare la temperatura della piastra fino a circa — 45 °C [4].

Il tetto della camera consiste di un disco in bronzo, nel quale è ricavata un'apertura circolare di 24 cm di diametro, chiusa mediante una lastra di cristallo; sul disco sono montati dei passanti per i conduttori dei riscaldatori e per gli elettrodi del campo chiarificatore e dei condotti per l'immissione dei

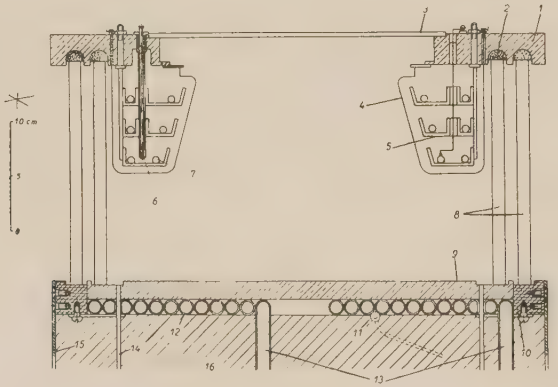

Fig. 1. – Sezione verticale della camera. (1) Tetto in bronzo della camera; (2) guarnizione di mastice; (3) disco di cristallo; (4) elettrodi del campo chiarificatore; (5) bacinelle porta-liquidi; (6) condotti per l'immissione dei liquidi; (7) resistenze blindate; (8) pareti laterali in vetro Pirex; (9) fondo della camera; (10) anello in bachelite; (11) bulbo termostatico; (12) serpentino frigorifero; (13) terminali del serpentino; (14) condotto per lo scarico dei liquidi; (15) cilindro in ottone; (16) blocco isolante di sughero autoespanso.

---

[2] C. SUCCI e G. TAGLIAFERRI: *Nuovo Cimento*, **9**, 1092 (1952).

[3] E. W. COWAN: *R.S.I.*, **21**, 991 (1950).

[4] Il gruppo frigorifero e la piastra sono stati costruiti dalla Ditta SAMIFI di Milano. Siamo grati al dott. ing. R. GIANESI per la cordiale collaborazione offertaci nella progettazione di queste parti e per la cura con cui ne ha seguito la costruzione.

liquidi da evaporare e per il ricambio dei gas: attraverso uno di questi condotti è possibile far scorrere una pinza termoelettrica per il rilevamento delle temperature nell'interno della camera.

L'evaporatore è costituito da tre bacinelle di forma anulare sovrapposte che complessivamente permettono di ottenere una superficie totale libera di liquido di circa 10 dm^2: ciascuna bacinella contiene una resistenza blindata che può dissipare una potenza regolabile da 5 a 20 W. I tre recipienti ed i tre riscaldatori sono alimentati indipendentemente per poter ottenere miscele di vapori diversi e nelle proporzioni volute.

Gli elettrodi del campo chiarificatore sono otto telai disposti attorno all'evaporatore e creano un campo diretto trasversalmente rispetto all'asse della camera.

Lo schizzo di fig. 1 mostra i particolari costruttivi della camera.

2. – Il funzionamento dello strumento.

La rivelazione delle particelle ionizzanti nella camera a diffusione si ottiene facendo diffondere un vapore attraverso i successivi strati di un gas, raffreddato per contatto da una parete fredda orizzontale: la diffusione verso il basso risulta grandemente facilitata se, sfruttando l'azione della gravità, si utilizzano vapori più pesanti del gas. Per temperature del fondo sufficientemente basse il gradiente termico verticale risulta abbastanza forte ed il flusso di vapore piuttosto intenso: in uno strato prossimo al fondo il vapore si soprassatura al di sopra del limite minimo necessario alla condensazione su ioni, permettendo di rivelare il passaggio di particelle cariche ([1,2,5]).

La superficie dell'evaporatore da noi realizzato è all'incirca uguale a quella della sezione della camera: ciò, oltre alla generazione di un flusso di vapore molto intenso, permette di evaporare a temperatura relativamente bassa, riducendo la probabilità di creazione di agglomerati molecolari al di sopra della zona sensibile e perciò di gocce di origine non ionica provenienti dall'alto; d'altra parte un limite superiore alla temperatura di evaporazione è imposto dalla necessità di non permettere la condensazione del vapore sulle pareti della camera: nel nostro caso ad entrambi questi inconvenienti era ovviato mantenendo i riscaldatori al di sotto dei 35 °C

In assenza di flusso di vapore la temperatura minima del fondo è intorno ai − 45 °C, ma durante il funzionamento essa subisce un aumento che dipende dalla natura del vapore e del gas impiegati: con argon ed alcool propilico, per esempio, questo aumento è di circa 8 °C.

L'intercapedine fra i due cilindri, opportunamente essiccata, assicura un

([5]) R. P. Shutt: *R.S.I.*, **22**, 730 (1951).

buon isolamento termico dall'ambiente circostante, impedendo la creazione di gradienti trasversali di temperatura, la cui presenza introduce spesso vorticosità nella camera.

L'osservazione della zona sensibile della camera a diffusione mostra, oltre alle tracce, una distribuzione praticamente uniforme di goccioline: le tracce sono dovute a condensazione del vapore su gli ioni all'atto della loro creazione da parte delle particelle ionizzanti; le goccioline sono dovute, invece, parte a fenomeni di condensazione spontanea nella zona sensibile e parte a condensazione sugli ioni prodotti nella zona inerte e diffusi nella zona sensibile. La nostra camera è in grado di rivelare tracce finchè il flusso di questi ioni si mantiene al di sotto di circa 200 ioni/cm^2 s.

Avvicinando ad una camera a diffusione una sostanza anche debolmente radioattiva, si nota che la capacità della camera a rivelare le particelle diminuisce nel tempo: questo fatto può essere messo in evidenza riprendendo durante l'irraggiamento della camera una sequenza di fotografie uniformemente distanziate nel tempo. Si osserva allora che la lunghezza totale di traccia misurabile nei singoli fotogrammi decresce nel tempo raggiungendo un valore limite che dipende dalla ionizzazione totale in tutto il volume della camera.

È evidentemente desiderabile che, al verificarsi dell'evento in istudio, sia disponibile nella zona sensibile la massima quantità di vapore: ciò si può ottenere utilizzando opportunamente l'azione di un campo elettrico. Con la disposizione degli elettrodi da noi adottata si riesce ad asportare ioni dalla zona inerte senza farli penetrare nella zona sensibile e a realizzare un campo abbastanza ben limitato alla parte superiore della camera, che perciò disturba poco la formazione delle tracce.

Per l'osservazione di eventi « prevedibili » viene utilizzato un campo piuttosto intenso ($\sim$ 100 V/cm), che viene tolto circa 1 s prima della produzione dell'evento per eliminarne l'azione sulle tracce; per l'osservazione, invece, di eventi « non prevedibili » l'applicazione di un campo costante di intensità notevolmente più bassa ($\sim$ 20 V/cm) non pregiudica la qualità delle tracce, pur mantenendo abbastanza vicino al massimo la lunghezza totale di traccia. Nel primo caso si introduce un « tempo morto » dell'ordine di due secondi, nel secondo il « tempo morto » è nullo.

3. – Le apparecchiature ausiliarie.

(i) *Il sistema di illuminazione e di osservazione.* – Per l'osservazione visuale delle tracce si illumina trasversalmente la zona sensibile della camera mediante una lampada ad incandescenza a filamento lineare.

Per la fotografia viene utilizzato il lampo di luce ottenuto scaricando su due « flash » lineari, posti nel fuoco di lenti cilindriche, due batterie di con-

densatori da 100 μF caricate a 2000 V. Opportune guide portano la luce alla camera delimitando un fascio abbastanza netto. Per la ricostruzione stereoscopica delle immagini vengono impiegate due macchine fotografiche disposte su una intelaiatura che permette la ripresa di fotografie sotto angoli variabili da 5° a 25° rispetto all'asse della camera e a distanze da 20 a 70 cm dal fondo. Vengono impiegate macchine fotografiche con otturatore comandato elettri-

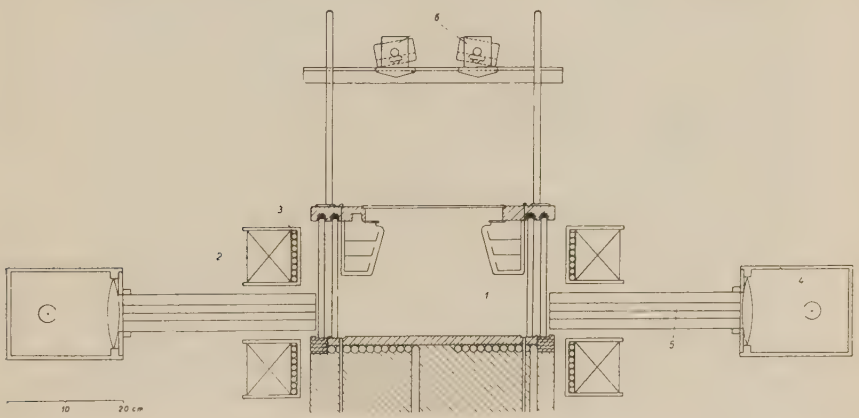

Fig. 2. – Schizzo della camera a diffusione e delle apparecchiature relative. (1) camera; (2) bobine generatrici del campo magnetico; (3) serpentino per la circolazione dell'acqua; (4) lampade a flash; (5) guide per la luce; (6) porta macchine fotografiche.

camente e con ricarica automatica per 200 fotogrammi formato 21 × 24 mm² (6). L'obbiettivo è un 36 mm « Supar » f/3,5 Wray.

Una ripresa cinematografica ha dato risultati molto soddisfacenti mediante l'illuminazione ottenuta isolando una lama di luce dal fascio di un proiettore ad arco voltaico. Per evitare la ionizzazione dovuta alla componente ultravioletta è stato necessario l'impiego di un filtro giallo.

Lo schizzo di fig. 2 mostra la camera con i particolari del sistema d'illuminazione e la disposizione delle macchine fotografiche.

(ii) *Il dispositivo per il ciclo delle operazioni.* – Per la ripresa di una serie di fotografie comandate su eventi « prevedibili » un automatismo ripete un ciclo di operazioni della durata minima di 3 secondi. La successione nel tempo delle varie operazioni è indicata nello schema di fig. 3.

Nelle fig. 4 e 5 sono mostrate alcune fotografie ottenute durante la messa a punto dello strumento: elettroni da radiofosforo venivano immessi nella camera comandando elettricamente un otturatore.

(6) Autocamera MK 3 della Ditta D. Shackman & Sons di Londra.

(iii) *Il campo magnetico.* – Per creare nella zona sensibile un campo magnetico la camera è posta nell'interno di due bobine complessivamente di 2 500 spire, alimentate con la corrente continua fornita da un raddrizzatore al selenio da 2 kW. Il campo massimo è di $\sim 1\,000$ gauss.

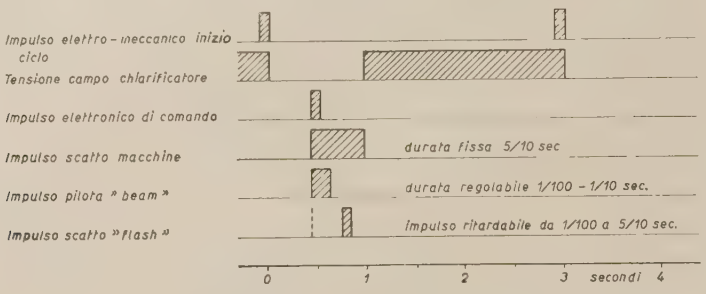

Fig. 3. – Ssuccessione nel tempo delle diverse operazioni.

Una circolazione di acqua raffredda le pareti delle bobine a contatto con la camera.

Una fotografia dello strumento e delle apparecchiature relative è riprodotta in fig. 6.

4. – Criteri orientativi per la scelta dei vapori.

Il caso più comune di impiego della camera a diffusione è l'osservazione di eventi che avvengono nel gas della camera: di conseguenza è importante poter conoscere qualche criterio orientativo per la scelta del vapore più opportuno da impiegarsi con il gas richiesto dall'esperienza.

Ci siamo perciò preoccupati di vedere come i coefficienti caratteristici dei vapori e dei gas [7] influenzano: *a*) l'altezza dello strato sensibile; *b*) la qualità delle tracce; *c*) la fedeltà delle tracce.

Nei grafici di fig. 8 sono riportati i risultati relativi alla distribuzione delle temperature, misurate per mezzo di una coppia termoelettrica, in funzione della quota fornendo sempre la stessa potenza ai riscaldatori.

Nel grafico di fig. 8*b* la curva *S* indica l'altezza dello strato sensibile in dipendenza dei vari gas usati: come si vede *l'altezza dello strato sensibile* diminuisce al crescere del rapporto fra il peso molecolare del vapore e quello del gas.

[7] Nella tabella I e nei grafici di fig. 7 sono raccolti alcuni dati relativi all'acqua, agli alcooli metilico, etilico e propilico ed ai gas idrogeno, aria ed anidride carbonica.

Fig. 4. Tracce di elettroni da radiofosforo.

Fig. 5. Evento prodotto dalla radiazione cosmica nelle pareti della camera.

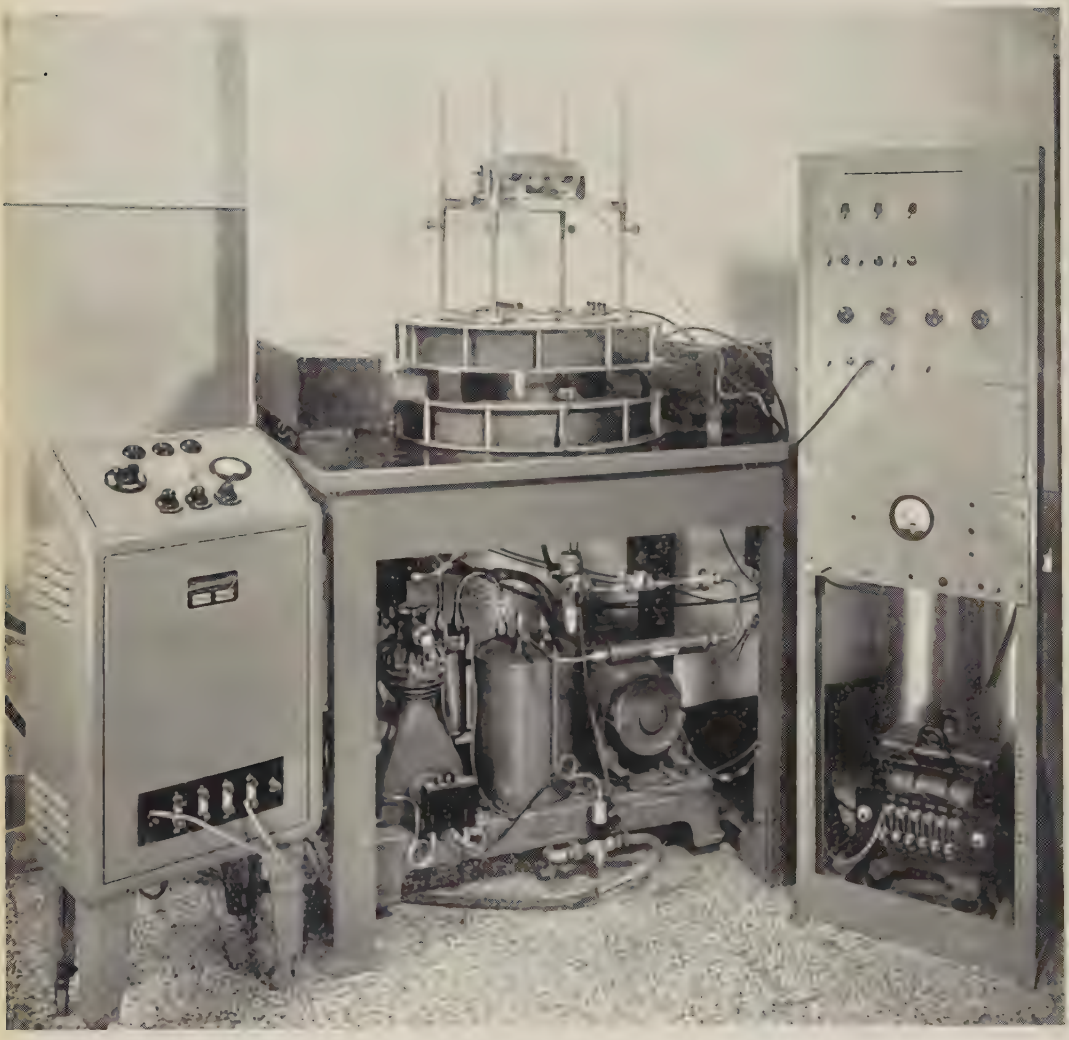

Fig. 6. – Veduta d'insieme della camera e delle apparecchiature relative.

L'esperienza ha mostrato che condizioni di instabilità, dovute a forti diversità fra i pesi molecolari dei vapori e dei gas, non insorgono se i riscaldatori vengono tenuti a temperatura sufficientemente bassa.

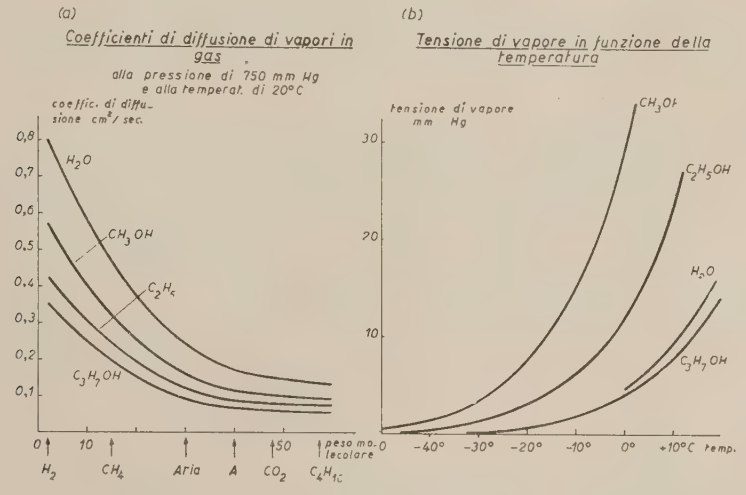

Fig. 7. – (*a*) Coefficienti di diffusione in gas del vapore d'acqua e degli alcooli metilico, etilico e propilico in funzione del peso molecolare dei gas. (*b*) Tensione di vapore dell'acqua e degli alcooli metilico, etilico e propilico in funzione della temperatura. (I grafici sono stati tracciati interpolando i dati pubblicati su: LANDOLT-BÖRNSTEIN: *Physikalisch-Chemische Tabellen*).

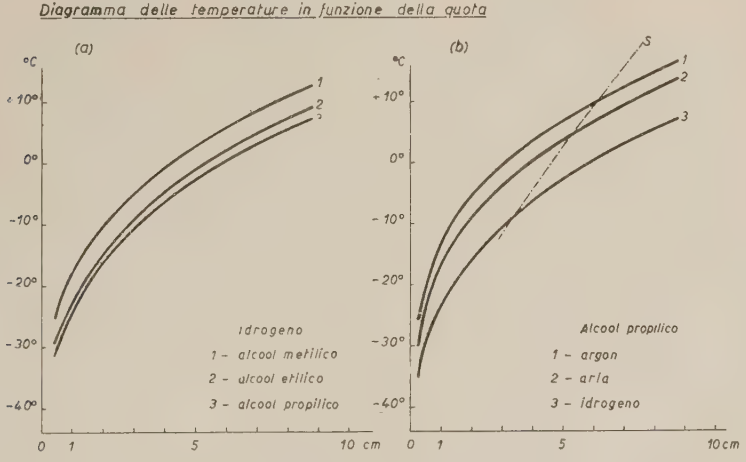

Fig. 8. – Diagramma delle temperature in funzione della quota nell'interno della camera per potenza costante ai riscaldatori: (*a*) temperatura relativa a vapori diversi che diffondono in idrogeno; (*b*) temperatura relativa all'alcool propilico che diffonde in gas diversi. La curva *S* mostra come varia l'altezza dello strato sensibile in corrispondenza ai pesi molecolari dei gas impiegati.

La qualità delle tracce dipende notevolmente dalle diverse combinazioni gas-vapore usate: le condizioni migliori per un dato gas si hanno in corrispondenza dei coefficienti di diffusione più elevati. Evidentemente in queste condizioni il vapore affluisce con maggior facilità verso centri di condensazione, l'ingrossamento delle goccioline diventa più rapido e la formazione delle tracce avviene prima che gli ioni abbiano potuto sensibilmente diffondersi.

TABELLA I. – *Costanti fisiche di alcune sostanze impiegate nella camera a diffusione.* (da LANDOLT-BÖRNSTEIN: *Physikalisch-Chemische Tabellen*).

Liquido	formula chimica	peso molecolare	densità (g/cm^3)	calore specif. (cal/g_m)	calore condens. a 20 °C (cal/g °C)	temperatura a 760 mm Hg		tensione superf. a 20 °C (dine/cm)
						solid. °C	ebull. °C	
Acqua	H_2O	18	1	0,999	586	0°	+100°	72,63
Alcool metilico .	CH_3OH	32	0,791	0,600	287	— 97°,1	+ 64°,7	23,02
Alcool etilico .	C_2H_5OH	46	0,789	0,593	224	—114°,15	+ 78°,3	22,03
Alcool propilico	C_3H_7OH	60	0,803	0,579	180	—127°	+ 97°,18	22,50

L'osservazione dei fotogrammi ottenuti durante la messa a punto dello strumento ha messo in evidenza una *alterazione di traccia* tipica delle camere continuamente sensibili: un breve tratto di traccia risulta talvolta o completamente mancante o attenuato e distorto. Questo fenomeno, che si verifica quando una particella ionizzante attraversa una regione della camera dove qualche istante prima ne era stata rivelata un'altra, è da attribuirsi all'abbassamento locale della soprassaturazione conseguente all'aumento di temperatura prodotto dal calore di condensazione liberato ed alla riduzione della quantità di vapore disponibile per effetto della condensazione sugli ioni della traccia precedente. Fissato il gas è opportuno di conseguenza scegliere un vapore che presenti, insieme ad un alto coefficiente di diffusione, un basso calore di condensazione ed una tensione di vapore poco variabile con la temperaura.

In base alle osservazioni fatte risulta infine giustificato l'uso di miscele di vapori diversi: con queste infatti si riesce di volta in volta a raggiungere soddisfacenti condizioni di compromesso, potendo ottenere dei « vapori » che presentano le caratteristiche più adatte per essere impiegati insieme ai gas imposti dai problemi che si devono studiare.

È nostro gradito dovere ringraziare il prof G. POLVANI, Direttore dell'Istituto di Scienze Fisiche dell'Università di Milano, ed il prof. P. CALDIROLA, Direttore della Sezione di Milano dell'Istituto Nazionale di Fisica Nucleare,

per aver seguito con vivo interessamento e costante appoggio la progettazione e la realizzazione dello strumento.

SUMMARY

A diffusion cloud chamber for use in nuclear research and its auxiliary equipment is described. The bottom of this chamber is cooled by an industrial refrigerator. Observations on the performance under different operating conditions are reported.

Energetic Nuclear Collisions in the Upper Atmosphere I. The Nucleon Pion Cascade.

U. Haber-Schaim (*)

Weizmann Institute of Science - Rehovoth, Israel

G. Yekutieli

Cosmic Ray Section, IAEC - Tel Aviv, Israel

(ricevuto il 10 Dicembre 1953)

Summary. — The nucleon pion cascade in the upper atmosphere is treated by an extension of the Fermi theory of pion production. The cascade equations are solved by an expansion in powers of the atmospheric depth. The contribution of primary alpha particles is considered in detail. The results are applied to the calculation of the attenuation mean free path of the nucleonic component and the ratio of neutral to charged nuclear particles.

1. – Introduction.

In recent years several papers were published on the nuclear cascade in the atmosphere. Most of these papers ([1-4]) describe the cascade of nucleons and pions below 10 Mc^2 ([5]) with the help of a « bremsstrahlung » type pro-

([1]) W. Heitler and L. Jánossy: *Proc. Phys. Soc.*, A **62**, 374 (1949); A **62**, 669 (1949).

([2]) H. Messel, R. B. Potts and C. B. A. McCusker: *Phil. Mag.*, **43**, 889 (1952).

([3]) P. Caldirola, R. Fieschi and P. Gulmanelli: *Nuovo Cimento*, **9**, 5 (1952). This reference has a detailed list of earlier publications.

([4]) P. Budini and G. Molière: *Kosmische Strahlung*, Ch. V (ed. Heisenberg, 2nd.ed.).

([5]) Note: Throughout this paper we shall put $M = 1$, $c = 1$ where M is the nuclear mass.

(*) At present: at *Physikalisches Institut der Universität Bern.*

duction spectrum. This procedure introduces in the above theories a number of free parameters to be fixed by the experiment. Exceptions are the papers by Rozenthal [6] and Amaldi [7] which deal with individual showers of very high energy.

It is the purpose of this work to study the cascade of nucleons and pions with energy above 100 Mc^2 in the upper atmosphere. The cascade equations are written with the help of Fermi's theory of pion production [8] generalized to include nucleon-nucleus effects. In particular we consider the influence of alpha primaries on the attenuation mean free path and the ratio of neutral to charged nuclear particles.

The production of heavy mesons is neglected in this work and therefore its results are incomplete. Yet we find it worthwhile to present the theory in its present form and to postpone to a later publication the discussion of the role played by the heavy mesons.

2. – The Primary Spectrum.

Intensity measurements at different geomagnetic latitudes showed that primary protons, α-particles, and heavier nuclei have similar energy spectra per nucleon [9]. The Bombay and Rochester groups [10] using emulsion cloud chamber techniques, found that this similarity of spectra holds up to 4000 Mc^2; namely, that 66% of the primary nucleons hit the top of the atmosphere as protons, 26% as α-particles and 8% as heavier nuclei, all with the same energy spectrum per nucleon.

The energy spectrum per nucleon is conveniently expressed in the form of a power law aE^{-s} nucleons, $(Mc^2)^{-1}\,s^{-1}\,cm^{-1}\,sterad^{-1}$. Several values have been suggested for the exponent s and the coefficient a. Barret *et al.* [11] give $s = 2.53^{+0.2}_{-0.1}$ and $a = 2.8^{+1.0}_{-0.5}$ whereas Haber-Schaim [12] gives $s = 2.56$ and $a = 0.57$. Final judgement on the coefficients and the exponents may be passed only when further experimental information is obtained.

In this paper we shall compare with experiment the ratio of neutral to

---

[6] L. L. Rozental: *Dokl. Akad. Nauk USSR*, **80**, 731 (1951). We are greatly indebted to Dr. M. Bruin, Amsterdam, for sending us an English translation of this paper.

[7] E. Amaldi, L. Mezzetti and G. Stoppini: *Nuovo Cimento*, **10**, 803 (1953).

[8] E. Fermi: *Prog. Theor. Phys.*, **5**, 570 (1950); *Phys. Rev.*, **81**, 683 (1951).

[9] B. Peters: *Progress in Cosmic Ray Physics*, Ch. 4 (Amsterdam, 1952).

[10] D. Lal, Yash Pal, M. F. Kaplon and B. Peters: *Phys. Rev.*, **86**, 569 (1952).

[11] P. H. Barret, L. M. Bollinger, G. Cocconi, Y. Eisenberg and K. Greisen: *Rev. Mod. Phys.*, **24**, 133 (1952).

[12] U. Haber-Schaim: *Phys. Rev.*, **84**, 1199 (1951) quoted as A.

charged particles and the attenuation length of the nuclear cascade. These two parameters are independent of the coefficient a, hence we choose the following spectra of protons and alpha particles.

(1) $$n_0(E) = aE^{-2.56} \qquad \text{for protons,}$$

and

(2) $$\alpha_0(E) = 0.4aE^{-2.56} \qquad \text{per nucleon for } \alpha\text{-particles.}$$

The contribution of heavier nuclei is neglected. The absolute intensities given in this paper are calculated with $a = 0.57$.

3. – The Nuclear Cascades Initiated by Primary Protons.

3·1. *The Cascade Equations.* – In what follows we shall neglect the lateral spread of the cascade. This is justified because in the energy region which is of interest to us most of the energetic particles are ejected within small angles to the primary direction. For example, at $E = 200$, 80% of the particles are ejected within 20° to the primary direction and they carry 98% of the total energy.

Let $n(E, p)$ and $\pi(E, p)$ be the differential vertical intensities of nucleons and pions at atmospheric pressure p g/cm², initiated by primary protons. They satisfy the following set of integro-differential equations:

(3)
$$\begin{cases} \dfrac{\partial n(E, p)}{\partial p} = -\dfrac{n(E, p)}{\lambda} + \\ + \dfrac{1}{\lambda}\displaystyle\int R_{nn}(E, E')n(E', p)\,\mathrm{d}E' + \dfrac{1}{\lambda}\int R_{n\pi}(E, E')\pi(E', p)\,\mathrm{d}E' , \\ \dfrac{\partial \pi(E, p)}{\partial p} = -\dfrac{126\pi(E, p)}{Ep} - \dfrac{\pi(E, p)}{\lambda} + \\ - \dfrac{1}{\lambda}\displaystyle\int R_{\pi n}(E, E')n(E', p)\,\mathrm{d}E' + \dfrac{1}{\lambda}\int R_{\pi\pi}(E, E')\pi(E', p)\,\mathrm{d}E' . \end{cases}$$

With the initial conditions: $n(E, 0) = aE^{-2.56}$ and $\pi(E, 0) = 0$. Where R_{nn} and $R_{n\pi}$ are the production spectra of nucleons resulting in nucleon and pion air-nucleus collisions respectively. Similarly $R_{\pi n}$ and $R_{\pi\pi}$, are the production spectra of pions resulting in nucleon and pion air nucleus collisions respectively. The collision mean free path of nucleons and pions in air $\lambda = 72$ g/cm² is assumed to be independent of energy. The above value of λ was obtained from the model used in (A) to describe the air nucleus, and is

due to its partial transparency to nuclear particles. Finally $pE/126$ is the mean free path for pion decay in the upper atmosphere calculated for a proper life time of $2.56 \cdot 10^{-8}$ s and an average temperature of -50 °C.

We shall solve equations (3) by expanding $n(E, p)$ and $\pi(E, p)$ in powers of (p/λ):

$$(4) \qquad \begin{cases} n(E, p) = \exp[-p/\lambda] \sum_{k=0}^{\infty} n_k(E)(p/\lambda)^k \\ \pi(E, p) = \exp[-p/\lambda] \sum_{k=0}^{\infty} \pi_k(E)(p/\lambda)^k . \end{cases}$$

The functions $n_k(E)$ and $\pi_k(E)$ have a simple physical interpretation, they are the energy spectra of the k-th generation of nucleons and pions respectively in the nuclear cascade. Inserting (4) into (3) we obtain the following recursion formulae for $n_k(E)$ and $\pi_k(E)$:

$$(5) \qquad \begin{cases} (k+1) n_{k+1}(E) = \int R_{nn}(E, E') n_k(E') \, \mathrm{d}E' + \int R_{n\pi}(E, E') \pi_k(E') \, \mathrm{d}E' , \\ \left(k - 1 - \frac{126}{E}\right) \pi_{k-1}(E) = \\ \qquad = \int R_{\pi n}(E, E') n_k(E') \, \mathrm{d}E' + \int R_{\pi\pi}(E, E') \pi_k(E') \, \mathrm{d}E' . \end{cases}$$

3·2. *The production Spectra R.* – The production spectra R_{nn}, $R_{n\pi}$, $R_{\pi n}$ and $R_{\pi\pi}$ are calculated on the basis of Fermi's theory of pion production [8] and the three layer model of the air nucleus [12]. According to this model the « average air nucleus » is described by an assembly of 15 nucleons fixed in three layers. A collision between an incident nucleon (or pion) with energy E' and an air nucleus is analysed in the following way. We distinguish three different cases:

(1) A nucleon-nucleon (or a pion-nucleon) collision, with energy E'. The relative frequency of this case is 0.40.

(2) A collision between δ_1 of the particles (nucleons and pions) produced in case (1) with one more nucleon from the second or third layer. The effective energy in this case is $k_1 E'$ with the relative frequency of 0.15.

(3) A collision between δ_2 of the particles produced in case (2) with a nucleon of the third layer. The relative frequency of this case is 0.45 and the effective energy is $k_2 E'$. The collision parameters of this model δ_1, δ_2,

k_1 and k_2 are functions of the incident energy E'. Their dependence on E' is given in (A) ([13]).

Following (A) we assume that the energy distribution of the pions produced in a nuclear collision is primarily determined by their angular distribution in the c.m. system. The energy distribution in the c.m. system is only of secondary importance and is neglected in our approximation i.e. we assume that all particles (pions and nucleons) have the same energy in the c.m. system. Using the angular distribution of Fermi $f_4(0.96\cos\theta)$ it can be shown that pions produced in nuclear collisions with effective energy E_{eff} have the following energy spectrum:

$$\varrho_\pi(E, E_{\text{eff}}) = 0.31 E_{\text{eff}}^{-1/2} f_4\left(0.96\left[\frac{1.93E}{E_{\text{eff}}^{3/4}} - 1\right]\right), \tag{6}$$

with the condition that $\varrho_\pi(E, E_{\text{eff}}) = 0$ for $1.93E_{\text{eff}}^{3/4} > 2$ and for all the three cases

$$R_{\pi n}(E, E') = 0.5\varrho_\pi(E, E') + 0.23\varrho_\pi(E, k_1E') + 0.4\varrho_\pi(E, k_2E') . \tag{7}$$

Small corrections have been introduced in the weighting factors to account for the partial transparency of the nucleus (the « left over particles » in (A)).

At energies $E' > 100$ the energy available for pion production in the c.m. system is practically the same for incident nucleons and pions. Hence we shall write

$$R_{\pi\pi}(E, E') = R_{\pi n}(E, E') . \tag{8}$$

The production of nucleons above 100 Mc^2 in nuclear collisions is treated in a similar way. We assume that in this region nucleons and pions have the same constant energy in the c.m. system, and that the energy spectrum in the laboratory system is governed by the same angular distribution. Therefore, the energy spectrum per nucleon of nucleons produced in nuclear collisions with effective energy E_{eff} will be:

$$\varrho_n(E, E_{\text{eff}}) = 0.30 E_{\text{eff}}^{-3/4} f_4\left(0.96\left[\frac{1.93E}{E_{\text{eff}}^{3/4}} - 1\right]\right) . \tag{9}$$

Now according to the analysis of the nucleon-air-nucleus collision given above, the number of nucleons that participate in the three cases of collisions are: 2, $2\delta_1+1$ and $(2\delta_1+1)\delta_2+1$ respectively. Hence the production spectrum

([13]) The factors k_i are related to h_i of (A) by $k_i = h_i^2$.

of nucleons in nucleon-air-nucleus collision is:

$$R_{nn}(E, E') = 0.5 \cdot 2\varrho_n(E, E') + 0.23[2\delta_1+1]\varrho_n(E, k_1E') + \\ + 0.4[(2\delta_1+1)\delta_2+1]\varrho_n(E, k_2E') . \tag{10}$$

Similarly the numbers of nucleons that participate in the three cases of a pion-air-nucleus collision are 1, δ_1+1 and $(\delta_1+1)\delta_2+1$ respectively. Therefore, the production spectrum of nucleons in pion-air-nucleus collision is:

$$R_{n\pi}(E, E') = 0.5\varrho_n(E, E') + 0.23(\delta_1+1)\varrho_n(E, k_1E') + \\ + 0.4[(\delta_1+1)\delta_2+1]\varrho_n(E, k_2E') . \tag{11}$$

3.3. *The Intensities of Pions and Nucleons in the Upper Atmosphere.* – Using the primary proton spectrum $n_0(E) = 0.57E^{-2.56}$ and the recursion formula (5) the values of n_1; n_2; $\pi_1 : \pi_2$ are calculated numerically. Some of their values are given in Table I.

TABLE I.

E	n_0	n_1	π_1	n_2	π_2
10	$1.5 \cdot 10^{-3}$	$3.15 \cdot 10^{-4}$	$3.5 \cdot 10^{-5}$	$4.7 \cdot 10^{-5}$	$1.1 \cdot 10^{-5}$
30	$9.5 \cdot 10^{-5}$	$1.4 \cdot 10^{-5}$	$4.5 \cdot 10^{-6}$	$9.8 \cdot 10^{-7}$	$7.5 \cdot 10^{-7}$
100	$4.3 \cdot 10^{-6}$	$3.0 \cdot 10^{-7}$	$3.8 \cdot 10^{-7}$	$2.0 \cdot 10^{-8}$	$3.9 \cdot 10^{-8}$
200	$7.3 \cdot 10^{-7}$	$4.4 \cdot 10^{-8}$	$7.8 \cdot 10^{-8}$	$2.5 \cdot 10^{-9}$	$7.1 \cdot 10^{-9}$
500	$7.0 \cdot 10^{-8}$	$3.1 \cdot 10^{-9}$	$8.2 \cdot 10^{-9}$	$1.2 \cdot 10^{-10}$	$5.1 \cdot 10^{-10}$
1 000	$1.2 \cdot 10^{-8}$	$3.6 \cdot 10^{-10}$	$1.3 \cdot 10^{-9}$	$1.1 \cdot 10^{-11}$	$6.0 \cdot 10^{-11}$

For $E > 250$ the following expressions hold:

$$\begin{cases} n_1(E) = 0.69E^{-3.08} \\ \pi_1(E) = 0.27 \dfrac{E^{-2.75}}{1 + 126/E} \\ n_2(E) = 0.34E^{-3.77} + 0.093E^{-3.33} \\ \pi_2(E) = \dfrac{0.29E^{-3.44} + 0.13E^{-3.0}}{2 + 126/E} . \end{cases} \tag{12}$$

We notice that $n_1(E)$ decreases with energy more rapidly than $\pi_1(E)$, this is due to the increased number of pions produced. The two terms in $n_2(E)$ and $\pi_2(E)$ are the contributions of $n_1(E)$ and $\pi_1(E)$ respectively.

In the upper atmosphere $n(E, p)$ and $\pi(E, p)$ are approximated by:

$$(13)\quad \begin{cases} n(E, p) = \exp[-p/\lambda][n_0(E) + n_1(E)(p/\lambda) + n_2(E)(p/\lambda)^2 + r_n(E, p) \\ \pi(E, p) = \exp[-p/\lambda][\pi_1(E)(p/\lambda) + \pi_2(E)(p/\lambda)^2 + r_\pi(E, p)\,. \end{cases}$$

Now according to Appendix A both $r_n(100, 216)$ and $r_\pi(100, 216)$ are smaller than $0.3\pi_2(100, 216)$. Hence the contributions of $r_n(100, 216)$ and $r_\pi(100, 216)$ to $n(100, 216)$ and $\pi(100, 216)$ are less than 8%. For $E > 100$ and $p < 216$ the contributions of r_n and r_π are even smaller and therefore neglected.

The integral intensities of nucleons $N(E, p)$ and pions $\Pi(E, p)$ are obtained by integrating both sides of (13) from E to infinity.

$$(14)\quad \begin{cases} N(E, p) = \exp[-p/\lambda]\{N_0(E) + N_1(E)(p/\lambda) + N_2(E)(p/\lambda)^2\} \\ \Pi(E, p) = \exp[-p/\lambda]\{\Pi_1(E)(p/\lambda) + \Pi_2(E)(p/\lambda)^2\}. \end{cases}$$

Some values of N_0, N_1, Π_1, N_2, and Π_2 are given in Table II.

TABLE II.

E	N_0	N_1	Π_1	N_2	Π_2
10	$1.0 \cdot 10^{-2}$	$1.7 \cdot 10^{-3}$	$5.3 \cdot 10^{-4}$	$1.8 \cdot 10^{-4}$	$7.5 \cdot 10^{-5}$
30	$1.8 \cdot 10^{-3}$	$1.9 \cdot 10^{-4}$	$1.2 \cdot 10^{-4}$	$1.2 \cdot 10^{-5}$	$1.5 \cdot 10^{-5}$
100	$2.8 \cdot 10^{-4}$	$1.8 \cdot 10^{-5}$	$2.4 \cdot 10^{-5}$	$9.2 \cdot 10^{-7}$	$2.3 \cdot 10^{-6}$
200	$9.4 \cdot 10^{-5}$	$4.8 \cdot 10^{-6}$	$1.0 \cdot 10^{-5}$	$2.2 \cdot 10^{-7}$	$7.4 \cdot 10^{-7}$
500	$2.3 \cdot 10^{-5}$	$7.5 \cdot 10^{-7}$	$1.9 \cdot 10^{-6}$	$6.3 \cdot 10^{-8}$	$2.1 \cdot 10^{-7}$
1000	$7.8 \cdot 10^{-6}$	$1.8 \cdot 10^{-7}$	$6.3 \cdot 10^{-7}$	$7.7 \cdot 10^{-9}$	$4.7 \cdot 10^{-8}$

4. – The Contribution of Alpha Primaries to the Nuclear Cascade.

4·1. *The Alpha-particle Air-Nucleus Collision.* – The differential energy spectrum per nucleon of alpha primaries on the top of the atmosphere is given by (2). The alpha's are absorbed with an attenuation mean free path of $\lambda_\alpha = 44.5$ g/cm^2 [8]; hence the differential energy spectrum at atmospheric pressure p is $0.4n_0(E) \exp[-p/\lambda_\alpha]$.

As a result of collisions between alpha particles and air nuclei pions and nucleons are produced. Let $g_n(E, p)$ and $g_\pi(E, p)$ be their differential production spectra at atmospheric depth p. In calculating $g_n(E, p)$ and $g_\pi(E, p)$ the following assumptions were made. The air nucleus was described by a

sphere of radius $3.4 \cdot 10^{-13}$ cm in which 15 nucleons were packed in three layers, each layer having a transparency of 0.37 for nucleons ([12]).

The alpha particle was described by a sphere of radius $2 \cdot 10^{-13}$ cm containing four nucleons. With this model we estimated that on the average 2.5 nucleons are stripped in the alpha air nucleus collision, whereas the other 1.5 nucleons produce mesons in the nuclear collision as if they were free.

Therefore:

$$(15) \qquad g_n(E,p) = \exp[\quad p/\lambda_\alpha] \left[0.25 n_0(E) + 0.15 \int R_{nn}(E, E') n_0(E')\, \mathrm{d}E'\right] =$$

$$= \exp[-p/\lambda_\alpha][0.25 n_0(E) + 0.15 n_1(E)]\,,$$

$$(16) \qquad g_\pi(E, p) = \exp[-p/\lambda_\alpha] 0.15 \int R_{\pi n}(E, E') n_0(E')\, \mathrm{d}E' =$$

$$= \exp[-p/\lambda_\alpha] 0.15 \pi_1(E) \left(1 + \frac{126}{E}\right).$$

4·2. *The Cascade Equations and Their Solutions.* – Let $\bar{n}(E, p)$ and $\bar{\pi}(E, p)$ be the differential intensities of nucleons and pions initiated by alpha primaries. They obey the following equations:

$$(17) \qquad \begin{cases} \dfrac{\partial \bar{n}(E, p)}{\partial p} = -\dfrac{n(E, p)}{\lambda} + \\ \quad + \dfrac{1}{\lambda} \int R_{nn}(E, E') \bar{n}(E', p)\, \mathrm{d}E' + \dfrac{1}{\lambda} \int R_{n\pi}(E, E') \bar{\pi}(E', p)\, \mathrm{d}E' + \dfrac{1}{\lambda_\alpha} g_n(E, p)\,, \\ \dfrac{\partial \bar{\pi}(E, p)}{\partial p} = -\dfrac{\bar{\pi}(E, p)}{\lambda} - \dfrac{126 \bar{\pi}(E, p)}{Ep} + \\ \quad + \dfrac{1}{\lambda} \int R_{\pi n}(E, E') \bar{n}(E', p)\, \mathrm{d}E' + \dfrac{1}{\lambda} \int R_{\pi\pi}(E, E') \bar{\pi}(E', p)\, \mathrm{d}E' + \dfrac{1}{\lambda_\alpha} g_\pi(E, p)\,. \end{cases}$$

With the initial conditions

$$\bar{n}(E, 0) = \bar{\pi}(E, 0) = 0\,.$$

To solve (17) we shalle expand $\bar{n}(E, p)$ and $\bar{\pi}(E, p)$ in powers of p/λ

$$(18) \qquad \begin{cases} \bar{n}(E, p) = \exp[-p/\lambda_\alpha] \sum_{k=1}^{\infty} \bar{n}_k(E) (p/\lambda)^k \\ \bar{\pi}(E, p) = \exp[-p/\lambda_\alpha] \sum_{k=1}^{\infty} \bar{\pi}_k(E) (p/\lambda)^k\,. \end{cases}$$

Inserting (18) into (17) we obtain the recursion formulae:

$$
(19)\quad
\begin{cases}
(K+1)\bar{n}_{k+1}(E)=\left(\dfrac{\lambda}{\lambda_\alpha}-1\right)\bar{n}_k(E)+\displaystyle\int R_{nn}(E,E')\bar{n}_k(E')\,\mathrm{d}E'+ \\
\qquad\qquad +\displaystyle\int R_{n\pi}(E,E')\bar{\pi}_k(E')\,\mathrm{d}E'+\delta_{0k}\frac{\lambda}{\lambda_\alpha}\left[0.25n_0(E)+0.15n_1(E)\right], \\
\left(K+1+\dfrac{126}{E}\right)\bar{\pi}_{k+1}(E)-\left(\dfrac{\lambda}{\lambda_\alpha}-1\right)\bar{\pi}_k(E)+\displaystyle\int R_{\pi n}(E,E')\bar{n}_k(E')\,\mathrm{d}E'+ \\
\qquad\qquad +\displaystyle\int R_{\pi\pi}(E,E')\bar{\pi}_k(E')\,\mathrm{d}E'+\delta_{0k}\frac{\lambda}{\lambda_\alpha}0.15\pi_1(E)\left(1+\frac{126}{E}\right).
\end{cases}
$$

Some values of $\bar{n}_k$ and $\bar{\pi}_k$ for $k=1$, 2, 3, and 4 are given in Table III. They were calculated for a primary energy spectrum of $0.23\cdot E^{-2.56}$ per nucleon on the top of the atmosphere.

TABLE III.

E	$\bar{n}_1$	$\bar{n}_2$	$\bar{n}_3$	$\bar{n}_4$	$\bar{\pi}_1$	$\bar{\pi}_2$	$\bar{\pi}_3$	$\bar{\pi}_4$
10	$7.3\cdot10^{-4}$	$2.9\cdot10^{-4}$	$7.7\cdot10^{-5}$	$1.5\cdot10^{-5}$	$8.5\cdot10^{-6}$	$1.5\cdot10^{-5}$	$7.1\cdot10^{-6}$	$1.9\cdot10^{-6}$
30	$4.1\cdot10^{-5}$	$1.6\cdot10^{-5}$	$4.0\cdot10^{-6}$	$7.0\cdot10^{-7}$	$1.1\cdot10^{-6}$	$1.7\cdot10^{-6}$	$7.3\cdot10^{-7}$	$1.8\cdot10^{-7}$
100	$1.8\cdot10^{-6}$	$6.3\cdot10^{-7}$	$1.4\cdot10^{-7}$	$2.5\cdot10^{-8}$	$9.0\cdot10^{-8}$	$1.3\cdot10^{-7}$	$5.3\cdot10^{-8}$	$1.3\cdot10^{-8}$
200	$3.0\cdot10^{-7}$	$1.0\cdot10^{-7}$	$2.6\cdot10^{-8}$	$4.1\cdot10^{-9}$	$1.9\cdot10^{-8}$	$2.6\cdot10^{-8}$	$1.0\cdot10^{-8}$	$2.5\cdot10^{-9}$
500	$2.9\cdot10^{-8}$	$9.9\cdot10^{-9}$	$2.1\cdot10^{-9}$	$3.6\cdot10^{-10}$	$2.0\cdot10^{-9}$	$2.5\cdot10^{-9}$	$9.8\cdot10^{-10}$	$2.3\cdot10^{-10}$
1000	$5.5\cdot10^{-9}$	$1.6\cdot10^{-9}$	$3.4\cdot10^{-10}$	$5.0\cdot10^{-11}$	$3.0\cdot10^{-10}$	$2.4\cdot10^{-10}$	$1.1\cdot10^{-10}$	$3.0\cdot10^{-11}$

In the upper atmosphere $\bar{n}(E,p)$ and $\bar{\pi}(E,p)$ are expressed by:

$$
(20)\quad
\begin{cases}
\bar{n}(E,p)=\exp\left[-p/\lambda_\alpha\right]\left\{\displaystyle\sum_1^4\bar{n}_k(E)(p/\lambda)^k+\bar{r}_n(E,p)\right\} \\
\bar{\pi}(E,p)=\exp\left[-p/\lambda_\alpha\right]\left\{\displaystyle\sum_1^4\bar{\pi}_k(E)(p/\lambda)^k+\bar{r}_\pi(E,p)\right\}.
\end{cases}
$$

According to Appendix B for $p<180$ g/cm^2 and $E\geqslant 100$ both $\bar{r}_n(E,p)$ and $\bar{r}_\pi(E,p)$ are bounded by $51\bar{n}_5(100)=1.86\cdot10^{-7}$ and with the help of Table III it can be shown that in this region $\bar{r}_n$ and $\bar{r}_\pi$ contribute less than 8% to the two sums of the right hand side of (20). Integrating both sides of (20) from E to infinity we obtain the integral intensities with about the

same accuracy:

$$(21)\qquad \begin{cases} \overline{N}(E,p) = \exp[-p/\lambda_\alpha] \sum_1^4 \overline{N}_k(E)(p/\lambda)^k \\ \overline{\Pi}(E,p) = \exp[-p/\lambda_\alpha] \sum_1^4 \overline{\Pi}_k(E)(p/\lambda)^k \end{cases}$$

The variation of $\overline{N}_k(E)$ and $\overline{\Pi}_k(E)$ for $k = 1, 2, 3$ and 4 with E are given in Table IV.

TABLE IV.

E	$\overline{N}_1$	$\overline{N}_2$	$\overline{N}_3$	$\overline{N}_4$	$\overline{\Pi}_1$	$\overline{\Pi}_2$	$\overline{\Pi}_3$	$\overline{\Pi}_4$
10	$4.5 \cdot 10^{-3}$	$1.8 \cdot 10^{-3}$	$4.0 \cdot 10^{-4}$	$8.7 \cdot 10^{-5}$	$1.2 \cdot 10^{-4}$	$2.0 \cdot 10^{-4}$	$8.6 \cdot 10^{-5}$	$2.0 \cdot 10^{-5}$
30	$7.7 \cdot 10^{-4}$	$2.8 \cdot 10^{-4}$	$6.8 \cdot 10^{-5}$	$1.2 \cdot 10^{-5}$	$2.9 \cdot 10^{-5}$	$4.7 \cdot 10^{-5}$	$1.9 \cdot 10^{-5}$	$3.9 \cdot 10^{-6}$
100	$1.2 \cdot 10^{-4}$	$4.0 \cdot 10^{-5}$	$9.2 \cdot 10^{-6}$	$1.6 \cdot 10^{-6}$	$5.9 \cdot 10^{-6}$	$9.2 \cdot 10^{-6}$	$3.4 \cdot 10^{-6}$	$9.3 \cdot 10^{-7}$
200	$3.9 \cdot 10^{-5}$	$1.3 \cdot 10^{-5}$	$3.0 \cdot 10^{-6}$	$5.0 \cdot 10^{-7}$	$2.4 \cdot 10^{-6}$	$3.3 \cdot 10^{-6}$	$1.3 \cdot 10^{-6}$	$3.1 \cdot 10^{-7}$
500	$9.3 \cdot 10^{-6}$	$3.1 \cdot 10^{-6}$	$6.7 \cdot 10^{-7}$	$1.1 \cdot 10^{-7}$	$4.6 \cdot 10^{-7}$	$5.5 \cdot 10^{-7}$	$2.0 \cdot 10^{-7}$	$4.8 \cdot 10^{-8}$
1000	$3.2 \cdot 10^{-6}$	$1.0 \cdot 10^{-6}$	$2.2 \cdot 10^{-7}$	$3.6 \cdot 10^{-8}$	$1.5 \cdot 10^{-7}$	$1.8 \cdot 10^{-7}$	$6.4 \cdot 10^{-8}$	$1.4 \cdot 10^{-8}$

The integral intensities of nucleons and pions above 100 Mc^2 as functions of v are plotted in Fig. 1.

5. – The Attenuation Mean Free Path of the Nuclear Component.

The attenuation mean free path (a.m.f.p.) of a given component of the cosmic radiation in the atmosphere is defined by the depth (in g/cm²) along which the intensity of this component, $I(p)$, is reduced by a factor e. When the intensity varies exponentially with pressure, the a.m.f.p. is a constant. In other cases it is better to use the average a.m.f.p. between two points p_1 and p_2 defined by:

$$L_{12} = -\frac{p_1 - p_2}{\log[I(p_1)/I(p_2)]}$$

According to Fig. 1, both $N(100, p)$ and $N(100, p) + \Pi(100, p)$ vary exponentially for $p < 216$ g/cm², with constant a.m.f.paths: $L = 1.06\lambda = 76.1$ g/cm² for nucleons and $L = 1.18\lambda = 85$ g/cm² for nucleons and pions initiates by primary protons only.

The total flux of nucleons and pions initiated by both primary protons and alpha particles $N+\Pi+\overline{N}+\overline{\Pi}$, does not vary exponentially with pressure.

Using (22) we calculated L_{12} for several values of p_1 and p_2 and $E = 100$. The results are given in Table V.

TABLE V.

p_1	p_2	L_{12}/λ	L_{12} g/cm^2
0	36	1.89	136
0	72	1.64	120
0	108	1.54	111
0	180	1.39	100
14	180	1.29	94
144	180	1.22	88

The high values of L_{12} near the top of the atmosphere are due to the large number of nucleons and pions directly produced by alpha primaries. The alpha primaries are, however, absorbed very rapidly in the atmosphere, and the average a.m.f.p. L_{0p} measured from the top of the atmosphere decreases with depth.

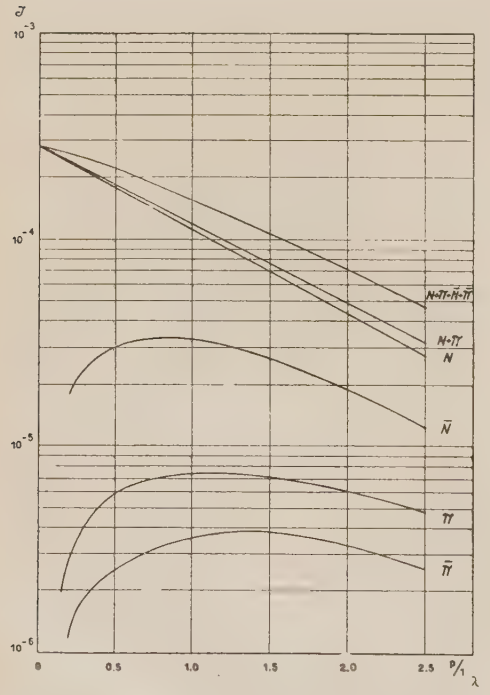

Fig. 1. – The integral (vertical) intensities of nucleons and pions at $E = 100$ as function of the atmospheric depth.

The dependence of L_{12} on the atmospheric pressure has important consequences. It appears from the above analysis, that the proton intensities on the top of the atmosphere deduced from nucleon and pion intensities measured at lower altitudes, on the assumption of a constant a.m.f.p., are too large.

The a.m.f.p. depends on the energy of the nucleons and pions. Now, each term N_k, Π_k, $\bar{N}_k$ or $\bar{\Pi}_k$ in the expansions (14, 21) is a monotonic decreasing function of the particle's energy and the slope of each function increases with k. Therefore, the a.m.f.p. is a decreasing function of the particle's energy.

The a.m.f.p. of the nuclear component in the atmosphere was measured by several authors. We shall quote the results of TICHO (14) and KAPLON *et al.* (15). TICHO found an average a.m.f.p. of 125 g/cm² for nuclear particles above 126 Mc² between $p_1 = 222$ g/cm² and $p_2 = 305$ g/cm². KAPLON *et al.* found an average a.m.f.p. of 129 ± 15 g/cm² measured between $p_1 = 15$ g/cm² and $p_2 = 180$ g/cm². Our value calculated between $p_1 = 144$ and $p_2 = 180$ g/cm² (i.e. 88 g/cm²) should be an upper limit to the value observed by TICHO. Similarly, the calculated a.m.f.p. between 14 and 180 g/cm² (i.e. 94 g/cm²) should be an upper limit to the value measured by KAPLON *et al.* It is evident that in both cases the calculated a.m.f.p. is lower than the observed one. This discrepancy can be explained in either of two ways:

(1) The values of the collision mean free path $\lambda = 72$ g/cm² used in this paper is too low. With $\lambda = 100$ g/cm² the calculated value will be in good agreement with the observed one.

(2) The nuclear collisions in this energy region are not so strongly inelastic as given by the Fermi theory. This has been suggested by GREISEN and WALKER (16). We shall return to this in the following sections.

6. – The Ratio of Neutral to Charged Nuclear Particles.

If we assume that on the average one half of the nucleons produced in nuclear collisions are neutrons, the number of neutrons $\mathcal{N}(E, p)$ with energy above E, at atmospheric pressure p will be:

$$\mathcal{N}(E, p) = \tfrac{1}{2}\{ N(E, p) - \exp[-p/\lambda] N_0(E) + N(E, p)\}. \tag{23}$$

The ratio $q(E, p)$ of neutral to singly charged nuclear particles is then:

$$q(E, p) = \frac{\mathcal{N}}{N + \Pi + \bar{N} + \bar{\Pi} - \mathcal{N}}. \tag{24}$$

Some values of $q(100, p)$ calculated with (23, 24) and Tables II and IV, are given in Table VI.

In the above calculation the contribution of primaries heavier then alpha particles is neglected. We estimate that these heavy primaries will increase the effective number of alpha primaries by 30%. The so corrected values are denoted by q^*.

(14) H. K. TICHO: *Phys. Rev.*, **88**, 236 (1952).

(15) M. F. KAPLON, J. Z. KLOZE, D. M. RITSON and W. D. WALKER: Private communication.

TABLE VI.

p g/cm^2	p/λ	$q(100, p)$	$q^*(100, p)$
36	0.5	0.089	0.114
12	1.0	0.147	0.178
180	2.5	0.220	0.244

The ratio of neutral to charged nuclear particles is strongly dependent on the degree of inelasticity of the nucleon-nucleus collision. As a rule, the ratio increases with decreasing inelasticity. An increase in the collision mean free path will only shift $q(E, p)$ along the p axis towards higher pressures. This holds, of course, only for pressures where the direct contribution of primary alpha particles is no longer important. Therefore, by comparing the calculated ratios with the observed, we shall be able to determine whether the discrepancy of the preceding chapter can be removed by increasing the collision mean free path or whether we shall have to assume a smaller degree of inelasticity in the nucleon-nucleus collision.

GREISEN and WALKER ([16]) found a ratio of 0.75 at p 724 g/cm^2. GOTLIEB ([17]), on the other hand, found at the same altitude a ratio between 0.04 and 0.16 for particles with energy above 15 Mc^2. The calculated value at $p = 180$ (Table VI) should be a lower limit to the observed ratios at 724 g/cm^2. Gotlieb's value is therefore too low. Unfortunately we cannot compare directly the ratios given in Table VI, with the experiments of GREISEN and WALKER, since our calculation does not hold at mountain altitudes. It is possible, however, that the calculated ratio would turn out too low also when the calculations are properly extended. This conclusion, if correct, would favor the assumption that the nucleon-nucleus collisions are not as inelastic as we have assumed here. This needs some explanation. Our calculation was based on two independent assumptions, (1) that the Fermi theory correctly describes the nucleon-nucleon collision; (2) that inside the nucleus the collision takes place between the composite particle and *one* nucleon at a time. A priori, we cannot exclude the possibility that the Fermi theory does hold but that more nucleons from the nucleus share the energy of the incoming particle, and by doing so, reduce a little the number of pions (and heavy mesons) produced. In other words, the collision is really strongly inelastic, but a large fraction of the energy lost by the incoming particle, is taken up by the nucleons of the nucleus.

([16]) K. GREISEN and W. D. WALKER: *Phys. Rev.*, **90**, 915 (1953).
([17]) M. B. GOTLIEB: *Phys. Rev.*, **82**, 349 (1951).

Appendix A

The terms of the nucleon-pion cascade initiated by protons, $n_k(E)$ and $\pi_k(E)$ are bounded by the terms $n_k^*(E)$ and $\pi_k^*(E)$ of a fictitious cascade in which the pions do not decay. n_k^* and π_k^* obey the following recursion formulae:

$$\text{(A1)} \qquad \begin{cases} (k+1)n_{k+1}^* = \int R_{nn} n_k^* \, dE' + \int R_{n\pi} \pi_k^* \, dE' , \\ (k+1)\pi_{k+1}^* = \int R_{\pi n} n_k^* \, dE' + \int R_{\pi\pi} \pi_k^* \, dE' . \end{cases}$$

According to (10) and (11) $R_{nn}(E, E') > R_{n\pi}(E, E')$, and for $E' > 100 \cdot R_{\pi n}(E, E') > R_{nn}(E, E')$. With (6, 7) and (9, 10) it can easily be shown that if: $g(E) \leqslant E^{-2}$.

Then:

$$\text{(A2)} \qquad 0.28 \int E'^{-\frac{1}{2}} f_4\left(0.96\left[\frac{1.93E}{E'^{\frac{1}{4}}} - 1\right]\right) g(E') \, dE' > \int R_{\pi n}(E, E') g(E') \, dE' .$$

Let us define $u_k(E)$ by:

$$\text{(A3)} \qquad (k+1)u_{k+1}(E) = 2 \cdot 0.28 \int E'^{-\frac{1}{2}} f_4\left(0.96\left[\frac{1.93E}{E'^{\frac{1}{4}}} - 1\right]\right) u_k(E') \, dE' \qquad k > 3 ,$$

and

$$\text{(A4)} \qquad u_3(E) = \pi_3(E_0)\left(\frac{E}{E_0}\right)^{-3.33} ; \qquad E > E_0 \quad \text{so that} \quad \pi_3(E_0) \geqslant n_3(E_0) .$$

Then we find that

$$\text{(A5)} \qquad n_k(E) \geqslant \pi_k^*(E) \geqslant n_k^*(E) . \qquad k > 3.$$

All the terms of the cascade $u_k(E)$ will be of the form

$$\text{(A6)} \qquad u_k(E) = n_k(E_0)(E/E_0)^{-s_k} \qquad k > 3 \text{ and } E > E_0 .$$

Using (A3) and (A6) we find that

$$\text{(A7)} \qquad \frac{(k+1)u_{k+1}}{u_k} = 1.02E^{\frac{3}{5}}(2.4E^{\frac{1}{5}}) \; s_k \int_{-1}^{+1} (1+\eta)^{(4s_k - 5)/3} f_4(0.96\eta) \, d\eta = D_k(E) .$$

In our case $s_{k+1} > s_k > 2$ and $E > 10$ Mc², therefore $D_k(E)$ is a decreasing

function of E and k. Hence with (A7) we find that:

$$k!\, u_k(E) < 3!\, D_3^{k-3}(E)\pi_3(E)\,. \tag{A8}$$

The residuals $r_n(E, p)$ and $r_\pi(E, p)$, (13) are smaller than $r_3(E, p)$ which is defined as:

$$r_3(E, p) = \sum_{k=3}^{\infty} n_k(E)(p/\lambda)^k\,. \tag{A9}$$

According to (A8)

$$r_3(E, p) = \frac{6\pi_3(E)}{[D_3(E)]^3}\left[\exp[D_3(E)p/\lambda] - 1 - D_3(E)(p/\lambda) - \frac{[D_3(E)(p/\lambda)]^2}{2}\right]. \tag{A10}$$

Now, $D_3(30) = 0.18$ and $r_3(30) = 0.07\pi_2(E)$ for $p \leqslant 216$ g/cm^2 and $E \geqslant 30$ Mc^2 we have then

$$r_3(E > 30, 216) < r_3(30, 216) \leqslant 0.3\pi_2(30)\,. \tag{A11}$$

Appendix B

Following the arguments of Appendix A, it can be shown that the terms $\bar{n}_k(E)$ and $\bar{\pi}_k(E)$ of the nucleon-pion cascade initiated by alpha primaries are bounded by terms $\bar{u}_k(E)$ defined by:

$$(k+1)\bar{u}_{k+1}(E) = \tag{B1}$$

$$= \left(\frac{\lambda}{\lambda_\alpha} - 1\right)\bar{u}_k + 0.55\int E'^{-\frac{1}{2}} f_4\left(0.96\left[\frac{1.93E}{E'^{\frac{1}{4}}} - 1\right]\right)\bar{u}_k(E')\,\mathrm{d}E'\,, \qquad k \geqslant 5$$

with the initial condition

$$\bar{u}_5(E) = \bar{n}_5(E_0)(E/E_0)^{-2.5} \quad \text{for} \quad E > E_0 \quad \text{and} \quad \bar{n}_5(E_0) > \bar{\pi}_5(E_0)\,. \tag{B2}$$

It follows that

$$\frac{(k+1)\bar{u}_{k+1}}{\bar{u}_k} = \frac{\lambda}{\lambda_\alpha} - 1 + D_k(E) \qquad k \geqslant 5\,, \tag{B3}$$

and $D_k(E)$ is defined by (A7). Hence

$$k!\,\bar{u}_k \leqslant 5!\left[\frac{\lambda}{\lambda_\alpha} - 1 + D_5\right]^{k-5}\bar{u}_5\,. \tag{B4}$$

Let us define $\bar{r}_5\ (E, p)$ as

$$\bar{r}_5(E, p) = \sum_{k=5}^{\infty} \bar{u}_k(E)(p/\lambda)^k \tag{B5}$$

then $\bar{r}_5(E, p)$ bounds both $\bar{r}_n(E, p)$ and $\bar{r}_\pi(E, p)$. In our case $D_5(100) = 0.41$ and $[(\lambda/\lambda_\alpha) - 1 + D_5] = 1.04$.

With (B4) and (B5) we find $\bar{r}_5(100, 180) < 51\bar{n}_5(100) = 1.86 \cdot 10^{-7}$.

For $p = 180$, $\sum_1^5 \pi_k(100)(p/\lambda)^k = 2.36 \cdot 10^{-6}$ and therefore, $\bar{r}_\pi(100, 180)$ contributes less than 8% to $\bar{\pi}(100, 180)$. The contribution of $\bar{r}_n(100, 180)$ to $\bar{n}(100, 180)$ is even smaller.

RIASSUNTO (*)

La cascata nucleoni-pioni nell'alta atmosfera è trattata per mezzo di un'estensione della teoria di Fermi sulla produzione dei pioni. Le equazioni della cascata si risolvono con uno sviluppo in serie di potenze della profondità atmosferica. Si considera dettagliatamente il contributo delle particelle α primarie. Si applicano i risultati al calcolo dell'attenuazione del cammino libero medio della componente nucleonica e del rapporto delle particelle neutre a quelle cariche.

(*) *Traduzione a cura della Redazione.*

A Theory of the Electron.

H. T. Flint and E. M. Williamson
Bedford College, University of London

(ricevuto il 16 Dicembre 1953)

Summary. — A theory of the electron is proposed by analogy with the gravitational theory of matter. It is essentially a classical theory based upon equations of the form suggested by Mie. The use of five-dimensional analysis results naturally in the appearance of a field of the Yukawa vector type in addition to the electromagnetic field. The theory of the electron is thus brought into line with theories of the nuclear field. The analogy leads directly to the results obtained by Bopp and accounts for the mass of the electron by means of the energy of the field.

This theory is based on an analogy with the relativistic theory of gravitation in the presence of matter. In the case when the region under consideration contains no matter, the law of gravitation is expressed in terms of geometrical quantities only. These are the coefficients (g_{mn}) of the line element,

$$\mathrm{d}s^2 = g_{mn}\,\mathrm{d}x^m\,\mathrm{d}x^n\,, \tag{1}$$

and their first derivatives.

The law of gravitation in this case takes the form

$$R_{mn} = 0 \tag{2}$$

(R_{mn}) being the curvature tensor, which is dependent only on the coefficients and their first derivatives.

When matter is present the law becomes

$$R_{mn} - \frac{1}{2}\,g_{mn}R = \frac{8\pi\varkappa}{c^4}\,T_{mn}\,, \tag{3}$$

(T_{mn}) being the tensor of matter and $R = g^{mn}R_{mn}$. If the space is the seat of electromagnetic energy, momentum and stresses but contains no matter, (T_{mn}) is the electromagnetic energy-momentum tensor. Its value is

$$T_{mn} = B_{ml}B_n{}^l - \frac{1}{4}\, g_{mn}B_{rs}B^{rs}\,, \tag{4}$$

where

$$B_{rs} = \frac{\partial \varphi_s}{\partial x^r} - \frac{\partial \varphi_r}{\partial x^s}\,,$$

(φ_r) denoting the electromagnetic potential.

The work of KALUZA and KLEIN [1] and of others who followed them has shown that by extending the forms of four-dimensional Riemannian geometry to five-dimensions it is possible to unite gravitation and electromagnetism so that they are together expressible in terms of geometrical quantities.

The same union has been expressed by means of the notation of projective geometry by VEBLEN and HOFFMANN [2].

The law of gravitation and electromagnetism has been developed as a geometrical law by ROSENFELD [3] who deduced the relation (3) by analogy with Einstein's derivation of relation (2). He showed that if the line element applicable to the five-dimensional continuum be taken as:

$$\mathrm{d}\sigma^2 = \gamma_{\mu\nu}\,\mathrm{d}x^\mu\,\mathrm{d}x^\nu\,, \qquad (\mu, \nu = 1, 2, 3, 4, 5)\,, \tag{5}$$

where

$$\left\{\begin{array}{l} \gamma_{mn} = g_{mn} + \gamma_{55}\alpha^2\varphi_m\varphi_n\,, \qquad \gamma_m = \alpha\gamma_{55}\varphi_m\,, \\ \gamma^{mn} = g^{mn}\,, \qquad \gamma^{55} = \dfrac{1}{\gamma_{55}} + \alpha^2\varphi_m\varphi^m\,, \\ \gamma^{5m} = -\,\alpha\varphi^m\,, \end{array}\right. \tag{6}$$

the curvature tensor (P^{mn}) hsa the value:

$$P_{mn} = R_{mn} - \frac{8\pi\varkappa}{c^4}\, B_m{}^l B_{nl}\,, \tag{7}$$

---

[1] TH. KALUZA: *Berliner Sitzungsberichte*, p. 966 (1921); O. KLEIN: *Zeits. f. Phys.*, **37**, 895 (1926).

[2] O. VEBLEN and B. HOFFMANN: *Phys. Rev.*, **36**, 810 (1930).

[3] L. ROSENFELD: *Bull. Acad. roy. de Belgique*, **13**, 6, 447 (1927).

so that the law expressed by equations (3) and (4) becomes

$$P_{mn} - \frac{1}{2} g_{mn} P = 0 \,, \tag{8}$$

where $P = g^{mn} P_{mn}$.

ROSENFELD proceeds to show that if charges are present in the space they must be represented by a tensor which replaces the zero on the right hand side of equation (8). This new tensor is thus introduced by analogy with that representing matter or electromagnetic phenomena in the theory of Einstein. In developing a theory of the electron it will be assumed that a quantity additional to those occurring in the geometry must be included and it will be the object of this work to derive an equation of the form (8) with a suitable tensor on the right hand side to represent the particle.

The Notation.

It is convenient to give a few particulars of the notation to be used.

The principle underlying the use of the notation of five-dimensional geometry or of that of projective geometry is that the extension by analogy of certain four-dimensional mathematical forms brings about a union of quantities and relations which remain separate in the analysis of four dimensions. This is a point which has been brought out particularly by O. KLEIN (1) and has since been developed and extended.

In applications to problems in physics it has been sufficient to assume a simple dependence upon the fifth coordinate, x^5, the position of the affix denoting the fact that the coordinate is a component of a contravariant vector. It has been assumed that when this coordinate occurs, it does so in the factor $\exp[\lambda x^5]$. In the theory of nuclear fields λ has been placed equal to a constant ik, $(i = \sqrt{-1})$, k being the reciprocal of the range of action of the nuclear force, the mass μ_0 of the meson associated with the field being given by the relation: $k = 2\pi\mu_0 c/h$.

The treatment here will not at first require that λ should be constant and it will be assumed to depend only on the four coordinates (x^m) with $m = 1, 2, 3, 4$. It will be necessary later to limit the treatment to the case when λ is constant, when it will be replaced by ik.

For the present purpose it is necessary to relate a five-dimensional vector and a five-dimensional antisymmetric tensor of the second rank with corresponding four-dimensional quantities.

The relations between the quantities result from those of equations (6) but these will be simplified by placing $\gamma_{55} = 1$ and $\alpha = e/m_0 c^2$. The former con-

dition is justified, since in the study of the equation of motion of an electron in an electromagnetic field, it is the ratio γ_{m5}/γ_{55} which is significant and which must be identified with a component of the electromagnetic potential. The second condition follows from the assumption that the path of the electron is a null geodesic ([4]) of the five-dimensional continuum.

If (A^μ) denotes a five-dimensional vector, it can be replaced in four dimensions by a vector (a^m) and a scalar magnitude $a_\cdot$. The relations between contravariant and covariant components are ([5]):

$$(9)\qquad \begin{cases} A^m = a^m\,, \qquad A^5 = a_\cdot - \alpha\varphi_m a^m\,, \\ A_m = a_m + \alpha\varphi_m a\,, \qquad A_5 = a_\cdot\,, \quad (m = 1, 2, 3, 4). \end{cases}$$

If $(A^{\mu\nu})$ denotes an antisymmetric tensor of the five-dimensional continuum, it can be related to an antisymmetric tensor and a vector in four dimensions.

If again small letters denote the four-dimensional quantities and capitals those of five dimensions:

$$(10)\qquad \begin{cases} A^{mn} = a^{mn}\,, \qquad A^{m5} = a^m{}_\cdot - \alpha\varphi_n a^{mn}\,, \\ A^m{}_n = a^m{}_n + \alpha\varphi_n a^m{}_\cdot\,, \qquad A^m{}_5 = a^m{}_\cdot\,, \\ A^5{}_m = a_{\cdot m} - \alpha\varphi_n a^n{}_m - \alpha^2\varphi_m\varphi_n a^n{}_\cdot\,, \\ A_{mn} = a_{mn} + \alpha\varphi_m a_{\cdot n} + \alpha\varphi_n a_m\,. \end{cases}$$

(a^{mn}) is the antisymmetrical tensor and $(a^m{}_\cdot)$ the vector.

The Field Equations for the Electron.

Theories of the electron have been based upon certain equations of a form similar to the electromagnetic equations of Maxwell. The difficulties and incompleteness of the older theories like that of H. A. LORENTZ ([6]) are well known. G. MIE developed a theory based on equations of similar form but essentially different in its principles from the theory of Lorentz, and equations of the same form as those of MIE ([7]) have been proposed on a number of occasions down to the present time. With the advent of the later form of the quantum theory and in particular with the discovery of Dirac's equation, new suggestions were made for the establishment of equations of the Maxwell

([4]) J. W. FISHER: *Proc. Roy. Soc.*, A **123**, 489 (1929).
([5]) H. T. FLINT: *Phil. Mag.*, **29**, 417 (1940).
([6]) H. A. LORENTZ: *The Theory of Electrons*, p. 213.
([7]) G. MIE: *Ann. der Phys.*, **37**, 511 (1912).

type as the basic equations of the quantum theory (8). The work of YUKAWA showed that the equations could be applied to the nuclear field associated with the vector meson.

One of the sets of equations proposed at this earlier period will be used again here. It is, in the five-dimensional continuum, analogous to the set of Maxwell's equations and it will be seen to lead to equations of Mie's type and also to the theory of the electron developed by F. BOPP (9). There are some differences between the assumptions made in the course of this work and in Bopp's presentation of his theory, but his ideas have been used and have guided the present development.

The first set of equations adopted as the basis of this theory are:

$$\frac{\partial F^{\mu\nu}}{\partial x^{\nu}} = J^{\mu}\,, \qquad (\mu, \nu = 1, 2, 3, 4, 5). \tag{11}$$

The second set are:

$$\frac{\partial F_{\mu\nu}}{\partial x^{\lambda}} + \frac{\partial F_{\nu\lambda}}{\partial x^{\mu}} + \frac{\partial F_{\lambda\mu}}{\partial x^{\nu}} = 0\,. \tag{12}$$

This set is satisfied automatically if $(F_{\mu\nu})$ is of the form

$$F_{\mu\nu} - \frac{\partial A_{\nu}}{\partial x^{\mu}} - \frac{\partial A_{\mu}}{\partial x^{\nu}}\,. \tag{13}$$

The vector (A_{μ}) is the element introduced to take account of the electron field and contains a quantity additional to the electromagnetic potential (φ_m). It is in terms of (A_{μ}) that the tensor required on the right hand side of equation (8) will be expressed.

In accordance with the notation it is proposed to adopt (A_{μ}) will be expressed in terms of (a_m) and $a_{\cdot}$ and the four-dimensional tensor (f_{mn}) and the vector $(f_{m\cdot})$ will replace $(F_{\mu\nu})$.

From equation (13)

$$\begin{cases} F_{mn} = \dfrac{\partial}{\partial x^m}(a_n + \alpha\varphi_n a_{\cdot}) - \dfrac{\partial}{\partial x^n}(a_m + \alpha\varphi_m a_{\cdot}) \\ F_{5m} = \dfrac{\partial}{\partial x^5}(a_m + \alpha\varphi_m a_{\cdot}) - \dfrac{\partial a_{\cdot}}{\partial x^m} \end{cases} \tag{14}$$

$$= \lambda a_m - \left(\frac{\partial a_{\cdot}}{\partial x^m} - \alpha\lambda\varphi_m a_{\cdot}\right). \tag{15}$$

(8) C. G. DARWIN: *Proc. Roy. Soc.*, A **118**, 604 (1928); TH. DE DONDER: *Bull. Acad. roy. de Belgique*, **14**, 2, 307 (1928); J. FRENKEL: *Zeits. f. Phys.*, **52**, 356 (1928); J. M. WHITTAKER: *Proc. Roy. Soc.*, A **121**, 543 (1928); J. W. FISHER anf H. T. FLINT: *Proc. Roy. Soc.*, A **126**, 644 (1929); A. PROCA: *Journ. Phys. et le Radium*, **7**, 347 (1936).

(9) F. BOPP: *Ann. d. Phys.*, **38**, 345 (1940).

It is assumed that (a_m) and $a_\cdot$ contain x^5 as already described but that (φ_m) is independent of this coordinate. It will be further supposed that the components (a_m) and also $a_\cdot$ can be expressed in the form

$$a_m = \theta_m \chi\,, \qquad a_\cdot = \theta_\cdot \chi\,. \tag{16}$$

The expression in the bracket in equation (15) takes the form:

$$\theta_\cdot \left(\frac{\partial \chi}{\partial x^m} - \alpha\lambda\varphi_m\chi \right)$$

and, again for the sake of simplicity, it is supposed that

$$\frac{\partial \chi}{\partial x^m} = \alpha\lambda\varphi_m\chi\,. \tag{17}$$

Thus

$$F_{5m} = \lambda a_m = f_{\cdot m} = -f_{m\cdot}\,. \tag{18}$$

By means of equations (10), (14), (16), (17) and (18) it follows that

$$f_{mn} = \left(\frac{\partial}{\partial x^m} - \alpha\lambda\varphi_m \right) a_n - \left(\frac{\partial}{\partial x^n} - \alpha\lambda\varphi_n \right) a_m + \alpha\theta_\cdot \left(\frac{\partial \varphi_n}{\partial x^m} - \frac{\partial \varphi_m}{\partial x^n} \right) \chi =$$

$$= \left(\frac{\partial \theta_n}{\partial x^m} - \frac{\partial \theta_m}{\partial x^n} \right) \chi + \alpha\theta_\cdot \left(\frac{\partial \varphi_n}{\partial x^m} - \frac{\partial \varphi_m}{\partial x^n} \right) \chi\,.$$

f_{mn} will be denoted by $h_{mn}\chi$ and it is convenient to write

$$\theta_{mn} = \frac{\partial \theta_n}{\partial x^m} - \frac{\partial \theta_m}{\partial x^n}\,, \qquad \varphi_{mn} = \frac{\partial \varphi_n}{\partial x^m} \quad \frac{\partial \varphi_m}{\partial x^n}\,. \tag{19}$$

φ_{mn} is thus a component of the electromagnetic intensity and has been denoted by B_{mn} in equation (4). It adds to simplicity and does not limit the present purpose to regard $\theta_\cdot$ as a constant and to place $\alpha\theta_\cdot = -1$. Thus

$$h_{mn} = \theta_{mn} - \varphi_{mn}\,. \tag{20}$$

This illustrates a characteristic feature of the five-dimensional notation, in which a quantity such as h_{mn} often appears as the sum or difference of two parts. It has been suggested that this division of an entity into two parts in four-dimensional representation may be the source of difficulties due to the appearance of infinities. An infinite value may arise in the separate parts

on account of the way they are separated, but there is no infinity in the entity thus artificially divided. The same feature is observed in the expression $(a_m + \alpha\theta.\varphi_m)$ or in $(\theta_m - \varphi_m)$. For the sake of uniformity h_m is introduced so that

$$h_m = \theta_m - \varphi_m$$

and consequently

$$h_{mn} = \frac{\partial h_n}{\partial x^m} - \frac{\partial h_m}{\partial x^n}. \tag{21}$$

Returning to equation (11) and placing $\mu = m$

$$\frac{\partial F^{m\nu}}{\partial x^\nu} = J^m$$

i.e.

$$\frac{\partial F^{mn}}{\partial x^n} + \lambda F^{m5} = J^m.$$

By means of equations (10) this takes the form:

$$\frac{\partial f^{mn}}{\partial x^n} + \lambda(f^{m}. - \alpha\tilde{\varphi}_n f^{mn}) = J^m.$$

On placing $f^{mn} = h^{mn}\chi$ and $J^m = s^m\chi$ this leads to

$$\frac{\partial h^{mn}}{\partial x^n} = s^m + \lambda^2\vartheta^m$$

by means of equation (18).

It is convenient to introduce the current vector

$$P^m = s^m + \lambda^2\varphi^m$$

so that the equation takes the form

$$\frac{\partial h^{mn}}{\partial x^n} = P^m + \lambda^2 h^m. \tag{22}$$

This is of the form postulated by MIE, the term $(P^m + \lambda^2 h^m)$ taking the place of the current density, but in Mie's theory h_{mn} is not of the form (21) and is not necessarily related to φ_{mn} by an equation of the form (20). The appearance of the term $\lambda^2 h^m$ as part of the current may be compared with a suggestion

made by Dirac that the electron current is represented by $\lambda^2\varphi^m$ [10], while in a wider treatment of the problem of the electromagnetic field B. HOFFMANN [11] has shown that his similarity theory of relativity requires the inclusion of such terms.

The presence of λ^2 as a function of the coordinates adds to the difficulty of interpreting the theory and of obtaining numerical results for comparison with experiment. It will thus be supposed that $\lambda^2 = -k^2$, where k is a constant. This means that x^5 occurs in the factor $\exp[ikx^5]$. It should be noted that this introduces a difficulty with regard to the function χ, defined in equation (17), for since φ_m is a non-integrable function $\int \varphi_m dx^m$ can only be determined if a path of integration is assumed. Nevertheless the same form of the equations will be adopted, λ^2 now being replaced by the constant $-k^2$.

The Energy-Momentum Tensor.

In order to carry out the analogy described at the beginning of this paper a tensor S_{mn} is required so that the law of gravitation may be expressed in the form

$$P_{mn} - \frac{1}{2} g_{mn} P = \frac{8\pi\varkappa}{c^4} S_{mn} . \tag{23}$$

The left hand side of this equation has the value

$$R_{mn} - \frac{1}{2} g_{mn} R - \frac{8\pi\varkappa}{c^4} \left(\varphi_{mt}\varphi_{nt} - \frac{1}{4} g_{mn} \varphi_{rs}\varphi_{rs} \right) ,$$

R_{mn} and R representing the contribution from gravitational effects and the remainder from electromagnetic effects. Together they arise from the geometry of the five-dimensional continuum.

For the sake of brevity let the electromagnetic terms within the bracket be denoted by M_{mn}. It is required to find the form of S_{mn} and to examine the divergence

$$\frac{\partial}{\partial x^n} (M_{mn} + S_{mn}) . \tag{24}$$

For the purpose of this theory gravitational effects can be neglected, it

---

[10] P. A. M. DIRAC: *Proc. Roy. Soc.*, A **209**, 291 (1951).
[11] B. HOFFMANN: *Phys. Rev.*, **89**, 1, 52 (1953).

being supposed that their influence in the theory of the electron is very slight. There is thus no need to distinguish between contravariance and covariance.

The tensor (S_{mn}) representing the electron will depend upon θ_{mn}, φ_{mn}, θ_m and φ_m. From the form taken by expressions corresponding to S_{mn} in Mie's theory, in the theories of nuclear fields and particularly in Bopp's theory it is anticipated that it will contain interaction terms of the type $\varphi_{ml}\theta_{ml}$, $k^2\varphi_m\theta_n$, $k^2\varphi_m\varphi_n$ and $k^2\theta_m\theta_n$. These considerations lead to the suggestion that it may be identified with the following expression

$$S_{mn} = \tfrac{1}{2}\delta_{mn}\{\varphi_{rs}\theta_{rs} + 2k^2\varphi_r\theta_r - k^2(\varphi_r\varphi_r + \theta_r\theta_r)\} - \\ - \varphi_{ml}\theta_{nl} - \theta_{ml}\varphi_{nl} - k^2(\varphi_m\theta_n + \theta_m\varphi_n) + k^2(\varphi_m\varphi_n + \theta_m\theta_n)\,.$$

Thus the sum $(M_{mn} + S_{mn})$ can be written in the form

$$M_{mn} + S_{mn} = h_{ml}h_{nl} + k^2h_mh_n - \theta_{ml}\theta_{nl} - \\ - \tfrac{1}{4}\delta_{mn}(h_{rs}h_{rs} + 2k^2h_rh_r - \theta_{rs}\theta_{rs})\,. \tag{25}$$

This form is convenient for the derivation of the divergence of $(M_{mn} + S_{mn})$.

If the forms of θ_{mn} and h_{mn} given by equations (19) and (21) be noted, it follows that

$$\frac{\partial}{\partial x^n}(M_{mn} + S_{mn}) = h_{lm}\left(\frac{\partial h_{ln}}{\partial x^n} + k^2h_l\right) + \theta_{ml}\frac{\partial\theta_{ln}}{\partial x^n}\,, \tag{26}$$

it being assumed that $\partial h_n/\partial x^n = 0$.

In the notation of equation (4) the divergence of the electromagnetic energy tensor is written in the form:

$$\frac{\partial T_{mn}}{\partial x^n} = -B_{mn}S_n\,,$$

where (S_n) is the current density. It is thus suggested that equation (26) should be converted to the same form. This change can be brought about by writing

$$\frac{\partial h_{ln}}{\partial x^n} + k^2h_l = P_l$$

in agreement with the field equation (22) when $\lambda^2 = -k^2$, and by placing

$$\frac{\partial\theta_{ln}}{\partial x^n} = P_l\,. \tag{27}$$

With these substitutions

$$\frac{\partial}{\partial x^n}(M_{mn} + S_{mn}) = \varphi_{mn} P_n \,, \tag{28}$$

since $h_{ml} = \theta_{ml} - \varphi_{ml}$.

In this way equations have been derived differing only slightly from those of BOPP.

The form of equation (28) calls to mind a relation derived in the quantum mechanical theory of the electron. In this theory the energy tensor is

$$T_{mn} = \frac{hc}{4\pi i}\left(\psi^+ \alpha_n \frac{\partial \psi}{\partial x^m} - \frac{\partial \psi^+}{\partial x^m}\alpha_r \psi\right) - e\varphi_m \psi^+ \alpha_n \psi \,, \tag{29}$$

the symbols having their usual meaning.

But in this form the tensor is not symmetric. The symmetric energy-momentum tensor is ([12])

$$\Theta_{mn} = T_{mn} - \frac{hc}{8\pi i}\frac{\partial}{\partial x^l}(\psi^+ \alpha_m \alpha_n \alpha_l \psi) \tag{30}$$

and satisfies the relation

$$\frac{\partial \Theta_{mn}}{\partial x^n} = e\varphi_{mn}\psi^+ \alpha_n \psi \,. \tag{31}$$

Thus if P_n and $e\psi^+\alpha_n\psi$ be regarded as denoting the current density, equations (28) and (31) may be regarded as expressing the same thing. The quantities in $(M_{mn}+S_{mn})$ and Θ_{mn} are differently expressed, but

$$\int (M_{mn} + S_{mn})\,\mathrm{d}v = \int \Theta_{mn}\,\mathrm{d}v \,, \tag{32}$$

the integration being over the three dimensional space volume v, denotes the equality of quantities measured in terms of the field and in terms of the electron considered as a particle. It is an expression of the idea at the basis of the theory of ABRAHAM and LORENTZ that the momentum and energy of the electron can be obtained from the electromagnetic momentum and energy of the field.

In conclusion the static case will be considered in order to find the value of the constant k in terms of familiar quantities. In this case the energy of the electron considered as a particle at rest is m_0c^2. This magnitude is derived from the right hand side of equation (32). This quantity is calculated from the integral of the left hand side by considering points of space where there is no current or charge ($P_l = 0$). The field quantities do not depend on the

([12]) W. PAULI: *Handbuch der Physik*, 2nd Edn., **24**/1, p. 235 (1933).

time and all the components of (θ_m) and (φ_m) vanish except the fourth, which will be denoted respectively by $\theta_4 = i\theta$ and $\varphi_4 = i\varphi$. Equation (22) becomes

$$\frac{\partial h_{mn}}{\partial x^n} = -k^2(\theta_m - \varphi_m) \tag{33}$$

and (27)

$$\frac{\partial \theta_{mn}}{\partial x^n} = 0 . \tag{34}$$

The relation $\partial\varphi_n/\partial x^n$ is assumed to hold as in the electromagnetic theory and as it has been supposed that $\partial h_n/\partial x^n = 0$, it follows that $\partial\theta_n/\partial x^n$ also vanishes. Thus it follows from (34) that in the present case $\nabla^2\theta = 0$. For the purpose of making a calculation it is more convenient to use ordinary electrostatic units instead of those of the rationalized system.

A solution is then $\theta = e/r$, where e is a constant which is identified as the fundamental unit of charge.

From (33) and (34) it follows similarly that

$$\nabla^2\varphi = -k^2(\theta - \varphi)$$

and with $\theta = e/r$ a spherically symmetrical solution is

$$\varphi = e(1 - e^{-kr})/r .$$

The corresponding component of (h_m) is $e\,e^{-kr}/r$. The energy density $(M_{44}+S_{44})$ obtained from the expression (25) is, in the static case, $\sum_l (h_{4l}^2 - \theta_{4l}^2 + k^2h_4^2)/8\pi$.

$$h_{4l} = \frac{\partial h_l}{\partial x^4} - \frac{\partial h_4}{\partial x^l} = i\frac{\partial}{\partial x^l}(\theta - \varphi)$$

in this case.

Thus $\sum_l h_{4l}^2 = \left\{\frac{\partial}{\partial r}(\theta - \varphi)\right\}^2$, on account of the spherical symmetry. In the same way $\sum_l \theta_{4l}^2 = -(\partial\theta/\partial r)^2$. On integrating this energy density over the whole of space it is found that the total energy is $ek/2$. The details of the calculation will be found in Bopp's paper.

Thus from the equation (32)

$$1/k = e^2/2m_0c^2 . \tag{35}$$

This account of the theory of the electron follows the lines previously sug-

gested as the basis of the theory of nuclear fields ([13]) and thus suggests that the theories of fundamental particles which are regarded as generators of fields may be developed in the same general way.

In conclusion it is of interest to examine the equations of the set (11) in which $\mu = 5$. It has not been required in the foregoing discussion but the assumption $\partial\theta_n/\partial x^n = 0$, which was made in considering the solution in the static case imposes a condition on the fifth equation. Since $(F^{\mu\nu})$ is antisymmetric, F^{55} vanishes and the equation with $\mu = 5$ is

$$\frac{\partial F^{5n}}{\partial x^n} = J^5 ,$$

and writing $F^{mn} = h^{mn}\chi$, $a^m = \theta^m\chi$ as before, and in addition $J^5 = s^5\chi$, $J^m = s^m\chi$, it is not difficult to show that it can be reduced to the form

$$\frac{\partial(\lambda\theta^n)}{\partial x^n} = S_5 - \frac{1}{2}\alpha\varphi_{mn}h^{mn} . \tag{36}$$

Thus when λ is constant the assumption $\partial\theta^n/\partial x_n = 0$ leads to $s_5 = \frac{1}{2}\alpha\varphi_{mn}h^{mn}$, which may be regarded as a definition or interpretation of this component of the current.

([13]) H. T. Flint: *Proc. Roy. Soc.*, **185**, 14 (1945); *Phil. Mag.*, **38**, 22 (1947); H. T. Flint and N. Symonds: *Phil. Mag.*, **39**, 413 (1948); E. M. Williamson: *Nuovo Cimento*, **10**, 113 (1953).

RIASSUNTO (*)

Si propone una teoria dell'elettrone in analogia con la teoria gravitazionale della materia. Si tratta essenzialmente di una teoria classica basata su equazioni della forma suggerita da Mie. L'uso dell'analisi pentadimensionale risulta naturale data l'apparizione, oltre il campo elettromagnetico, di un campo del tipo del vettore di Yukawa. Si porta così la teoria dell'elettrone sullo stesso piano con le teorie del campo nucleare. L'analogia conduce direttamente ai risultati ottenuti da Bopp e dà conto della massa dell'elettrone per mezzo dell'energia del campo.

(*) *Traduzione a cura della Redazione.*

Relativistic Scattering of Electrons and the Born Approximation.

E. CORINALDESI

Dublin Institute for Advanced Studies

(ricevuto il 19 Dicembre 1953)

It is generally accepted that, for scattering of high energy electrons by a potential $V(r)$, the validity of the Born approximation does not improve with increasing energy. In fact, PARZEN [1] has shown that the exact phase shift $\delta_l(k)$ for the Dirac and for the Klein-Gordon equation tends to the limit

$$\delta_l(\infty) = \int_0^\infty V(r)\,\mathrm{d}r$$

for $k \to \infty$, if the potential is such that the integral converges, while the Born approximation yields the formula

$$\big(\exp\,[2i\delta_l(\infty)] - 1\big)/2i = \int_0^\infty V(r)\,\mathrm{d}r\,.$$

Therefore, if $V(r)$ is large, the approximate value of $\delta_l(\infty)$ differs appreciably from the exact value.

It may now be noted that the non-validity of the Born approximation at infinite energy has thus been proved only for the calculation of the single phases, and not for the scattering amplitude $f(\theta)$. Since with increasing energy an increasing number of phases must be considered for the calculation of $f(\theta)$, until for $k \to \infty$ all are equal and must be included, it is natural to compare the exact scattering amplitude at infinite energy with the one given by the Born approximation. One then finds that they are both expressions of the type

$$\lim_{k\to\infty} \frac{1}{k} \sum_{l=0}^{\infty} (2l+1) F\big(\delta_l(k)\big) P_l(\cos\theta)\,:$$

for $k \to \infty$, the factor $F\big(\delta_l(\infty)\big)$ becomes independent of l and can be taken out of

[1] G. PARZEN: *Phys. Rev.*, **80**, 261, 355 (1950).

the summation leaving an expression proportional to

$$\lim_{k\to\infty} \frac{1}{k} \sum_{l=0}^{\infty} (2l+1) P_l(\cos\theta) ,$$

which is of ambiguous meaning. In fact, the series of Legendre's polynomials can be summed to zero for $\theta \neq 0$, but diverges for $\theta = 0$.

In order better to illustrate the nature of the discontinuity, one can take as an example the amplitude

$$f(\theta) = -\frac{1}{4\pi} \int \exp\left[ik(\boldsymbol{n}_0 - \boldsymbol{n})\cdot\boldsymbol{r}\right](2E \exp\left[-ar\right] - \exp\left[-2ar\right]) \, \mathrm{d}\boldsymbol{r} =$$

$$\frac{4a}{\pi}\left[\frac{E}{(a^2 + k^2|\boldsymbol{n}_0 - \boldsymbol{n}|^2)^2} - \frac{1}{(4a^2 + k^2|\boldsymbol{n}_0 - \boldsymbol{n}|^2)^2}\right]$$

derived from the Born approximation as applied to the Klein-Gordon equation with $V(r) = \exp\left[-ar\right]$. For $k \to \infty$, $f(\theta) \to 0$ as long as $\boldsymbol{n}_0$ and $\boldsymbol{n}$ do not coincide, but diverges if one first takes $\boldsymbol{n}_0 \equiv \boldsymbol{n}$ and then lets the energy tend to infinity.

The above argument holds also for the case of a potential without singularity at the origin and behaving like $V(r) = (\beta/r) + O(1/r^2)$ for large r, also yielding a value of $\delta_l(\infty)$ which is independent of l.

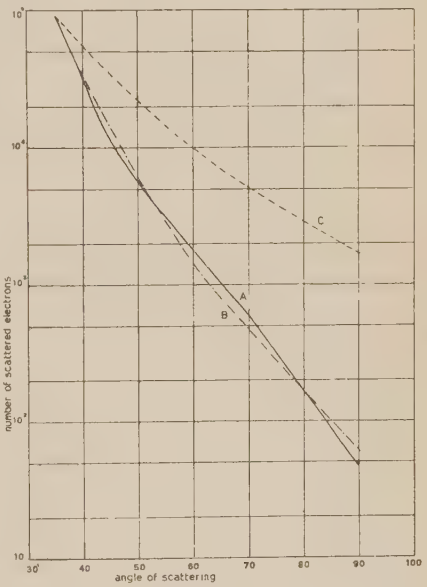

Fig. 1. – *A*) Typical angular distribution obtained at 116 MeV with a 0.002-inch gold foil. *B*) Scattering by potential $V(r) = -(Ze^2/r)(1 - \exp\left[-r/R\right])$ (R = radius of the nucleus of gold) according to the Born approximation for the Dirac equation. *C*) Scattering by a point charge.

One concludes that there is no particular reason to disbelieve that the validity of the Born formulae for the amplitude [1]

$$f_3(\theta) = \frac{E+1}{2}\left[1 + \left(\frac{k}{E+1}\right)^2 \cos\theta\right] f_{\text{n.r.}}(\theta) ,$$

$$f_4(\theta) = \frac{E+1}{2}\left(\frac{k}{E+1}\right)^2 \sin\theta \, f_{\text{n.r.}}(\theta) \quad \text{(Dirac eq.)}$$

[1] R. HOFSTADTER H. R. FECHTER and J. A. MCINTYRE: *Phys. Rev.*, **91**, 422 (1953).

with

$$f_{\text{n.r.}}(\theta) = \frac{1}{2\pi}\int \exp\left[ik(\boldsymbol{n}_0 - \boldsymbol{n})\cdot\boldsymbol{r}\right] V(r)\,\mathrm{d}\boldsymbol{r}$$

improves with increasing energy. (The same holds for the corresponding formula in the Klein-Gordon case).

Consequently attempts can be made to fit the differential cross-section for scattering of 116 MeV electrons, recently published by HOFSTADTER, FECHTER and MCINTYRE [2], with the theoretical cross-section given by the Born approximation. Taking e.g. the potential $V(r) = -(Ze^2/r)(1 - \exp[-r/R])$, which, although somewhat artificial from a physical viewpoint, is smooth enough to exclude the presence of diffraction peaks (not actually found experimentally), one obtains the encouraging agreement shown in the figure.

I have pleasure in expressing my thanks to Prof. MARIO AGENO for his interest in this work and for generously providing working facilities in the Physics Laboratory of Istituto Superiore di Sanità in Rome.

IL NUOVO CIMENTO Vol. XI, N. 2 1° Febbraio 1954

On Corben's Formulation of the Dirac Equation.

O. Bergmann and N. Baker

Department of Mathematical Physics, University of Adelaide, South Australia

(ricevuto il 21 Dicembre 1953)

In a series of papers which appeared recently in this journal (1), Corben has proposed a new formulation of Dirac's equation using as starting point the five-dimensional method of unified field theory. It is assumed that the wave-function is periodic in the fifth coordinate and that only the averages (over a period) of the fifth coordinate have physical significance. He obtains for particles of spin 1/2

$$[\gamma_k \partial_\kappa + i\lambda\gamma_5 + \mu]\Psi = 0 \,, \tag{1}$$

which differs from Dirac's equation by the term $i\lambda\gamma_5$; where λ may be real or imaginary and is proportional to the charge of the particle.

A study of this equation has been made by Caldirola and Gulmanelli (2). Loinger and Bellomo and Loinger (3). The latter authors found a transformation which reduces equation (1) to Dirac's equation with the mass given by $m = (\mu^2 + \lambda^2)^{\frac{1}{2}}$. Their transformation can be written more simply in the form

$$\Psi' = \exp[-i\gamma_5 N]\Psi = U^{-1}\Psi \tag{2}$$

with

$$\operatorname{tg} 2N = -\lambda/\mu \,. \tag{3}$$

Then Ψ' fulfills

$$\begin{cases} [\gamma_k \partial_k + m]\Psi' = 0 \\ m = (\mu^2 + \lambda^2)^{\frac{1}{2}} \,. \end{cases} \tag{4}$$

The transformation (2), which is incidentally a special case of Foldy's transformation (4), is also valid for imaginary λ, although it is no longer unitary and does not conserve the normalization of Ψ. Bellomo and Loinger deduce from the unitary character of the transformation (2) for real λ the complete physical equivalence of Corben's with Dirac's theory. The case of imaginary λ has not been considered by them, probably because it cannot be put into a five-dimensional form. However, we think that even for real λ the equivalence of both formulations is not of such a universal character. It is obvious that, if

(1) H. C. Corben: *Nuovo Cimento*, **9**, 235, 580, 1071 (1952); *Phys. Rev.*, **88**, 677 (1952).

(2) P. Caldirola and P. Gulmanelli: *Nuovo Cimento*, **9**, 834 (1952).

(3) A. Loinger: *Nuovo Cimento*, **9**, 885 (1952); E. Bellomo and A. Loinger: *Nuovo Cimento*, **9**, 1240 (1952).

(4) L. L. Foldy: *Phys. Rev.*, **84**, 168 (1951), also J. M. Berger, L. L. Foldy and R. K. Osborn: *Phys. Rev.*, **87**, 1061 (1952).

the operators O' and $O = UO'U^{-1}$ represent the same physical quantity in Dirac's and Corben's theory respectively, the equivalence of the two is complete. It is not clear, however, why an operator which represents an interaction of the spin 1/2 particles with other fields (meson or neutrino fields, etc.) should be transformed in this way; indeed, it seems more natural to insert the interaction terms in their conventional form in the fundamental equation (1) of Corben's formalism. Any interaction term can be split into two terms:

$$P = A_k\gamma_k + B_k\gamma_k\gamma_5 \tag{5}$$

which anticommutes with γ_5 and

$$Q = C\cdot 1 + D_{ik}\gamma_i\gamma_k + iE\gamma_5 \tag{6}$$

which commutes with γ_5. The addition of a term (5) to (1) leaves the equivalence unaffected, i.e. it follows

$$[\gamma_k\partial_k + m + P]\Psi' = 0\,. \tag{7}$$

The functions A_k can be interpreted e.g. as electromagnetic four-potentials, whereas B_k may be a pseudovector coupling with a meson field. An interaction term Q, however, will not appear in the same form in the transformed equation, which runs

$$\left[\gamma_k\partial_k + m + Q\frac{1}{m}(\mu - i\gamma_5\lambda)\right]\Psi' = 0. \tag{8}$$

Consequently, the equivalence does not hold in this case for *charged* particles ($\lambda \neq 0$). The quantites C, D_{ik} and E might be interpreted as scalar, tensor and pseudoscalar coupling of Corben's particle with other fields.

We should like to remark that a consistent application of the five-dimensional formalism requires that the interaction terms are covariant in five dimensions, which implies that a coupling term involving derivatives of field variable will generally contain a term in ∂_5 – this derivative has to be replaced by $i\lambda$ and thus appears only for charged particles.

It is perhaps not without interest that in the Dirac equation a similar transfomation can be used to transform a term $\gamma_i p_i + \mu$ (no summation) into a multiple of the unit matrix provided p_i is a constant and the interaction terms involve only matrices which anticommute with γ_i.

IL NUOVO CIMENTO Vol. XI, N. 2 1° Febbraio 1954

The Anomalous Large Angle Scattering of μ-Mesons.

J. P. Davidson

Centro Brasileiro de Pesquisas Fisicas - Rio de Janeiro, Brazil

(ricevuto il 29 Dicembre 1953)

Several recent experiments ([1-5]) indicate an anomalous large angle scattering of μ-mesons with a cross-section of the order of 10^{-28} cm^2/nucleon. Calculations of the cross-section for inelastic collisions of the μ-mesons with individual protons of the nucleus made by Amaldi and Fidecaro ([1]) (in iron) and by George, Redding and Trent ([3]) (in lead) account only for a very small percentage of the observed anomalous scattering. This would seem to indicate that the mechanism responsible for this scattering involves the entire nucleus rather than the individual nucleons.

A mechanism for the production of stars by μ-mesons has been given ([6]) in which the coulomb field of the rapidly moving meson is replaced by its equivalent photon spectrum (the Weizsäcker-Williams method). In the present case the virtual photon beam does not give rise to appreciable star production since the energy is only of the order of a few hundred MeV; however, it is well known that all nuclei possess a « giant » photon resonance in the neighborhood of 15-20 MeV which could be excited by the virtual photons.

One may consider a rapidly moving charged particle of energy E to be equivalent to a beam of photons whose number with energy between $\hbar\omega$ and $\hbar\omega + \mathrm{d}(\hbar\omega)$ is given by

$$N(\hbar\omega)\,\mathrm{d}(\hbar\omega) = \frac{2\alpha}{\pi} \ln\left(\frac{E}{\hbar\omega}\right) \frac{\mathrm{d}(\hbar\omega)}{\hbar\omega}\,, \tag{1}$$

α being the fine structure constant.

For $\hbar\omega_0$, the energy at which the photon absorption is a maximum, recent experiments on the photonuclear effect give ([7])

$$\hbar\omega_0 = 37\, A^{-0.186}\ \mathrm{MeV} \tag{2}$$

([1]) E. Amaldi and G. Fidecaro: *Nuovo Cimento*, **7**, 537 (1950).
([2]) W. L. Whittemore and R. P. Shutt: *Phys. Rev.*, **88**, 1312 (1952).
([3]) E. P. George, J. L. Redding and P. T. Trent: *Proc. Phys. Soc.*, A **64**, 533 (1953).
([4]) M. L. T. Kannangara and G. S. Shrikantia: *Phil. Mag.*, **44**, 1091 (1953).
([5]) B. Leontic and W. A. Wolfendale: *Phil. Mag.*, **44**, 1101 (1953).
([6]) E. P. George and J. Evans: *Proc. Phys. Soc.*, A **63**, 1248 (1950).
([7]) R. Montalbetti, L. Katz and J. Goldemberg: *Phys. Rev.*, **91**, 659 (1953).

and for the cross-section integrated from 0 to 27.5 MeV ([8])

$$\int_0^{27.5} \sigma_n(\hbar\omega)\,\mathrm{d}(\hbar\omega) = 5.2\cdot 10^{-4}\,A^{1.8}\ \text{MeV-barns}\,. \tag{3}$$

If one considers the « giant » resonance to have the character of a delta function centered at $\hbar\omega_0$ then one may write

$$\sigma_n(\hbar\omega) = 10.4\cdot 10^{-4} A^{1.8}\,\delta(\hbar\omega - \hbar\omega_0)\ \text{barns}\,. \tag{4}$$

Assuming the photon absorption results only from this « giant » resonance then no harm is done in writing $\hbar\omega_{\max} \approx \infty$ even for incident μ-mesons with $E = 300$ MeV. Thus

$$\sigma_n = \frac{1}{A}\int_0^{\infty} \sigma_n(\hbar\omega) N(\hbar\omega)\,\mathrm{d}(\hbar\omega) = \tag{5}$$

$$= 6.54 A^{0.986} \ln (E A^{0.186}/37)\cdot 10^{-32}\ \text{cm}^2/\text{nucleon}\,.$$

When evaluated for lead with $E = 300$ MeV, equation (5) gives $\sigma_n = 3.34\cdot 10^{-25}$ cm^2/nucleon. While this is somewhat lower than the observed values it must be remembered that no account has been taken of the not insignificant high energy « tail » to the photon absorption cross-section. Finally, it is of interest to note that σ_μ is essentially proportional to A, which seems to be in agreement with the experimental evidence (cf. Table 4, reference ([5])).

Of course all charged particles of sufficient energy should produce such scattering; however, for sufficiently energetic electrons the effect will be masked by the bremsstrahlung while for protons and π-mesons it will be masked by the strong nuclear scattering.

It would seem that the anomalous scattering of μ-mesons can be explained by the interaction of the meson's coulomb field with the entire target nucleus, and thus it is not necessary to postulate an interaction between the μ-meson field and the nucleon field in addition to the Fermi interaction. A more complete discussion of this scattering process will be published elsewhere.

The author wishes to express his appreciation to Profs. U. Camerini and J. Leite Lopes for stimulating conversations.

([8]) L. W. Jones and K. M. Terwilliger: *Phys. Rev.*, **91**, 699 (1953).

IL NUOVO CIMENTO Vol. XI, N. 2 1° Febbraio 1954

On a Possible Negative K→π-Meson Decay.

E. Amaldi, G. Baroni, C. Castagnoli, G. Cortini, C. Franzinetti and A. Manfredini

Istituto di Fisica dell'Università - Roma
Istituto Nazionale di Fisica Nucleare - Sezione di Roma

(ricevuto il 12 Gennaio 1954)

In an emulsion exposed at high altitude during the International Expedition held in Sardegna 1953, we have observed a star due to a neutral particle containing 11 black prongs, 6 gray and 6 shower particles.

Among the gray tracks two are due to K-mesons.

The first one crosses 8 emulsions with a total range of 12.1 mm. At the end of its range it apparently decays into a σ-meson which crosses 7 emulsions with a total range of 23.2 mm. The σ-meson gives a 3 prong star; of the three prongs whose lenghts are 138 μ, 69 μ and 40 μ respectively, the first two have the typical appearence of proton tracks.

The probability that such a star is due to the capture of a μ-meson, is not larger than $8 \cdot 10^{-4}$ [1]. Furthermore two independent determinations of the mass of this particle based on its range and the grain density measured in 2 emulsions close to its origin, give

$$(1) \qquad \begin{cases} m_\sigma = 305 \pm 43 \ m_e , \\ m_\sigma = 274 \pm 43 \ m_e . \end{cases}$$

From these three independent facts one can conclude that the probability that this track is due to a μ-meson, is certainly not larger than $5 \cdot 10^{-6}$.

Therefore we can assume in the following that the particle emitted at the end of the K-meson is a negative π-meson whose kinetic energy turns out to be, from its range,

$$(2) \qquad T_{\pi^-} = 38.5 \pm 2.5 \text{ MeV} .$$

The grain-density variation along the track of the corresponding K-meson shows clearly that this particle has been emitted from the star.

From grain density measurements in the first 4 emulsions one can conclude that the value of its mass is

$$(3) \qquad m_{K_1} = 1\,060 \pm 50 \ m_e .$$

[1] H. Morinaga and W. F. Fry: *Nuovo Cimento*, **10**, 308 (1953).

The second K-meson crosses 9 emulsions with a total range of about 18 mm. It shows a scattering or a decay 3 mm before to escape from the last emulsion. From preliminary measurements of its grain density variation one gets $m_{K_2} \sim$ $\sim 1000\ m_e$.

A more detailed experimental study of the star and in particular of these two K-mesons is in progress.

We would like however to point out that the simplest interpretation of event K_1 is to attribuite it to a K-meson decaying in a π-meson, although other interpretations can not be ruled out. For instance, as pointed out to us by Dr. LEVI SETTI, one could try to interpret K_1 as a particular case of that unusual type of stars associated to the capture of K-mesons which have been observed by LAL and coworkers (2). The present case would then correspond to a nuclear interaction of a K-meson with emission of a π^- and only invisible prongs.

At the moment it is impossible to evaluate the probability of such an event, although one would expect it to be low. Therefore in the following we shall stick to the assumption of a decay process.

Under this assumption K_1 constitutes the first example of a negative K-decay observed in nuclear emulsions and the probability that the decay happens when the K_1-meson is still in flight, is not larger than 10%.

Its time of flight between the emission from the star and the decay is $1.4 \cdot 10^{-10}$ s. On the other hand we know that the probability that a meson is captured by a light or a heavy element inside the emulsion are respectively 30 and 70%.

In heavy elements its K-orbit is almost completely inside the nucleus and there fore one has to consider three alternative possibilities. If the K-meson has a not too weak interaction with nucleons the observed event must be due to a K-meson captured by a light element. If the K-meson has an extremely low interaction with nucleons it could also be captured by a heavy element; in this case however one has to consider that a π-meson of 40 MeV has a probability of about 20-30% of escaping from a heavy nucleus without producing at least a small recoil. One has finally to consider also the possibility that the time necessary for the K-meson to be captured in the K-orbit is longer or at least of the same order of magnitude of its mean life (let us say $\gtrsim 10^{-10}$ s).

Apart from this problem one can make the following remarks on the various possible interpretations of the observed event considered as a decay:

1) It is not a new example of the well established K-meson, decaying according to the process

$$K \to \mu + ? + ? \,. \tag{4}$$

2) It is not a χ-meson decaying according to the process (3)

$$\chi \to \pi + \gamma \,, \tag{5}$$

because the $p\beta$ of the π-meson emitted in process (5) is about 180 MeV/c while the π-meson in the present case has a $p\beta$ of about 70 MeV/c.

The possibility that our event is due to a χ-meson decaying in flight can be excluded because in order to justify the low energy of the π-meson it would be necessary to attribute to it such a high velocity that the grain density would be about 1.6 g_{min} while it is much higher.

3) If we admit the existence of processes of the following types

$$\chi^{\pm} \to \pi^{\pm} + \gamma + \gamma \,, \tag{6}$$

$$\chi^{\pm} \to \pi^{\pm} + \nu + \nu \,, \tag{7}$$

(2) D. LAL, Y. PAL and B. PETERS: *Phys. Rev.*, **92**, 438 (1953).

(3) M. G. K. MENON and C. O'CEALLAIGH: *Cosmic Ray Conference Bagnères de Rigorre*, 1953.

they would explain both the present event as well as the χ-meson observed by other authors ([3]).

4) The observed event could be interpreted also according to the following process

$$\tau^- \to \pi^- + \pi^0 + \pi^0 \,. \tag{8}$$

In this case, assuming for the τ^--meson a mass equal to that of the

$$\tau^+ \cdot \pi^+ + \pi^+ + \pi^- \,,$$

the maximum kinetic energy of the π^- would be slightly higher than the observed values (2).

Finally, from what we have stated above, it is clear that if the present event is due to a two body decay the neutral particle would have a mass of about 550 m_e; we are now looking for its possible decay products.

On the Possible Ejection of a Meson-Active Triton from a Nuclear Disintegration.

A. Bonetti, R. Levi Setti, M. Panetti

Istituto di Scienze Fisiche dell'Università - Milano
Istituto Nazionale di Fisica Nucleare - Sezione di Milano

L. Scarsi

Istituto Nazionale di Fisica Nucleare - Sezione di Milano

G. Tomasini

Istituto di Fisica dell'Università - Genova

(ricevuto il 12 Gennaio 1954)

During the scanning of a batch of stripped emulsions flown at high altitude in the International Expedition of Sardinia 1953, we observed the ejection of an unstable heavy particle from a nuclear disintegration.

The particle is emitted in the forward hemisphere from a star of the type $22+3$ n; it travels for 8 mm in the first plate and comes to rest after 5 mm in the next plate. Two tracks seem to originate from the end of the primary track; one is 9.6 microns long and heavily ionizing and at first sight could be considered as a final scattering of the primary; the other one is ejected in the exactly opposite direction and has an ionization of about 1.7 minimum. The latter track was followed through 22 plates of the batch and was found to stop in the emulsion and to give rise to a 5 branch σ-star; its total range is 2.38 cm. See fig. 1.

Full mass measurements have been performed on the primary particle: $x - R$ with constant cells gives 5150 ± 1000 m_e; $x - R$ with constant sagitta gives $5150 \pm \pm 900$ m_e; blob-counting versus range, limited to 5 mm of the track in the first plate, gives $6400^{+1300}_{-1000} \cdot m_e$. The gradient of development, which limited a realiable blob-counting to the first five mm of the track, made gap-length versus range measurements unreliable: however this latter measurements also give a mass much higher than that of the proton, inside the limits of uncertainty due to difficulties in the calibration. From δ-ray counting it can be concluded that the particle is singly charged. The fast secondary has been shown by grain-counting and scattering-range measurements, to be a light meson; the evidence given by the σ-capture leading to a 7 branch star, whose visible energy is about 50 MeV, makes it practically

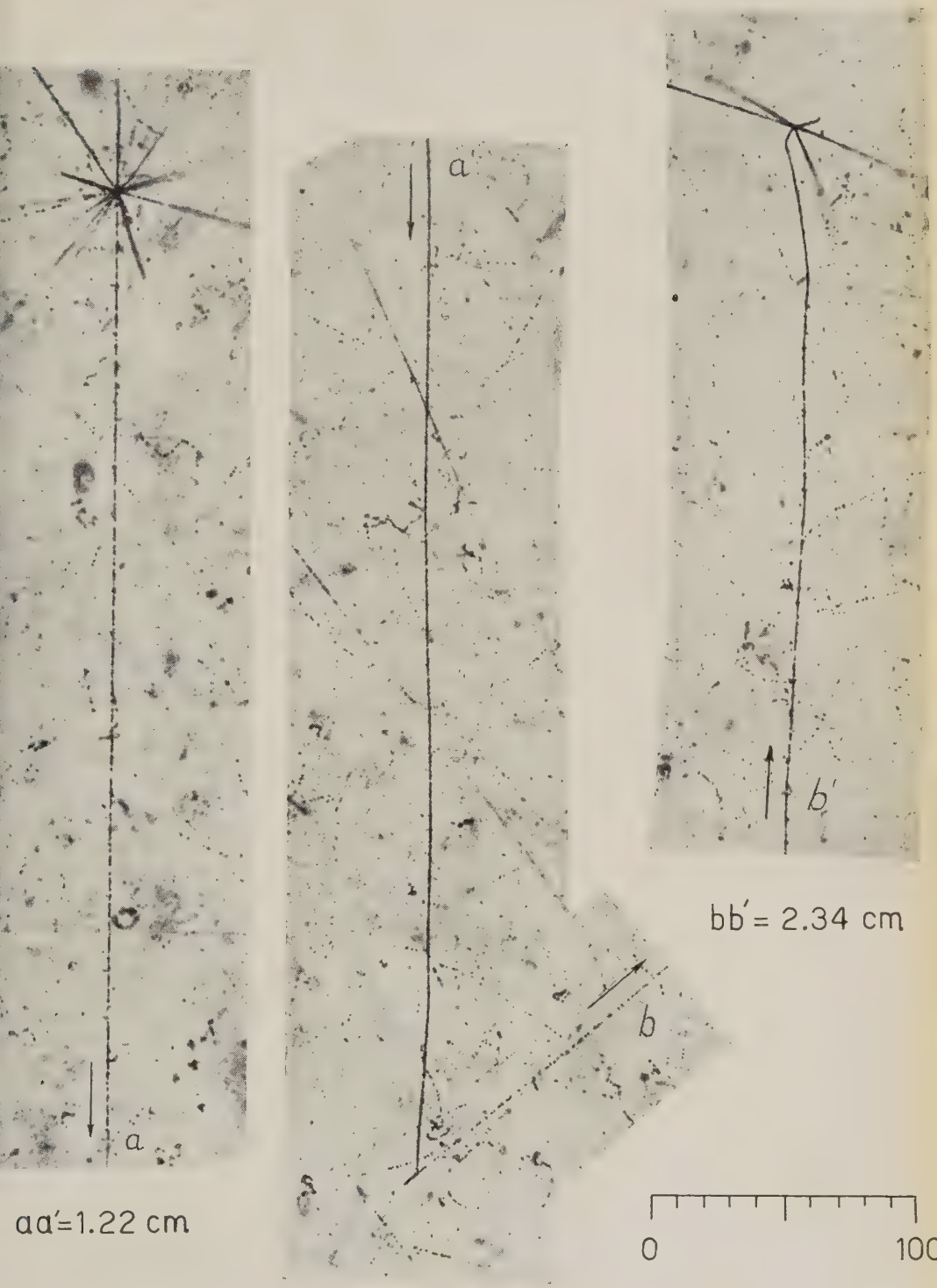

Fig. 1. (*Observed by* S. Conti)

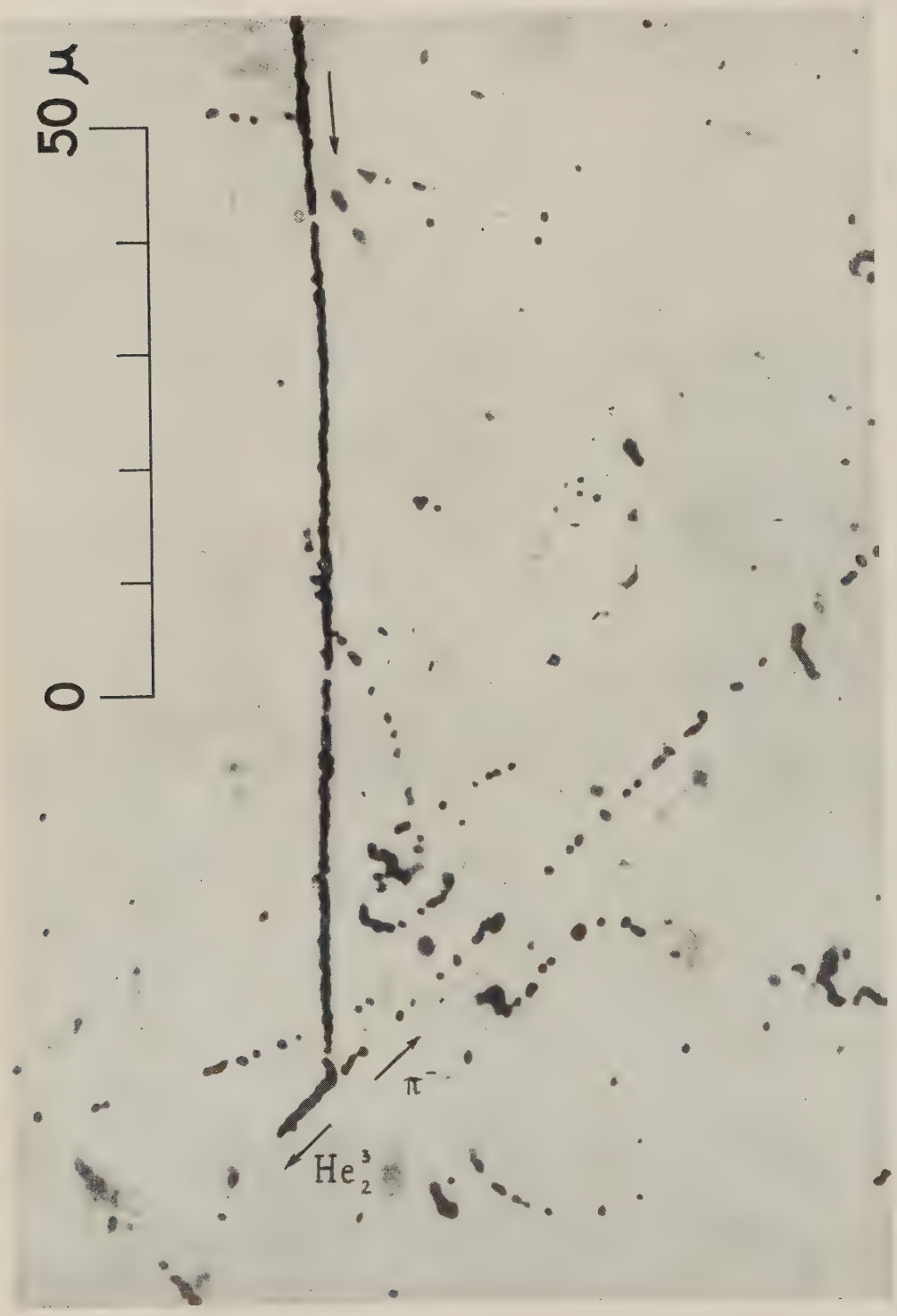

Fig. 2.

certain that the particle is a π^--meson. Its energy then turns out to be $39.4 \pm \pm 1$ MeV.

The end of the primary track has been investigated with the highest resolving power and magnification from both sides of the emulsion, in order to identify the point of origin of the meson: it was indistinguishable from the point of apparent scattering. This particular of the event is shown in fig. 2.

Apart that of a chance juxtaposition, several interpretations of this event are possible.

If the short branch is the continuation of the primary track and is not a recoil, the event could be the decay or the capture of a negative particle. In the first case the balance of energy and momentum would be ensured by some heavy neutral particle. In the second, the π^--meson would be the only visible product of the capture.

If the short branch is an evaporation track or a recoil, the event could still represent the capture of a negative particle. There is also the possibility that a negative heavy meson bound to a nucleus of charge 2 has either suffered internal capture or decayed with the emission of a π^--meson.

These hypotheses must remain purely speculative since the experimental data are insufficient to support anyone of them.

The most convenient interpretation is that of a two-body decay of the primary particle at rest. The short branch would then be the recoil. As we shall see, this interpretation fits very well all the experimental data.

Since the primary has been shown to be singly charged, the principle of charge conservation requires *a*) that the primary be positive, *b*) that the recoil be a fragment of charge $+2$. The collinearity of the two decay products suggests that the parent particle is at rest; this fact is supported by scattering and ionization measurements on the primary. If we assume that the recoil is a He_2^3-nucleus, knowing the kinetic energy of the π^--meson, we deduce the kinetic energy of the recoil from the conservation of momentum, and the mass of the primary particle from the conservation of both momentum and energy.

The energy of the recoil turns out to be 2.3 MeV, to be compared with $2.7 \pm \pm 0.6$ MeV as deduced from the range. The calculated mass of the primary is $5860 \pm 2\ m_e$; the energy release of the disintegration, 41.7 ± 1 MeV.

The assumption of a two-body decay appears therefore to fit very satisfactorily the experimental facts, if we identify the recoil with a He_2^3-nucleus. In this way we account for the measured charge and mass of the primary, as well as for the collinearity of the secondary tracks, and ensure the balance of momentum.

It cannot be excluded that the disintegration is accompanied by the emission of some light neutral particle of low momentum.

Neglecting this possibility, the process represents the spontaneous decay of an excited positive isobar of mass-number 3 and charge-number 1:

$$H_1^{3*} \to He_2^3 + \pi^- + Q\ .$$

The life-time of the excited isobar is longer than $3 \cdot 10^{-10}$ s.

The first example of an excited nuclear fragment undergoing spontaneous disintegration at rest with a life-time longer than 10^{-12} s was reported by DANYSZ and PNIEWSKI [1]. Further examples have been observed by TIDMAN *et al.* [2] and by CRUSSARD and MORELLET [3].

An interpretation proposed for this type of phenomena is that it represents

[1] M. DANYSZ and J. PNIEWSKI: *Phil. Mag.*, **44**, 348 (1953).

[2] D. A. TIDMAN, G. DAVIS, A. J. HERZ and R. M. TENNENT: *Phil. Mag.*, **44**, 350 (1953).

[3] J. CRUSSARD et D. MORELLET: *Compt. Rend. des Séances de l'Ac. Sc.*, **236**, 64 (1953).

a bound-V_1^0 decay. The Q-value as reported by CRUSSARD and MORELLET is very close to that of the free V_1^0 decay. So is ours.

If our event has been correctly interpreted, it gives a very precise example of this type of process, in accord with the theoretical picture of CHESTON and PRIMAKOFF (4), concerning the mesonic decay of bound-V_1^0 particles, and of PEASLEE (5), on V-fragments.

The following of the secondary to its end was made possible by the loan by Brussels of the other half of the stack of emulsions. For this we express our thanks to Prof. BAUDOUX. We are very grateful to Prof. G. P. S. OCCHIALINI for his invaluable criticisms of this work.

(4) W. B. CHESTON and H. PRIMAKOFF: *Cosmic Ray Conference Report*, Bagnères de Bigorre (1953), p. 179.

(5) D. C. PEASLEE: *Progress. Theor. Phys.*, **10**, 227 (1953).

PROPOSTE E DISCUSSIONI

(La responsabilità scientifica degli scritti inseriti in questa rubrica è completamente lasciata dalla Direzione del periodico ai singoli autori)

Symbols for Fundamental Particles.

E. AMALDI, C. D. ANDERSON, P. M. S. BLACKETT, W. B. FRETTER, L. LEPRINCE-RINGUET, B. PETERS, C. F. POWELL, C. D. ROCHESTER, B. ROSSI, B. W. THOMPSON

(ricevuto il 12 Dicembre 1953).

In recent years we have witnessed startling developments in the field of fundamental particles. One of the consequences has been the appearance in the scientific literature of a new jargon and of a large number of new symbols. Some symbols (such as π, μ, τ) designate specific kinds of particles. Others (such as ρ, σ) have been used to describe merely a phenomenological behavior. Various authors have called the same particle by different names or have attached different meaning to the same symbol. Sometimes the meaning of a symbol has changed through the years. To give an example, the Greek letter $\varkappa$ was used initially to describe a heavy meson which stops in the emulsion and subsequently decays giving rise to a single ionizing particle. Later the latin letter K replaced the Greek letter $\varkappa$ as a code for the above phenomenological description, while the letter $\varkappa$ acquired a more definite physical meaning: that of a heavy meson which decays into one charged and two neutral particles. Sometimes, however, the letter K is also used to designate any charged particle heavier than a π-meson and lighter than a proton, whose mode of decay is unknown. As another example, the neutral particle of mass about 1 000 m_e; which decays into two π-mesons, has been variously named V^0, V_2^0, V_4^0, whereas some authors have used the letter V_2^0 to designate any V^0-particle different from the so-called V_1^0:

It seems to us that, in order to avoid confusion, the time has come to agree upon a co-ordination of the symbols used to indicate fundamental particles or groups of fundamental particles. Our specific suggestions are listed in the table to follow.

We propose first to subdivide fundamental particles into three groups according to their mass and to denote each group by a latin letter. We tentatively suggest the name *hyperon* for a particle of mass intermediate between that of the neutron and the deuteron.

We then suggest the use of Greek letters to indicate specific particles (as opposed to groups of particles). We note that this procedure has been widely followed in the past (recall the symbols γ, μ, ν, π, τ). We do not propose, however, to change the accepted symbols for the proton (p) or the neutron (n).

We finally suggest to retain and make more precise the phenomenological classification already in use, based on the empirical features of the decay process (V-particles, S-particles).

CLASSIFICATION OF PARTICLES.

A) *Groups of Particles.*

Light mesons (L-mesons): π-mesons-μ-mesons, any other lighter meson which may be discovered.

Heavy mesons (K-mesons): all particles

heavier than π-mesons and lighter than protons.

Hyperons (Y-particles): all particles with mass intermediate between that of the neutron and the deuteron (this definition might be revised if fundamental particles heavier than deuterons are discovered).

B) « *Christian Names* ».

Use capital Greek letters for hyperons and small Greek letters for mesons.

(1) *Hyperons*

Λ^0: particle previously known as V_1^0 characterized by the decay scheme $\Lambda^0 \rightarrow p + \pi^-$. If it turns out (as suggested by some results) that there are particles with this decay scheme and different Q-values, they could be designated by different subscripts.

Λ^+: the positive counterpart of Λ^0 with the possible decay schemes:

$$\Lambda^+ \rightarrow n + \pi^+$$

$$\Lambda^+ \rightarrow p + \pi^0 .$$

The existence of these particles is indicated by recent experiments.

(2) *Heavy Mesons*

$\tau \rightarrow 3\pi$ (considered certain).

$\varkappa \rightarrow \mu + 2$ neutral particles (considered very probable; however the nature of the neutral product is still unknown).

$\chi \rightarrow \pi + 1$ neutral particle (considered as probable; nature of neutral particle unknown).

θ^0: particle previously known as V^0, V_2^0, V_4^0, characterized by the decay scheme $\theta^0 \rightarrow \pi^\pm + (\pi^\mp$ or $\mu^\mp)$. If it turns out (as suggested by some results) that there are particles with this decay scheme and several Q-values, they could be designated by different subscripts.

C) *Phenomenological Categories.*

V-event: phenomenon which can be interpreted as the decay in flight of K-meson or Y-particle. Subdivisions: V^0-event; decay of a neutral particle; $V^\pm$-event, decay of a charged particle.

S-event: phenomenon which can be interpreted as the decay at rest of a charged K-particle or Y-particle.

LIBRI RICEVUTI E RECENSIONI

H. Eyring, J. Walter and G. E. Kimball – *Chimica quantistica*. Edizioni Sansoni, Firenze, 1953 (traduzione a cura di E. Scrocco).

Il libro di Eyring, Walter e Kimball è uno dei testi più usati per lo studio delle applicazioni della meccanica quantistica a problemi di strutturistica molecolare ed è sostanzialmente destinato a chi desideri iniziare ricerche in questo campo: non è perciò evidente l'utilità di una sua traduzione italiana in quanto esso si rivolge a lettori che dovranno poco dopo prendere contatto diretto con la letteratura originale. Lo scopo del libro è quello di illustrare nei particolari l'applicazione dei metodi e non quello di discutere le linee generali o le questioni di fondamento. Non sorprende quindi che queste ultime quando debbono essere trattate lo siano solo in maniera superficiale.

Il libro è suddiviso in 18 capitoli più 9 appendici. I primi otto capitoli costituiscono una introduzione non autosufficiente alla meccanica quantistica; quelli dal nono al quattordicesimo discutono l'applicazione dei metodi quantistici alla strutturistica e spettroscopia molecolare ed atomica e rappresentano certo la parte più utile del libro. I capitoli successivi accennano ad argomenti diversi quali la meccanica statistica quantistica, la teoria delle velocità di reazione, la teoria del potere rotatorio, le forze di van der Waals, ecc. C'è una certa disuniformità fra le varie parti, dovuta indubbiamente ai differenti punti di vista dei tre autori. Alle volte manca anche la coordinazione fra i diversi capitoli: così, ad esempio, nel capitolo 7 sui metodi di approssimazione non è discusso il metodo della variazione lineare che è poi ripetutamente utilizzato nei capitoli successivi (§§ 11*b* 11*e*, 13*a* (pag. 234), ecc.).

L'edizione originale del libro (Wiley, New York, 1944) conteneva numerosi errori molti dei quali sono stati corretti nella edizione italiana: così, ad esempio, quelli del § 9*h* sulla struttura fine e del § 14*f* sugli spettri di vibrazione delle molecole poliatomiche. Altri errori sono purtroppo rimasti invariati: fra questi, quelli della tabella 12.2 e l'equazione (4.74) data correttamente sul Condon e Shortley, *The Theory of Atomic Spectra* (Cambridge), pag. 52, eq. (17). Un ultimo commento: il sistema periodico riportato in fig. 9.3 risale al 1944 data del volume originale e quindi richiede sostanziali completamenti.

F. G. Fumi

Valerio Tonini – *Epistemologia della Fisica Moderna*. 1 vol. in-16° di 578 pagg. Fratelli Bocca Editore, Milano-Roma 1953 – Prezzo L. 2500.

Perchè i nostri lettori si possano fare un'idea del tutto chiara del contenuto di questo libro, mandato in recensione, è sufficiente riportare alcune frasi tratte, completamente a caso, dalle 578 pagine di esso.

(Pag. 11): « L'ambizioso scopo del presente libro è quindi proprio quello di perseguire una severa analisi, scevra di pre-

concetti, delle sconvolgenti teorie fisico-matematiche moderne per ritrovare il linguaggio adatto ad una nuova apertura di razionalità, la quale possa sovrastare unitariamente gli attuali frantumati livelli di cultura ».

(Pag. 105, in corsivo): « Il fenomeno fisico sperimentato inerentemente a una certa plaga ed invariante rispetto ad essa è indipendente dalla particolare funzione che lo rappresenti rispetto ad uno o ad un altro sistema teorico di riferimento ».

(Pag. 361): « L'esistenza di una realtà, altra-da-io, è un dato testimoniato da un'esperienza totale ».

(Pag. 448): « ... un'individuazione elettronica è qualcosa di più di un nome ed è da presumere che nessuno avrebbe mai inventato " elettroni " se alcune serie cospicue di esperimenti non avessero suggerito che in natura c'è qualche cosa di individuato... ».

Basta. In conclusione il libro è del tutto privo di qualsiasi valore scientifico.

M. Ageno

Direttore responsabile: G. POLVANI Tipografia Compositori - Bologna

Questo fascicolo è stato licenziato dai torchi il 24-I-1954